Hydrogeology and Geochemistry of Arsenic Contaminated Shallow Alluvial Aquifers in Florida and Alabama

by

Peter Haynes Starnes

A thesis submitted to the Graduate Faculty of
Auburn University
in partial fulfillment of the
requirements for the Degree of
Master of Science

Auburn, Alabama
August 1, 2015

Keywords: arsenic, bioremediation, pyrite, adsorption

Approved by

Ming-Kuo Lee, Chair, Professor of Geosciences
James Saunders, Professor of Geosciences
Ashraf Uddin, Professor of Geosciences

Abstract

This study integrates groundwater geochemical data and modeling with hydrogeological modeling to study the geochemistry and hydrogeology of arsenic contaminated shallow alluvial aquifers in Florida and Macon County, Alabama. Geochemical data collected for the Florida site showed levels of arsenic (As) in groundwater from 0.0002 to 0.577 ppm, above the US EPA drinking standard for As concentration. Geochemical data also suggest a high degree of mixing of meteoric and carbonate groundwater in the surficial aquifer. The main hydrochemical facies of groundwater in the surficial aquifer is characterized as a Ca-HCO_3-Na-Cl type. Groundwater is enriched in Ca, Mg, and HCO_3^- relative to the conservative mixing line of seawater. Groundwater geochemistry data indicate that reduced ferrous iron (Fe^{2+}) and arsenite ($As(OH)_3$) are the dominated species under moderately reducing conditions (Eh = -77 to 130.4 mV). Geochemical modeling utilizing reaction path models and Eh-pH diagrams predict that a further drop in current redox conditions will lead to the precipitation of Fe-sulfides (i.e. pyrite) and arsenic sequestration.

XRF and XRD data from both sites indicate that biogenic pyrite is naturally forming at the site, and had removed arsenic, presumably by co-precipitation and sorption. XRF analyses of dark sediment slurry recovered from monitoring wells indicate elevated concentrations of Fe, S, and As. XRD analyses indicate pyrite and perhaps other forms of iron sulfides are currently forming at both sites in reducing environments.

Hydrogeological modeling and historical water table data show a general flow trend from east to west at a velocity of a few to a few tens of meters per year across the Florida industrial site and the main factors controlling to arsenic transport at this site include advection, dispersion, and adsorption. Varying the K_d values (1 to 10 ml/g) for different adsorption models showed that the higher the degree of sorption (high K_d values) the more arsenic transport is inhibited. Sensitivity numerical analysis shows that adsorption can lower the peak concentration and cause time lag of transport.

Field data and geochemical and hydrogeologic modeling provide the basis for a future bioremediation strategy of the Florida industrial site. The Florida site is sulfate-limited (sulfate concentration < 9 mg/L) and thus should be amended with labile organic carbon and iron sulfate to stimulate metabolism of indigenous sulfate-reducing bacteria. The strategy will utilize the biogeochemical reaction involving natural sulfate reducing bacteria to form iron sulfide solids. With time, perhaps within months, groundwater is expected to become more reducing, and most dissolved arsenic will be removed due to precipitation of iron sulfide once biogenic sulfate-reduction begins.

Acknowledgments

Without grants from the National Science Foundation (#1425004), the Geological Society of America, the Gulf Coast Association of Geological Societies, and Auburn University this study would not have been possible. Many thanks are given to the following people who gave their time, advice, and constructive criticism: Dr. Ming-Kuo Lee, Dr. James Saunders, Dr. Ashraf Uddin; the entire faculty in the Auburn University Department of Geoscience. Field sampling and data collection were made possible by Dr. Jim Redwine (ANCHOR QEA, LLC) and Rick Hagendorfer. I thank Dr. Mehmet Billor and Robin Governo for their assistance in XRD and total organic carbon analyses. Gratitude must also go out to the author's fellow graduate students who provided moral support throughout this long process. The author's parents also deserve thanks for all the encouragement and financial assistance they provided. The author's wife, Leslie Starnes, was an irreplaceable part of this undertaking, providing endless hours of moral and emotional support.

Table of Contents

List of Tables

List of Figures

List of Abbreviations

As	Arsenic
AU	Auburn University
COC	Contaminant of Concern
EARP	Enhanced Anaerobic Reductive Precipitation
EPA	Environmental Protection Agency
ERD	Enhanced Reductive Dechlorinization
HFO	Hydrous Ferrous Oxide
Fe	Iron
FDEP	Florida Department of Environmental Protection
ICP-MS	Inductively Coupled Plasma Mass Spectroscopy
SRB	Sulfate Reducing Bacteria
SRS	Savannah River Site
XRD	X-Ray Diffraction
XRF	X-Ray Fluorescence
Zn	Zinc

Style manual or journal used: Geology

Computer software used: Microsoft Word 2010, Microsoft Excel 2010, Microsoft Power Point 2010, Geochemist's Workbench 10.0, Surfer 8, Visual MODFLOW Classic, Visual MODFLOW Flex, ArcMap 10

Introduction

Arsenic is the second most common contaminant of concern (COC) for sites listed on the Superfund National Priorities List (USEPA, 2002). A total of 1209 sites are on this list and 752 of this total list arsenic as the COC in either sediments, aquifers, or groundwater (Ford et al., 2007). The maximum contaminant level for arsenic in drinking water according to the U.S. EPA is 0.01 mg/L or parts per million (ppm).

Remediation technologies for arsenic found in sediments vary from those targeting arsenic in groundwater. Remedial technology for arsenic-bearing sediment includes treatments that effect containment, immobilization, or sequestration within the solid matrix (Ford et al., 2007). Technologies targeting arsenic-laden groundwater are based on either ex-situ or in-situ approaches. Pump and treat (ex-situ) technologies represent a common water treatment process for the removal of arsenic. In-situ approaches are far less common and involve the application of permeable reactive barriers or bioremediation utilizing natural bacterial reactions, such as those described in this thesis. Permeable reactive barrier technology involves the installation of reactive solid material into the subsurface to treat the plume as it is intercepted by the reactive barrier (Ford et al., 2007).

The number of groundwater arsenic contamination cases has been increasing across the world in the last few decades (Figure 1). Bangladesh and India have been hit harder by this epidemic than perhaps any other region and millions of people are being affected (Nickson et al., 2000; Harvey et al., 2002; Smedley and Kinniburgh, 2002; Charlet and Polya, 2006). In recent years, a shift of water supply from surface water to shallow alluvial

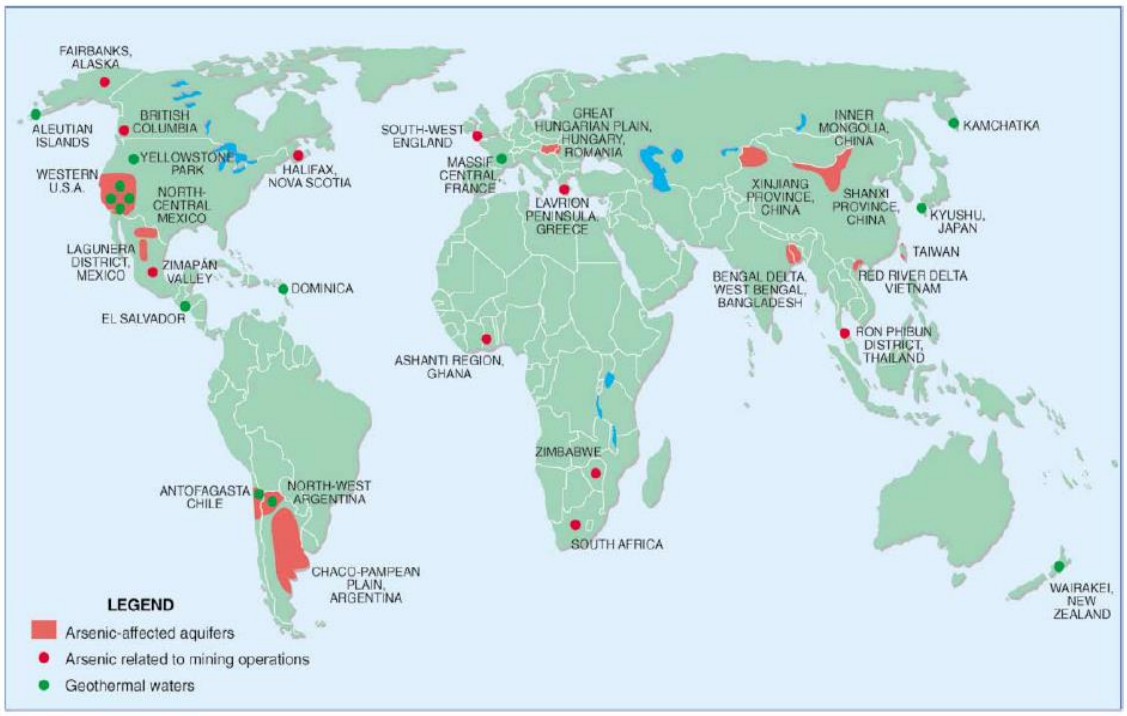

Figure 1. Global map of major arsenic groundwater contamination from Smedley and Kinniburgh (2001).

aquifers has occurred due to pollution of major rivers (Shamsudduha et al., 2008). For countries like India and Bangladesh the situation went from bad (polluted rivers) to worse (human exposure to arsenic-contaminated groundwater) because of this switch.

In contrast to Bangladesh, the United States has a much different arsenic situation. The concentration of arsenic fluctuates regionally, due to a combination of both geology and climate. Groundwater in Alabama and Florida coastal plain sediments does not normally have high concentrations of arsenic (Welch et al., 2000). The sediments in Alabama are much older (Cretaceous) than the younger Holocene sediments of the Bangladesh coastal plain, and the arsenic (if present) has been largely flushed out by gravity driven regional flow over a longer geologic period of time.

The sources of arsenic found in groundwater can be either natural or anthropogenic (Harvey et al., 2002). In either case, the remediation of the contaminated water must be addressed. In the past, remediation usually consisted of pump and treat methods, but in places where funds are low this is not a feasible option. In these situations, in-situ bioremediation is more cost effective and thus represents the preferred method of treatment (Saunders et al., 2008).

The objectives of this research stem from the need for finding a cost effective way to treat arsenic-contaminated groundwater. These objectives include: 1) assessing how biomineralization and geochemical sorption work together to remove dissolved arsenic from groundwater at the field scale, 2) investigating the arsenic contaminant assimilative capacity of iron sulfide (pyrite) biominerals formed in shallow alluvial aquifers, 3) developing a plan to use biomineralization of sulfides for immobilizing arsenic at a contaminated industrial site located in Florida, based on field data and geochemical and hydrological models.

Background

Geologic Setting

The first site of this study is located in Macon County, Alabama. At this site the coastal plain aquifers and associated sediments rest in the Tuscaloosa Formation, which consists of non-marine alluvial deposits that are considered undifferentiated (Penny et al., 2003). These undifferentiated sediments consisting of gravel, sand, silt, and lignitized wood were derived from the weathering and erosion of the Appalachians and were deposited in a Holocene floodplain (Saunders et al., 2008). At this location (Figure 2), groundwater discharges locally into stream banks of Uphapee Creek and Choctafaula Creek within Tuskegee National Forest (Saunders et al., 1997). Age dating of organic clay at the base of the aquifer produced a date of 7000 years before present (Markewich and Christopher, 1982). Arsenic and other trace metals (e.g., Co, Ni, Cu, etc.) all occur in significant concentrations in biogenic pyrite found at this site (Saunders et al., 1997). All of these hydrogeologic characteristics are similar to Holocene sediments of southern Asia, permitting the comparison of the geochemical characteristics at the Macon County site to those in Bangladesh.

The second location for this study is the Florida industrial site, where shallow groundwater and sediments contain high levels of arsenic derived from pesticides. The Florida industrial site lies within the Gulf Coastal Plain of the Florida panhandle (Figures 3 and 4). The Florida panhandle falls within the East Gulf Coastal Plain section of the Coastal Plain physiographic province. Within Bay County itself are four different physiographic subdivisions:

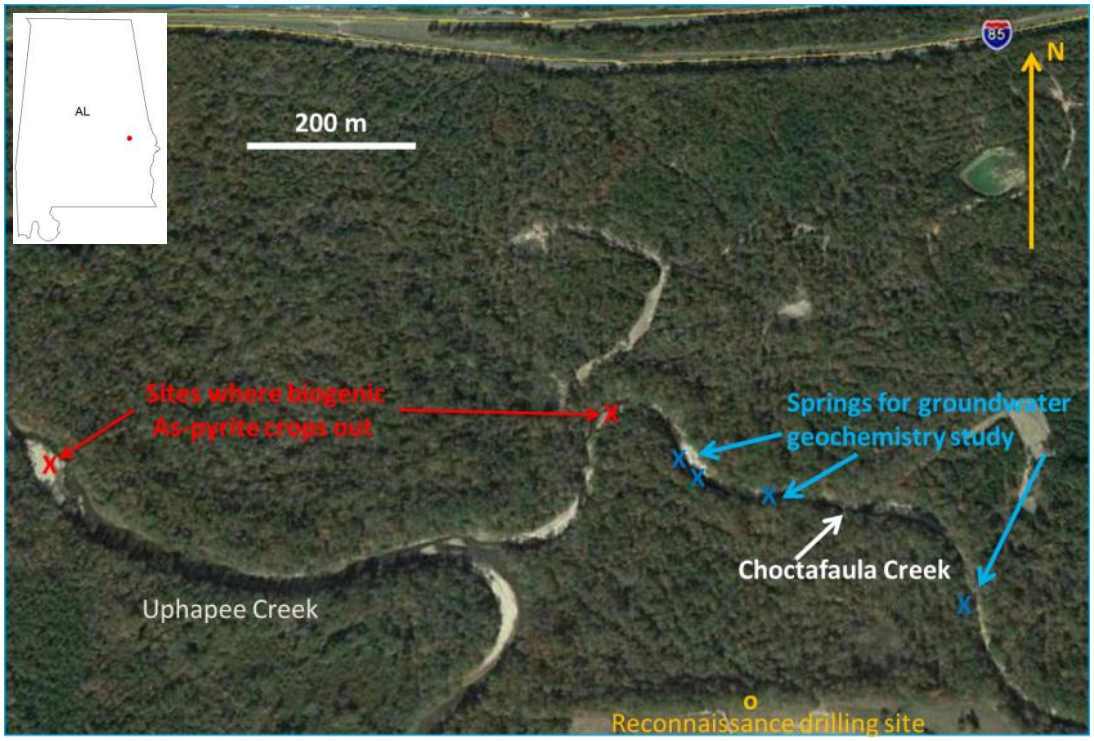

Figure 2. Location of the Macon County site (Alabama) where arsenic-rich biogenic pyrite replaces wood fragments near the base of the coastal plain alluvial aquifer. The occurrence of pyrite supports localized sulfate-reducing conditions in which arsenic is sequestered in solids.

Figure 3. A map of northwest Florida showing the location of the Florida industrial site.

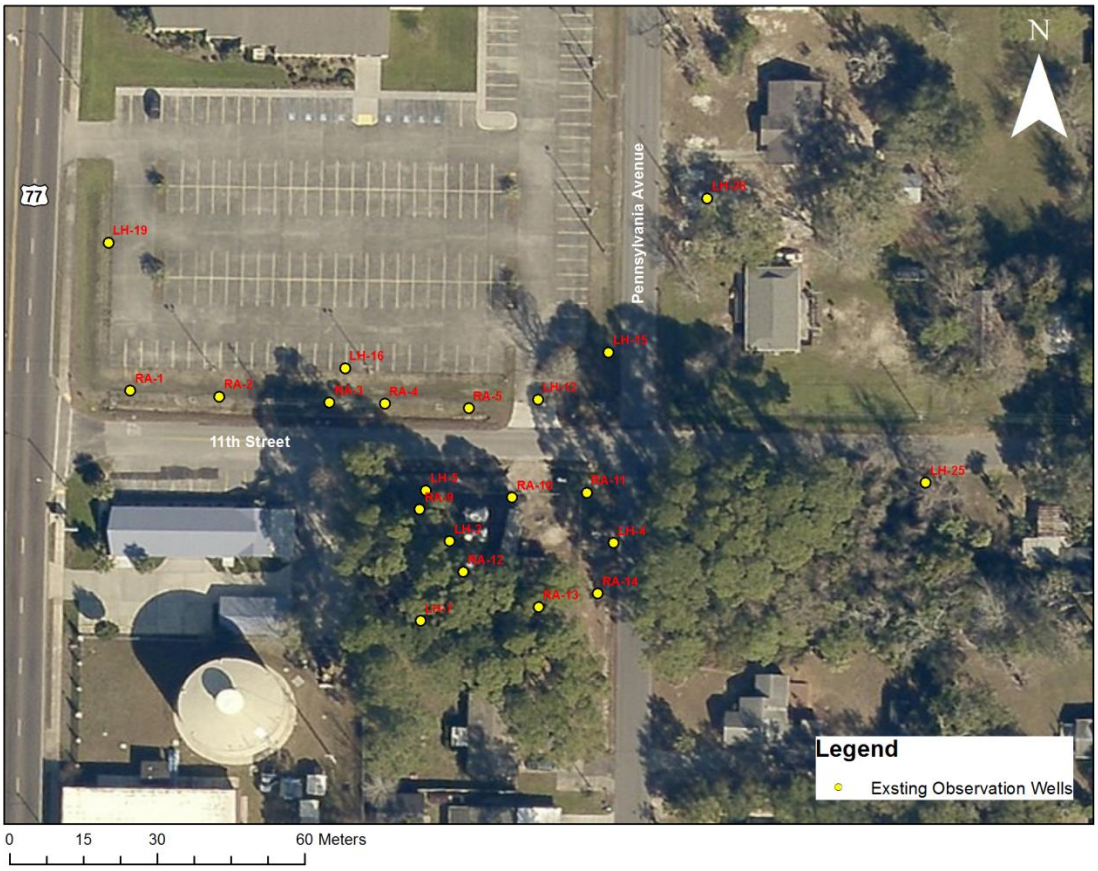

Figure 4. Site map of the Florida industrial site showing existing monitoring wells.

Sand Hills, Sinks and Lakes, Flat-Woods Forest, and Beach Dunes and Wave-cut Bluffs. The Flat-Woods Forest subdivision takes up the largest portion of Bay County. Located within Bay County the Florida industrial site rests in the Flat-Woods subdivision, and can be observed as having a slightly rolling to flat topography covered in pine trees (except where it has been cleared). Areas of the lowest elevations are likely to become flooded in times of heavy rainfall (Schmidt and Clarke, 1980).

The deposition of thick sequences of marine sediments underneath Bay County is controlled by the Apalachicola Embayment. The Apalachicola embayment is a regional basin whose axis plunges to the southwest, producing increased sediment thickness towards the coastline (Schmidt and Clarke, 1980). These sediments can be called marine terraces that represent ancient sea floors receiving sedimentation. In addition to the Apalachicola Embayment, other regional structures that may affect geology and sedimentation of the Gulf Coastal Plain are the Chattahoochee Anticline and the Ocala Arch (Veach and Stephenson, 1911).

The oldest rocks found in outcrops exposed in the county are Early Miocene limestone units. The youngest rocks found in the county are Pleistocene to recent aged undifferentiated quartz sands, clayey sands, and gravels. These sands overlie the limestone units which can extend to depths of 3000 feet, and below the limestone units, sandstones and shales extend to granitic basement rock (Schmidt and Clarke, 1980).

There are four major hydrogeologic units that are recognized in the state of Florida: surficial aquifer system, intermediate aquifer system (or the intermediate confining unit), the Floridan aquifer system, and the sub-Floridan confining unit. The surficial aquifer system is

made up of undifferentiated terrace marine and fluvial deposits in the northern Florida panhandle and normally consists of clayey sands and gravels near the coast (Schmidt and Clarke, 1980).

Specifically in Bay County, the surficial aquifer is mainly composed of quartz sand and gravel with occasional clayey sand and sandy clay lenses (Schmidt and Clark, 1980). Groundwater from the surficial aquifer discharges into local streams or springs, or it may migrate into the deeper Floridan aquifer system where the two aquifer systems are hydraulically interconnected. Underneath the surficial aquifer is the Jackson Bluff Formation, which is an important intermediate confining unit that separates the surficial aquifer from the intermediate aquifer. The Jackson Bluff Formation is characterized as sandy clay to clayey sand possessing large portions of mollusk shells (Schmidt and Clark, 1980). Because of irregular deposition and erosion, the Jackson Bluff Formation occurs intermittently in the southern portion of Bay County and is more common in northern parts of the county.

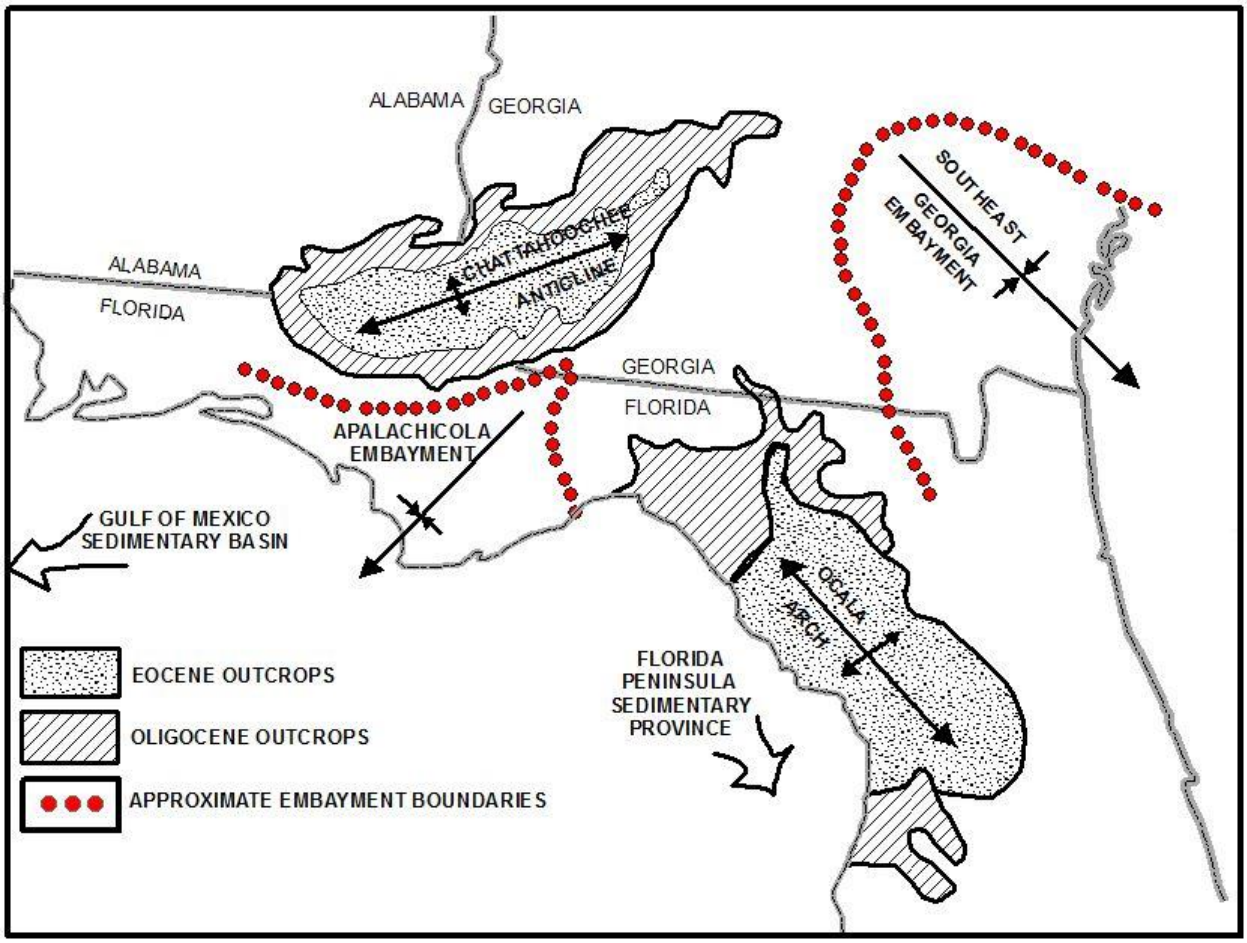

Figure 5. Regional geologic structures of the Gulf Coastal Plain in Alabama, Florida, and Georgia. This map shows the main structures controlling the deposition and geologic properties of the Florida industrial site and surrounding areas (Modified from Schmidt and Clark, 1980).

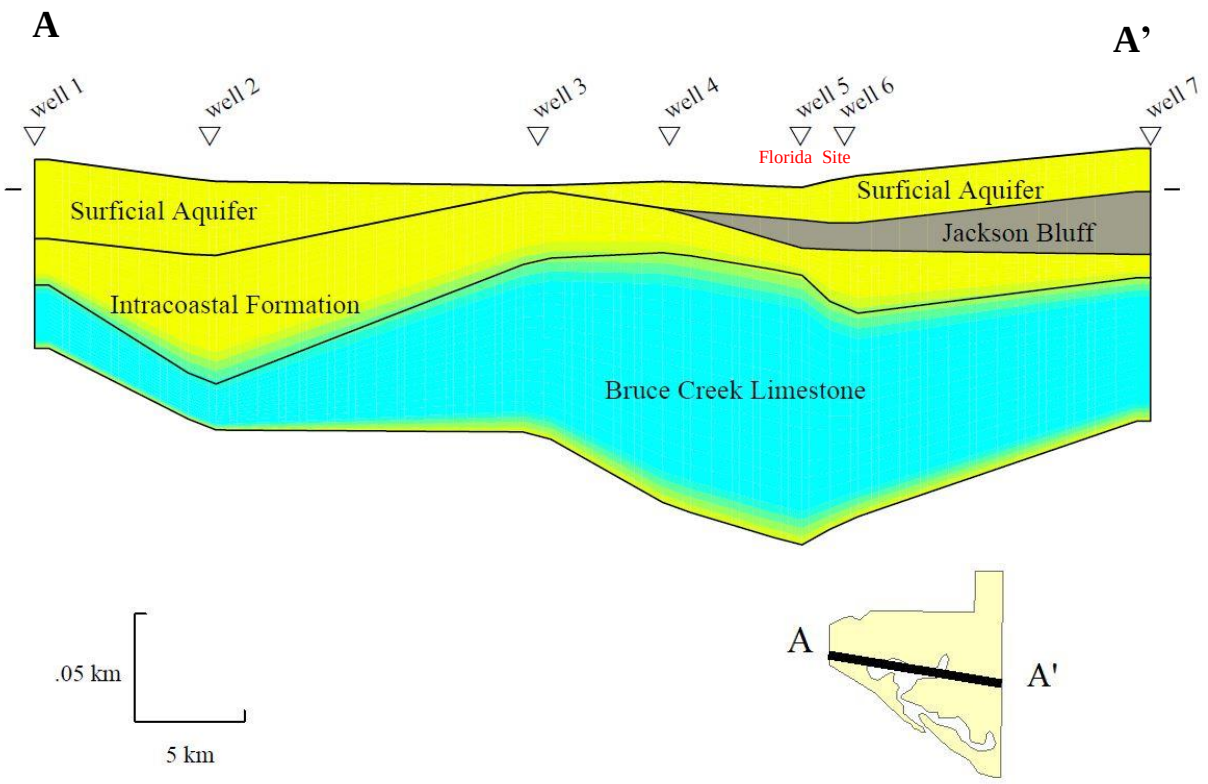

Figure 6. Geologic cross-section of Bay County showing the hydrogeologic units from west to east across the county (Modified from Schmidt and Clark, 1980).

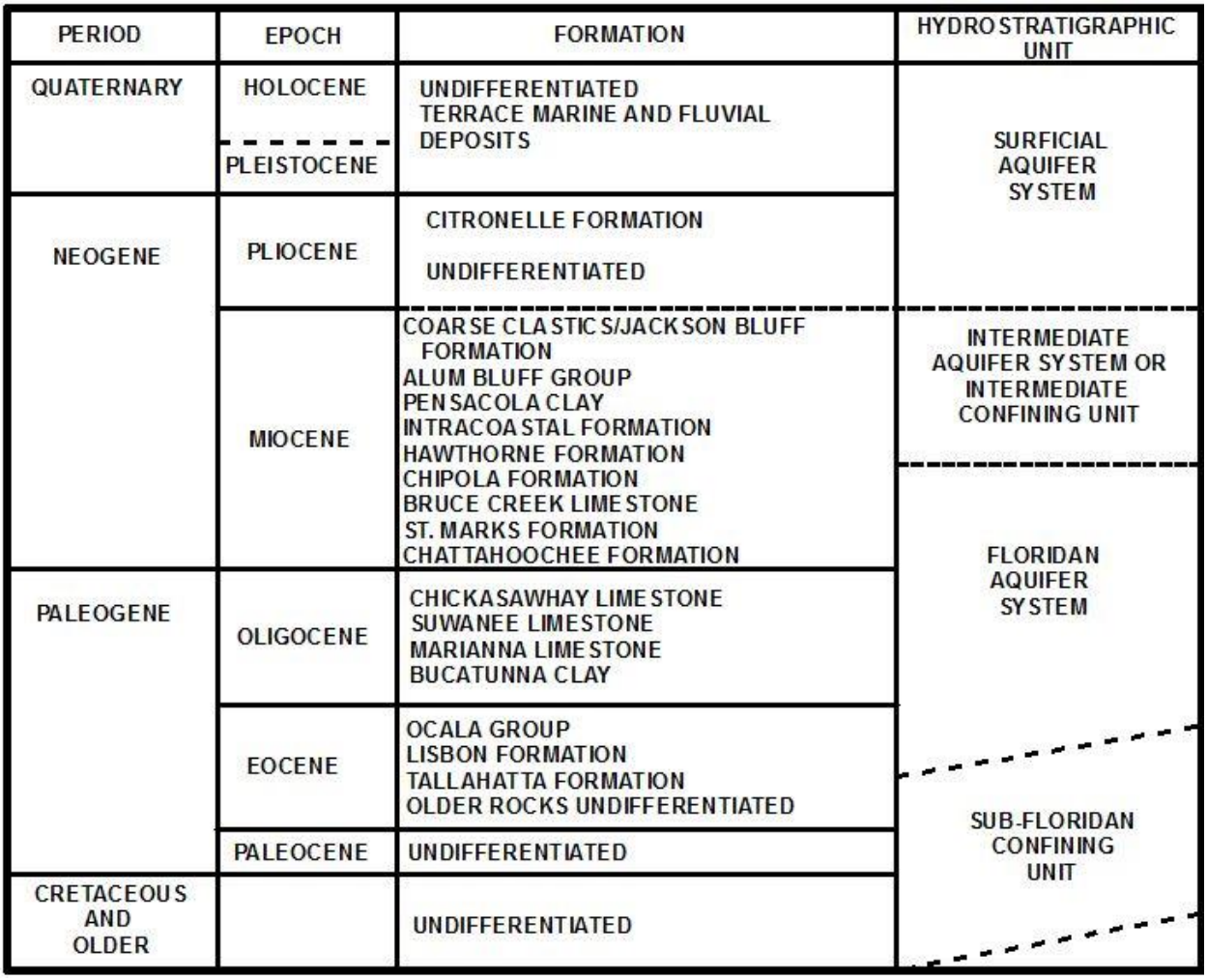

Figure 7. Generalized stratigraphic column for the Florida panhandle showing the main stratigraphic and hydrostratigraphic units (Modified from Schmidt and Clark, 1980).

Florida Industrial Site History

Groundwater in the surficial aquifer beneath the Lynn Haven industrial site (Figure 3) was contaminated via the use herbicides containing arsenic trioxide (a common by-product of the copper smelting process). Extensive contamination assessment activities and analysis were performed from 1989 to 1993 and confirmed that the contamination extended off-site to the north and west with the highest arsenic concentration reaching about 4.5 ppm (Mintz and Miller, 1993).

In 1992, approximately 770 cubic yards of arsenic contaminated soil were removed and disposed of in a nonhazardous waste landfill. In areas of close proximity to the soil excavation arsenic concentrations in groundwater were reduced from 30 to 70 percent.

Remedial actions began at this site with the installation of a pump and treat system utilizing a combination of iron co-precipitation, ceramic membrane filtration, and soil flushing with selected reagents in 1994. These operations ended in 1999 due to the failure to further lower arsenic concentrations below Florida Department of Environmental Protection (FDEP) and EPA levels. At this time the site then began a monitor only program that was approved by FDEP.

The last excavation at this site occurred in 2008, at the suggestion of the FDEP. Impacted soils along 11th street were removed based on data from previously collected soil samples.

Arsenic Geochemistry

Arsenic that occurs in soil and groundwater can originate from both natural and anthropogenic sources (USEPA, 1997). Natural sources of arsenic come from a large array of

geologic material such as sedimentary, igneous, and metamorphic rocks (Korte and Fernando, 1991). Arsenic can also accumulate during the precipitation of secondary minerals during diagenesis. Anthropogenic sources are derived from arsenic bearing pesticides and herbicides and/or arsenic bearing waste disposal from the processing of metal ores (USEPA, 1995).

Hounslow (1980) and Smedley and Kinniburgh (2002) provided evaluations of different geochemical triggers that could lead to the mobilization of arsenic in subsurface geologic materials. Included are three scenarios: 1) desorption at high pH under oxidizing conditions or due to the influx of dissolved ions that compete for sorption sites on aquifer minerals, 2) dissolution from change to a more reducing environment, and 3) mineral dissolution that is not redox driven. The first scenario arises from the addition dissolved ions (e.g., from seawater or brines) that compete and displace arsenic that is already adsorbed onto mineral surfaces. The second scenario arises from a change in groundwater chemistry to different redox conditions where the sorbent material is no longer stable. Lastly, the third scenario arises from changes in groundwater geochemistry (not redox) to where arsenic-bearing minerals are no longer stable.

Once arsenic is mobilized into groundwater it can occur in several oxidation states (-3, 0, +3, and +5), but is most common as the oxyanions arsenate [As(V)] and arsenite [As(III)] (Smedley and Kinniburgh, 2002). Many toxic trace metals that occur in solution as cations (Pb^{2+}, Cu^{2+}, Cd^{2+}, Zn^{2+}, etc.) generally become more insoluble as pH conditions increase in a system. Thus, in near neutral conditions of most natural groundwaters the solubility of trace metal cations is quite limited (Smedley and Kinniburgh. 2002). However, negatively charged oxyanions including arsenate and arsenite usually become less strongly sorbed during pH increase, so in near neutral groundwaters oxyanions can persist in larger concentrations than cations (Dzombak and Morel, 1990).

The most important factors controlling arsenic speciation are pH and redox potential (Eh) (Figures 8 and 9). Under oxidizing conditions at low pH the aqueous species $H_2AsO_4^-$ is dominant, and at high pH $HAsO_4^{2-}$ becomes dominant. Both of these species contain arsenate. Under reducing conditions and at pH less than 9 the dominant aqueous species of arsenite is $H_3AsO_3^0$ (Smedley and Kinniburgh, 2002). Under even more reducing conditions, solid arsenic sulfides (orpiment or realgar) or thioarsenite aqueous complexes become the dominant phases in S-rich systems, if there is little or no Fe (Figure 9). Sulfide produced by bacterial sulfate reduction tends to react with metals to form sulfide minerals including pyrite (FeS_2), orpiment (As_2S_3), galena (PbS), and sphalerite (ZnS). Previous studies also showed the adsorption or co-precipitation of arsenic on Fe-S or As-S solids formed under sulfate reducing conditions (e.g., Huerta Diaz and Morse, 1992; Saunders et al., 1997; O'Day et al., 2004; Lowers et al., 2007). The precipitation of arsenic sulfide or iron sulfide (Figure 8) would reduce the dissolved arsenic concentration in solution, whereas the formation of thioarsenite aqueous complexes may enhance arsenic mobility in aquifers.

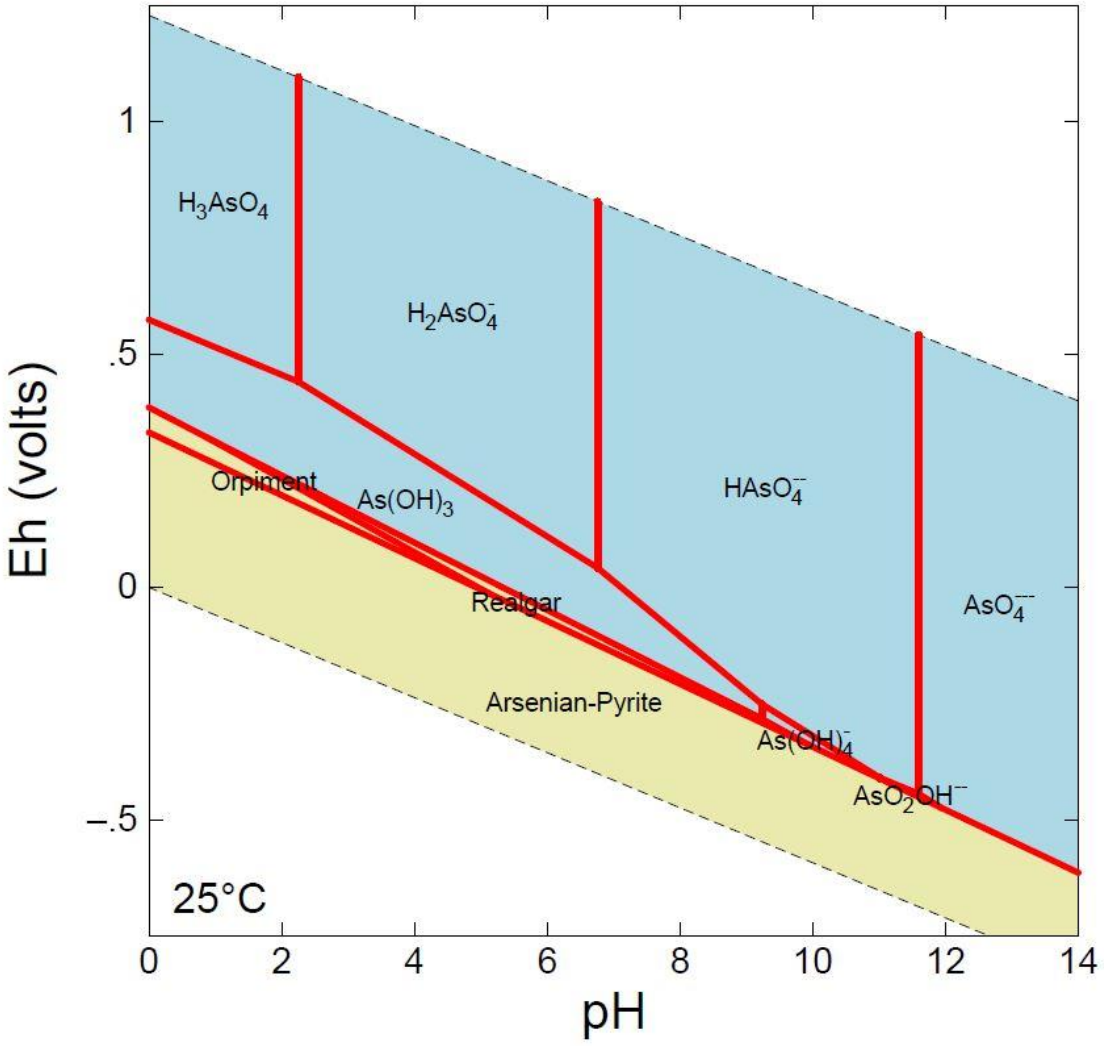

Figure 8. An Eh-pH diagram for aqueous arsenic species in the system As-Fe-S-O_2-H_2O at 25°C and 1 bar pressure. The diagram was generated with Geochemist's Workbench.

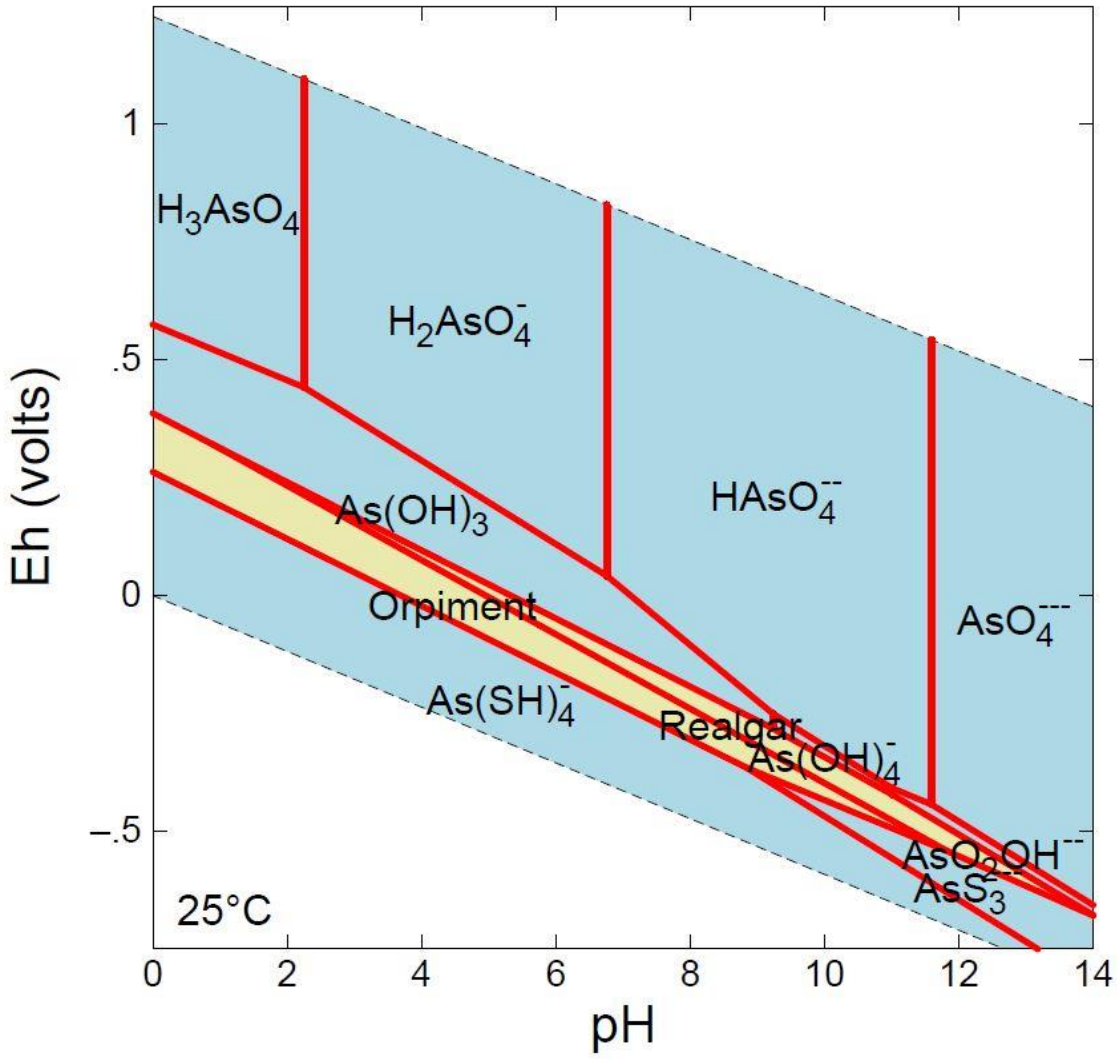

Figure 9. An Eh-pH diagram showing the dominant solid phase arsenic species in low Fe systems (As-S-H_2O). Realgar and orpiment dominate moderately reducing conditions and thioarsenate ($As(SH)_4^-$) aqueous complexes dominate at even more reducing conditions. The diagram was generated with Geochemist's Workbench.

Previous Works

There are many published studies that characterize the speciation, mobilization, and remediation of arsenic within aquifers. Examples include Lee and Saunders (2003), Saunders et al. (2005 and 2008), Keimowitz et al. (2007), Shamsudduha et al. (2008), DeFlaun et al. (2009), and Lutes et al. (2014).

Lee and Saunders (2003) and Saunders et al. (2005) presented studies in which a geochemical reaction path model was constructed to trace the geochemical evolution (including precipitation and adsorption reactions) of minerals and groundwater during an in-situ bioremediation experiment. The in-situ bioremediation experiments were carried out at the Sanders Lead car-battery recycling plant in Troy, Alabama. The geochemical models showed the effects of redox potential (Eh) on mineral precipitation and pH controls on the sorption of heavy metals. Modeling results showed that most metal ions remained in solution when pH was below 3.5 and as pH increased over the reaction the sorption of metals on HFO's became significant. Dissolved Pb was strongly sorbed at low pH (less than 4), consistent with their field observations. For As, increases in pH triggered increases in sorption for both arsenate and arsenite (Figure 10A). However, arsenite dominates at lower pH than arsenate. The modeling also showed that at low oxidation state As desorbs with increasing pH at approximately 5.8, because of reactions with dissolved sulfide leading to the formation of arsenic sulfides (Figure 10B).

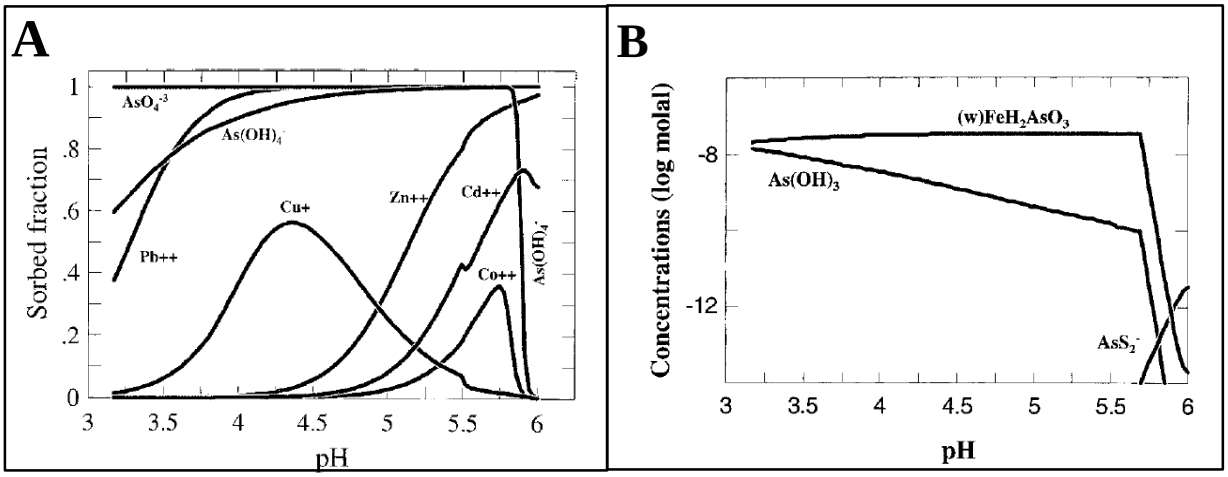

Figure 10. **A**. Plot showing sorbed fractions of common metal ions versus an increase in pH. **B**. Plot showing the concentration of sorbed As species versus a rise in pH. (From Lee and Saunders, 2003).

Saunders et al. (2005) studied the natural occurrence of arsenic in Holocene alluvial aquifers and concluded arsenic derived from different geological sources such as mountain belts or glacial deposits will be weathered, transported, and deposited in alluvial aquifers. This study collected geochemical data from two sites in the United States where biogeochemical and hydrogeologic conditions are comparable to arsenic contaminated sites in southern Asia. To explain the mechanisms behind the natural contamination of arsenic, Saunders et al. (2005) proposed that different geomicrobiologic, geochemical and hydrogeologic processes work together to cause long distance transport and mobilization of arsenic in alluvial aquifers. Tectonic uplift coupled with weathering and glaciation of bedrocks allowed for the release of arsenic into streams where the As-bearing sediments were ultimately deposited and buried. Eventually, anaerobic conditions will develop in these aquifers, and iron reducing bacteria will

release the sorbed arsenic into solution. The steps in this geochemical cycling model explain and help predict locations of potential arsenic contamination based on their geologic locations, transport history, and local biogeochemical conditions.

Keimowitz et al. (2007) studied whether the method of enhanced sulfate reduction could be a viable remediation strategy. Their samples were taken from a landfill in Maine that was contaminated with arsenic. In both of their experiments, sediment, water, and acetate (carbon source) were incubated. The first experiment analyzed small aqueous phase samples from large vessel incubations, and the second experiment analyzed aqueous phase and sediment samples

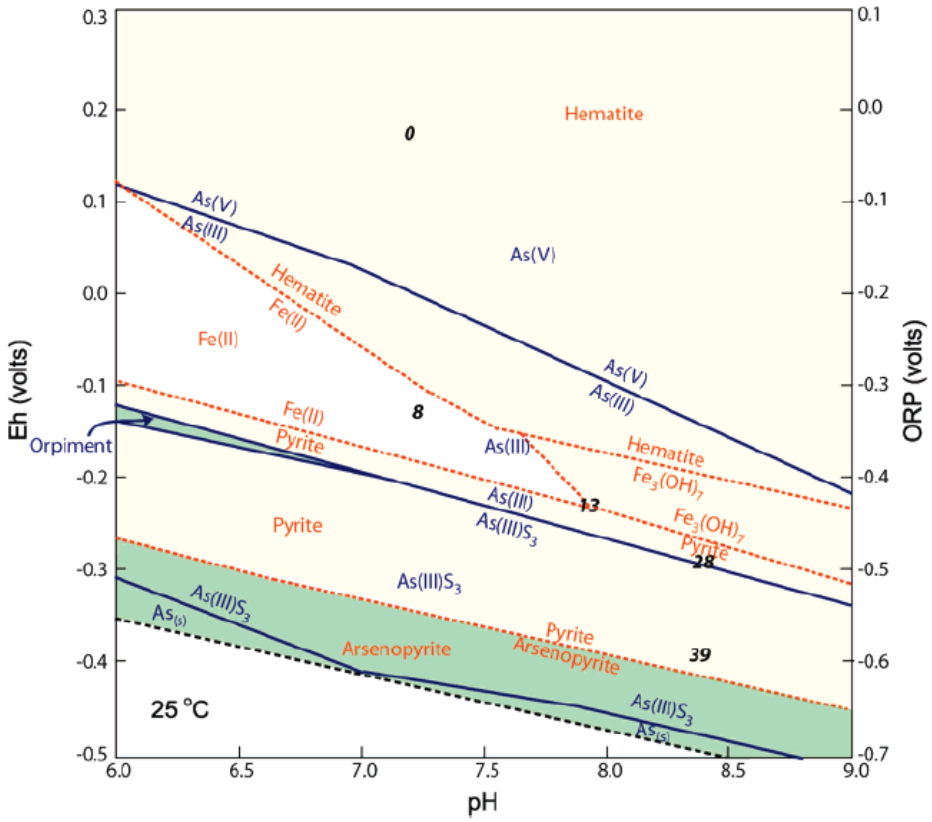

Figure 11. An Eh and pH diagram showing the stability fields of Fe and As with increasing pH as the microcosm experiment progressed with time (number of days in bold). Sulfate reducing condition is established after about 39 days (from Keimowitz et al., 2007).

from microcosm incubation. The results of this study showed that significant amounts of arsenic were removed from solution by the forming of biogenic pyrite under highly reducing conditions (with low negative Eh values) at the end of the both incubations (Figure 11). For the large vessel incubation there was an approximate decrease in arsenic concentration of fifty percent. For the microcosm experiment the arsenic concentration decreased by approximately 85 percent.

Saunders et al. (2008) presented new data from field bioremediation experiments and geochemical modeling to illustrate the principal geochemical behavior of arsenic in anaerobic groundwater. Two field bioremediation experiments were carried out, one in Bangladesh, where carbon and $MgSO_4$ were added to a shallow Holocene aquifer to stimulate sulfate reducing bacteria. Another was in the United States, where groundwater was amended with sucrose and methanol to stimulate sulfate reducing bacteria. These studies again showed that arsenic is mobile and released from iron oxides under iron-reducing conditions and becomes immobile under sulfate reducing conditions (Figure 12). Thus, if sulfate reduction can be engineered and maintained, it is possible to reduce the arsenic concentration at the field scale.

The objectives of DeFlaun et al. (2009) were to examine the mineralogy of iron hydroxides harboring arsenic and to measure the dissolution rate of the pyrite under aerobic conditions. If arsenic sulfides formed in a lab setting would be stable on a decadal time scale under changing redox conditions, then this technology may be feasible for a field remediation strategy. The results of DeFlaun et al. (2009) showed successful sequestration of As under anaerobic, sulfate reducing conditions, and that As precipitates were resistant to dissolution under aerobic conditions (Figure 13).

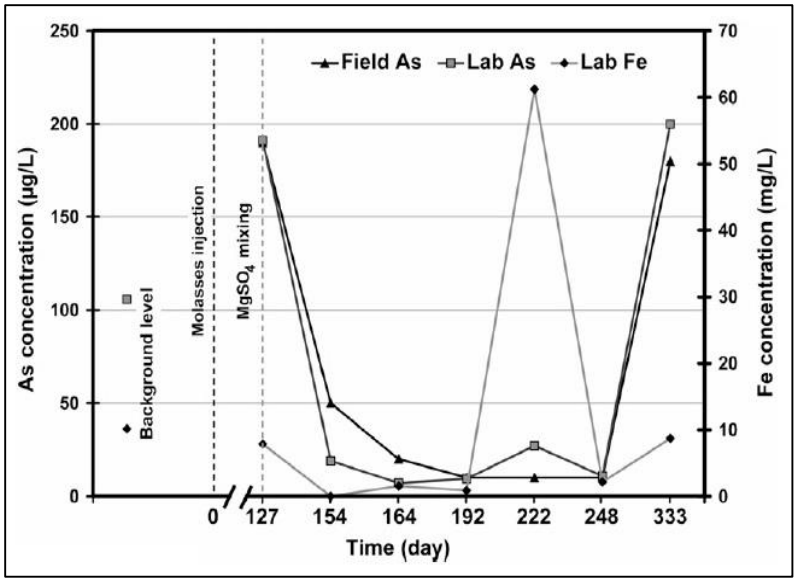

Figure 12. Plot showing As and Fe concentration versus time for the Bangladesh site. Arsenic concentrations were dramatically reduced one month after $MgSO_4$ amendment (from Saunders et al., 2008).

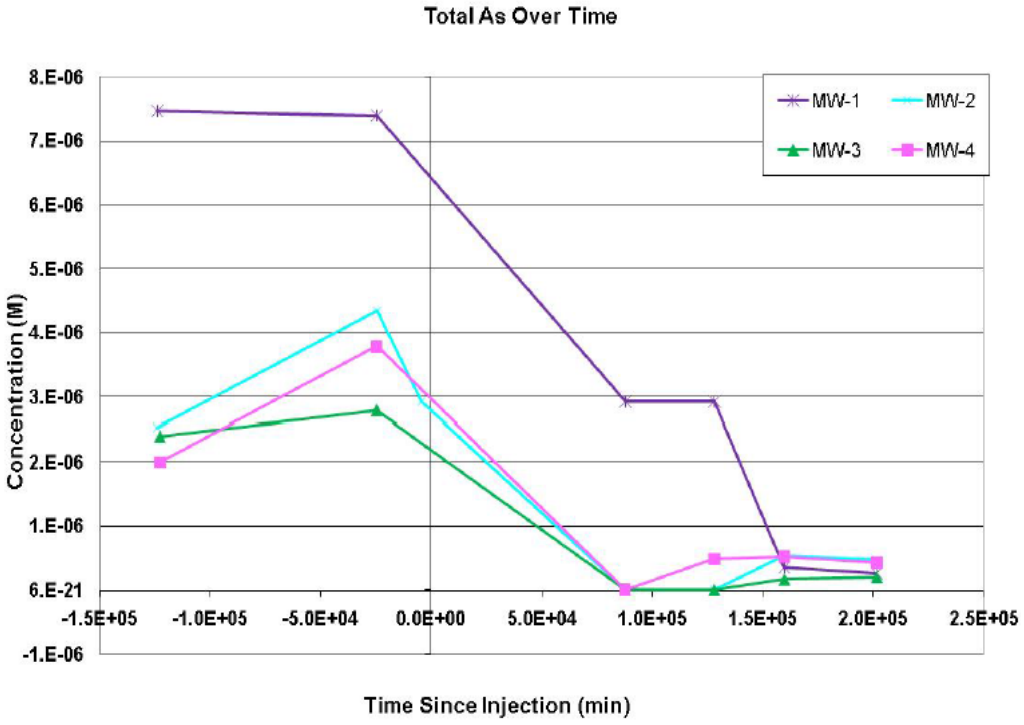

Figure 13. The decrease in arsenic concentration with time from the DeFlaun et al. (2009) pilot study.

Lutes et al. (2014) presented a study in which a field demonstration of in-situ groundwater remediation technology was carried out. This technology was termed enhanced anaerobic reductive precipitation (EARP) and enhanced reductive dechlorination (ERD). The location of this study was the U.S. Department of Energy's Savanah River Site (SRS). At this location three key contaminants were targeted for remediation: uranium radionuclides, technetium, and nitrate.

EARP involves the use of a food-grade carbohydrate substrate that acts as a food source for microbiological processes. By injecting this food source into the subsurface, an aquifer that is currently aerobic or mildly anoxic can be amended to a strongly anaerobic zone. This newly amended anaerobic zone is suitable for the precipitation of metals and radionuclides in insoluble forms or for the degradation of chlorinated solvents.

The goals of this field demonstration at the SRS were the attainment of continuous sulfate-reducing biogeochemical conditions for a period of 18 months, achievement of treatment goals for specific contaminants within two years in the main area of the reactive zone, and the presence of precipitated uranium and technetium in insoluble sulfide forms following the treatment.

By the end of the active treatment period redox zones were changed from aerobic to methanogenic. At the target date of 18 months after injections the reactive zone of the SRS was observed to be returning to original redox conditions, but still exhibited methane concentrations suggesting that sulfate-reducing conditions were still ongoing.

The treatment goal for the key contaminants of concern at the SRS ended with mixed results. The long-term trends for all contaminants fell sharply immediately after injection.

However, within a year of injection nitrate and strontium-90 were elevated above GWPS levels. The remaining contaminants (U-233/234, U-238, and Tc-99) were still observed to be below GWPS levels one year after injection.

Finally, the presence of precipitated insoluble forms of uranium and technetium can be indicated by the continuing of long-term monitoring at the SRS site. For a successful test precipitated uranium and technetium will not be re-dissolved at an unacceptable rate after aerobic conditions are re-established. Most recent data collected 2.5 years after injections shows that conditions have returned to background levels and the uranium radionuclides and technetium concentrations have remained low, suggesting that sorbing mineral phases have formed and remained stable in the aquifer.

Materials and Methods

Sample Collection and Water Quality Measurements

During January 21st through 24th 2015, Peter Starnes, Shahrzad Saffari, and Dr. Ming-Kuo Lee of Auburn University, collected both sediment and water samples from the study site in Lynn Haven, Florida. In addition to the collection of samples, in-situ measurements of water quality parameters were also taken.

In order to collect representative sediment samples of the surficial aquifer at the Lynn Haven site a peristaltic pump was used. Once the pump was placed into the well and lowered to the bottom, sediments were collected into a clean beaker and then frozen in a test tube on dry ice to preserve any bacteria or redox states of chemical species present in the well sediments.

To collect representative groundwater samples in the aquifer a peristaltic pump was used to purge the wells. At least three well volumes of water were removed and all water quality parameters readings became stable before sampling. This purging makes sure that all of the stagnant groundwater residing inside the well casing is flushed out and fresh groundwater percolates through the well screen. This procedure allows for the sample to accurately represent the groundwater geochemistry of the aquifer being analyzed. After the well purging was completed, water quality parameters including temperature, pH, dissolved oxygen, oxidation-reduction potential, and electrical conductivity were measured in the field using YSI 556 hand-held multiparameter probes. Measured ORP values are often normalized to a standard hydrogen electrode (SHE), depending on the type of ORP electrode (e.g., Ag/AgCl) used. Since pH and ORP electrodes are built together as a single probe for YSI 556, ORP is read relative to the standard SHE, so no conversion of ORP measurements to Eh values is needed.

After a water sample was collected in a clean beaker, it was then filtered with a 45 micron filter and acidified with 5% nitric acid for preservation before trace metal and cation analysis using inductively coupled plasma mass spectrometry (ICP-MS). A second sample was filtered for anion analysis using ion chromatography (IC), as well as, DOC analysis. A third sample for each well was filtered through arsenic speciation cartridges for an arsenic speciation study. The sample was first filtered through a 45 micron filter and about 50 mL of the water sample was passed through the cartridge using a syringe (with luer slip tip). The first 5 mL of filtrate was discarded before collecting the filtered solution for analysis. The adsorbent in the cartridges retains arsenate anions [As(V), $H_2AsO_4^-$], but allows the uncharged arsenite complex [As(III), or H_3AsO_3] to pass through. As(III) is then measured in the effluent filtered through the cartridges and As(V) is calculated from the difference between total As and As(III). All water samples were refrigerated for transport and preservation before chemical analysis.

Redox sensitive ions were measured in the field using HACH Spectrophotometers. A HACH DR2700 was used to measure dissolved sulfide concentrations in the field via the standard Methylene Blue Method (USEPA Method 8131). Ferrous iron concentrations were measured by the 1.10 Phenanthroline Method (USEPA Method 8146) using a HACH DR820. Alkalinity was also measured in the field using the standard titration method (USEPA Method 8203).

Monitoring Wells

Groundwater and sediment samples were collected from a total of 22 monitoring wells at the Lynn Haven study site. All wells were drilled using hollow stem auger drilling procedures. 11 of the 22 wells were constructed of 2 inch diameter PVC casing, with a well screen of 0.01

inch slotted PVC, and are named “LH” wells. Each well had a fifteen-foot screened interval used to monitor the surficial aquifer and to avoid breaching the Jackson Bluff confining layer. Sand filter packs surround the screened interval and are placed at least one foot above the interval. Over top of the sand filter pack, a bentonite seal of at least one foot was installed, and all wells were grouted to the surface.

The remaining wells were installed as recovery and injection wells for the pump and treat process that previously operated at this site, and are named “RA” wells. These wells were also installed via hollow stem auger procedures. The RA wells were constructed with 6 inch PVC pipe with five feet of screen below the water table.

Geochemical and Mineralogical Analyses

A total of 44 groundwater samples were shipped on ice to Actlabs Ltd. for major ion and trace element analysis. 22 samples were tested for major anions using ion chromatography, and the other 22 samples were tested for trace elements and cations using ICP-MS technology.

Biogenic pyrite samples (Figure 14) were also taken from the Macon County site, and submitted to ACME Labs Inc. for aqua regia digestion followed by ICP-MS testing of the remaining leachate. The aqua regia (3:1 volume ratios of HCl to HNO_3) digestion procedure (ISO standard 11466) is considered adequate for analyzing total acid leachable heavy metals in sediments.

Figure 14. Biogenic pyrite sample from Macon County, AL submitted to ACME Labs Inc. for aqua regia digestion and ICP-MS testing.

Dissolved organic carbon (DOC) analyses were performed to quantify the level of organic matter contents in groundwater. 22 filtered groundwater samples from each well were prepared for DOC analysis in the AU School of Forestry and Wildlife Sciences using a Shimadzu TOC-V Combustion Analyzer.

X-ray fluorescence (XRF) and X-ray diffraction (XRD) technology were used to determine the chemical compositions and mineralogical make-up of sediment samples collected at the bottom of each well. Determining the mineralogy and chemistry of these sediments can show the hydrogeology and geochemical conditions of the aquifer. The XRD and XRF analyses were conducted using the Bruker D2 Phaser X-ray Diffraction spectrometer and the Bruker X-ray Fluorescence Elemental Tracer IV-ED in the Department of Geosciences at Auburn University. For XRD analysis, samples were run from 2 theta values of 27 degrees to 60 degrees with a 0.004 degree step interval. The mineral composition of the samples was determined by a peak search and match procedure using DIFFRAC.EVA software. XRD pattern also reveals semi-quantitative make-up of a sample since the areas under the peak reflect the amount of each phase present in the sample.

XRF technology analyzes the energy emission of characteristic fluorescent X-rays from a sample that has been excited by bombardment with high-energy (i.e., short-wavelength) X-rays. The XRF technology can quantify the elemental composition of a material because each element has unique electronic orbitals of characteristic energy and the intensity of each characteristic radiation is directly related to the amount of each element in the material. Major elements and most trace elements (Ba, Cr, Co, Cu, Mo, Nb, Ni, Pb, Rb, Sr, U, Th, V, Y, Zn, Se, As, etc) of sample, in the range of parts per million (ppm), were measured in the laboratory.

Hydrogeologic and Geochemical Modeling

To develop an effective remedial plan for the Lynn Haven industrial site, geochemical and hydrogeologic modeling techniques were employed to characterize the site's hydrogeochemistry and groundwater flow regimes. The software Geochemist's Workbench (Bethke, 2008) was used to calculate speciation and geochemical reactions associated with sulfate reduction based on the current field hydrochemical environment. Field parameters measured (temperature, pH, Eh, etc.) and the concentrations of major ions and arsenic were uploaded in a spreadsheet into Geochemist's Workbench. Activity diagrams and hydrochemical facies analysis were used to graphically characterize the geochemical conditions of Lynn Haven surficial aquifer. Eh-pH diagrams are particularly useful in showing stable fields of various solid and aqueous phases under different redox and geochemical conditions. Piper diagrams are used to show the characteristic hydrochemical facies of groundwater in the surficial aquifer. In addition, a reaction path model was created in Geochemist's Workbench to predict what might happen minerogically and chemically as a result of sulfate reduction within the surficial aquifer.

Three dimensional numerical modeling of groundwater flow and contaminant transport at the Lynn Haven site was performed using the U.S. Geological Survey model MODFLOW (McDonald and Harbaugh, 1988). The governing equation for 3D groundwater transient simulation is:

$$S_s \frac{\partial h}{\partial t} - R^* = \frac{\partial}{\partial x}\left(K_x \frac{\partial h}{\partial x}\right) + \frac{\partial}{\partial y}\left(K_y \frac{\partial h}{\partial y}\right) + \frac{\partial}{\partial z}\left(K_z \frac{\partial h}{\partial z}\right)$$

where h is hydraulic head, S_s is specific storage, and K_x, K_y, and K_z are hydraulic conductivity in x, y, and z directions. R^* represents a source term derived from water pumping or injection. The

solute transport equation involved advection, dispersion, and adsorption processes in one dimension is given by:

$$\frac{\partial C}{\partial t} = -v\frac{\partial C}{\partial x} + D\frac{\partial^2 C}{\partial x^2} - \frac{\rho_b}{\varphi}\frac{\partial (K_d C)}{\partial t}$$

where C is the concentration of a given contaminant (mol cm^{-3}), v is groundwater flow velocity (cm sec^{-1}), t is time (sec), and D is hydrodynamic dispersion (cm^2 sec^{-1}), which accounts for molecular diffusion of solutes as well as mechanical dispersion. The model calculates the coefficients of hydrodynamic dispersion D from the following equation:

$$D = D^* + \alpha v_x$$

where D^* is the diffusion constant (cm^2 sec^{-1}) and α is the dispersivity (cm) in the x direction.

Graphic interface modeling was carried out with the programs Visual Modflow Classic and Visual Modflow Flex. These two programs are industry standards in characterizing the groundwater hydrogeology of an aquifer and are distributed by Schlumberger Water Services. The input parameters required for modeling a system were: conductivities, porosities, storage capacity, initial heads, concentration observations, observed head values, contaminant concentrations, hydraulic gradient, recharge, precipitation, and groundwater boundaries. All of these variables were gathered through the January 2015 sampling event and in previous studies (Mintz and Miller, 1993). By using measured field hydrogeologic parameters and proper boundary and initial conditions numerical models of groundwater flow were generated. Sensitivity analysis was also conducted to examine the effects of adsorption on arsenic transport.

Results and Discussion

Groundwater Geochemistry

Tables 1 and 2 show the complete results of the geochemical analyses of this study. Table 1 lists the field parameters that were measured during the January 2015 sampling event. The water temperatures encountered in the wells ranged from 14.5˚C to 22.4°C. The mean groundwater temperature was 18.46°C with a standard deviation of 1.74°C.

The pH values for groundwater in the Lynn Haven surficial aquifer were observed to be near-neutral to slightly acidic, as expected for a coastal plain surficial aquifer. The observed pH ranges from 4.46 in LH-25 and 6.82 in RA-11. The mean pH was calculated to be 5.72 with a standard deviation of 0.65.

Oxidation-reduction potential (ORP) was also measured in the field during the January 2015 sampling event. The highest ORP recorded occurred in well LH-25 at 130.4 mV, and the lowest ORP value was recorded in well RA-4 at -77 mV. The mean value for field ORP was 46.72 mV and the standard deviation of ORP was 40.03 mV. ORP is determined by measuring the potential of a chemically-inert electrode which is immersed in the solution. The sensing electrode potential is then read in reference to the electrode of the pH probe and presented in mV. Because the values are already referenced to the standard hydrogen electrode (SHE) in the pH probe they do not need to be referenced again to be used as Eh values. This will be discussed in more detail in the results of the geochemical modeling section.

Well ID	Temp (°C)	pH	ORP (mV)	Conductivity (µs/cm)	S^{2-} (mg/L)	Fe^{2+} (mg/L)	Alkalinity (mg/L)	DO (mg/L)
LH-2	18	5.29	42	164	0.01	0.42	40	0.42
LH-4	17.7	5.86	78.4	149	0.14	0.67	80	0.6
LH-5	16.45	6.42	56	227	0.01	0.17	79	1.59
LH-7	16.9	5.7	33.7	200	0.06	1.48	78	0.25
LH-12	19.6	5.5	36	233	0.30	0.25	20	0.24
LH-15	19.45	4.7	44.1	80	0.19	0.78	4	0.18
LH-16	18.65	5	51.2	109	0.43	0.81	8	0.19
LH-19	20.2	4.58	90	62	0.16	0.25	8	0.95
LH-25	22.4	4.46	130.4	94	0.34	0.09	4	0.1
LH-26	20.8	5.1	61	110	0.09	0.64	30	0.16
LH-27	17.2	5.76	105	124	0.04	0.32	18	0.95
RA-1	19.4	6.15	28	77	0.02	1.63	35	0.15
RA-2	18.5	5.83	63	206	0.01	2.74	46	0.14
RA-3	18.1	6.27	-12	125	0.00	2.44	60	0.76
RA-4	18.2	6.1	-77	167	0.06	1.25	68	0.09
RA-5	20.5	5.72	41	233	0.18	1.56	45	0.09
RA-9	17.1	6.12	35	130	0.07	0.03	31	1.53
RA-10	16.7	6.71	46	278	0.01	0.11	95	0.55
RA-11	14.5	6.82	49	166	0.03	0.12	51	1.55
RA-12	18.4	5.74	36	299	0.04	0.91	28	1.49
RA-13	17.6	5.73	39	102	0.01	0.13	25	0.85
RA-14	19.7	6.38	52	133	0.03	0.08	48	0.81
Mean	18.46	5.72	46.72	157.64	0.10	0.77	40.95	0.62
Stan. Dev.	1.74	0.65	40.03	66.21	0.12	0.78	26.81	0.53

Table 1. Field parameter results from the January 2015 sampling event. Electrical conductivity is measured in µS/cm. Units for sulfide (S^{2-}) and ferrous iron (Fe^{2+}) are mg/L. Field ORP values were measured in reference to the electrode of the pH meter of YSI-556, thus can be used as Eh values without being referenced.

Well ID	NO_3 (mg/L)	DOC (mg/L)	F (mg/L)	Na (mg/L)	Mg (mg/L)	PO_4 (mg/L)	SO_4 (mg/L)	Cl (mg/L)	K (mg/L)	Ca (mg/L)	Fe (mg/L)	As (mg/L)	Br (mg/L)	TDS (mg/L)	CBE
LH-2	< 0.01	26.37	< 0.01	10.70	1.59	< 0.02	< 0.03	< 0.03	0.96	12.10	0.39	0.4830	< 0.03	52.59	0.00%
LH-4	0.04	31.81	< 0.01	24.40	0.92	< 0.02	6.39	15.10	0.66	5.10	0.36	0.0015	< 0.03	84.78	0.13%
LH-5	0.11	31.31	< 0.01	3.61	2.06	< 0.02	9.34	7.35	0.36	36.70	0.29	0.5620	< 0.03	91.69	0.09%
LH-7	< 0.01	51.70	0.19	14.00	2.84	< 0.02	1.71	9.84	1.11	21.90	1.25	0.0029	0.12	104.66	0.07%
LH-12	< 0.01	40.76	< 0.01	17.20	2.21	< 0.02	12.00	33.40	2.21	19.70	0.25	0.0119	0.23	127.97	0.74%
LH-15	< 0.01	90.05	< 0.01	4.83	0.29	1.52	4.58	3.01	0.19	4.80	0.97	0.0063	0.06	110.31	0.63%
LH-16	0.05	20.48	< 0.01	7.98	0.96	0.95	3.30	12.50	1.26	4.70	0.55	0.1640	< 0.03	52.90	0.65%
LH-19	< 0.01	77.94	< 0.01	3.27	0.27	< 0.02	< 0.03	4.69	1.54	1.00	0.24	0.0004	0.23	89.18	0.20%
LH-25	0.06	11.22	< 0.01	4.75	1.86	< 0.02	7.08	9.91	0.57	5.50	0.11	0.0002	0.11	41.17	1.18%
LH-26	0.04	25.69	< 0.01	2.28	0.37	< 0.02	3.71	2.98	0.32	1.40	0.46	0.0147	< 0.03	37.27	0.07%
LH-27	0.09	15.20	< 0.01	6.59	1.40	< 0.02	12.70	8.22	0.33	9.10	0.39	0.0005	< 0.03	54.02	0.33%
RA-1	0.03	20.17	< 0.01	4.83	0.91	< 0.02	1.02	3.42	0.49	8.70	2.08	0.0080	< 0.03	41.65	0.05%
RA-2	0.05	21.59	< 0.01	26.30	1.15	< 0.02	11.30	22.50	1.05	7.00	4.40	0.0159	0.09	95.45	0.28%
RA-3	0.05	23.04	< 0.01	3.46	2.15	< 0.02	2.17	5.97	0.93	18.30	2.61	0.0240	< 0.03	58.70	0.06%
RA-4	0.05	26.26	< 0.01	9.11	1.89	< 0.02	6.01	15.60	1.11	27.00	1.25	0.5440	< 0.03	88.82	0.14%
RA-5	0.01	27.21	< 0.01	18.40	4.67	< 0.02	11.50	30.70	1.77	19.30	1.44	0.5770	0.14	115.72	0.36%
RA-9	0.06	26.47	< 0.01	5.14	2.02	< 0.02	10.40	10.20	0.18	20.70	0.24	0.4850	< 0.03	75.90	0.22%
RA-10	0.13	35.83	0.05	2.65	3.05	< 0.02	6.73	4.03	0.43	50.00	0.10	0.3340	< 0.03	103.33	0.05%
RA-11	0.16	18.45	0.16	2.65	4.34	< 0.02	4.88	3.62	0.35	15.40	0.15	0.0197	< 0.03	50.18	0.06%
RA-12	< 0.01	34.60	0.02	25.90	4.36	< 0.02	33.70	50.60	0.22	36.70	0.65	0.1090	0.14	187.00	0.98%
RA-13	0.04	23.34	< 0.01	3.34	2.33	< 0.02	7.73	8.94	0.08	13.60	0.29	0.0038	< 0.03	59.69	0.21%
RA-14	0.04	22.49	< 0.01	2.12	2.19	< 0.02	6.22	4.89	0.17	23.90	0.05	0.0025	< 0.03	62.07	0.08%
Mean	**0.06**	**31.91**	**0.11**	**9.25**	**1.99**	**1.24**	**8.12**	**12.74**	**0.74**	**16.48**	**0.84**	**0.15**	**0.14**	**81.14**	0.30%
Stan. Dev.	**0.04**	**19.09**	**0.08**	**8.10**	**1.26**	**0.40**	**6.98**	**12.22**	**0.58**	**12.73**	**1.04**	**0.22**	**0.06**	**35.65**	0.33%

Table 2. Geochemical analyses results from Actlabs Ltd. All units are in ppm. CBE are calculated charge balance errors.

Conductivity values ranged from 62 μS/cm in well LH-19 to 299 μS/cm in well RA-12. The mean conductivity for the surficial aquifer was 157.64 μS/cm and the standard deviation was 66.21 μS/cm. Conductivity values correspond to the total dissolved solids (TDS) of the groundwater. The more dissolved solids are present in the water the higher the electrical conductance of a sample, especially if there are dissolved metals and metalloids present.

Alkalinity can be defined as the net concentration of strong base in excess of a strong acid with a pure CO_2 system as a point of reference (Morel, 1983). In natural groundwater, the generation of a net positive charge through the dissolution of carbonate minerals is usually greater than the contribution of negative charges from the ionization of strong acids (Domenico and Schwartz, 1990). Thus, as a general rule of thumb, natural groundwaters typically will display a positive alkalinity, unless there is some point of strong acidic contamination. The results of our field measurements of alkalinity (as HCO_3^-) yielded an average mode of 40.95 mg/L with a standard deviation of 26.81 mg/L. These results can be expected for the Lynn Haven aquifer, since there are few carbonate minerals in the surficial aquifer and recharge is mainly of a meteoric origin. Groundwater in the surficial aquifer may still acquire alkalinity via mixing with deeper groundwater associated with the Bruce Creek Limestone.

Dissolved oxygen (DO) was also measured in the field with the YSI-556. The highest DO measurement was taken at well LH-5 at 1.59 mg/L. The lowest DO was observed at wells RA-4 and RA-5 at 0.09 mg/L. DO values are generally low as compared to those in shallow aquifers or surface water under oxidizing conditions. Dissolved oxygen concentration will reduce to low levels due to breakdown or degradation of organic matter in the aquifer. The relatively low DO values are consistent with ORP values that indicate a moderately reducing environment.

Table 2 shows the results of geochemical analyses including measured major cation concentration, major anion concentration, trace element (As and Fe) composition, dissolved organic carbon (DOC), and TDS calculated from these concentrations. NO_3 (nitrate) concentrations ranged from below the detection limit (0.01 ppm) in several wells to 0.16 ppm in well RA-11. The average NO_3 concentration was calculated to be 0.06 ppm with a standard deviation of 0.04 ppm. The relatively low values for this aquifer are expected, since there are no surficial sources of excess nitrate in the area (fertilizers).

Naturally occurring dissolved organic carbon (DOC) in groundwater is produced by biological and biochemical decay of organic matter in the aquifer. Results indicate the lowest DOC value of 11.22 ppm in well LH-25 and the highest value of 90.05 ppm in LH-15. The mean DOC value was calculated to be 31.91 ppm with a standard deviation of 19.09 ppm. The relatively low DOC values indicate that the aquifer needs to be amended with organic carbon and nutrients to boost the activity of sulfate-reducing bacteria during biostimulation.

Fluorine, which usually occurs as fluoride (F^-) in natural groundwaters, was measured. In all but 4 wells, LH-7, RA-10, RA-11, and RA-12, fluoride concentrations were below detection limits. The main sources for fluoride in groundwater are the minerals fluorite and apatite. None of these minerals are present in aquifer materials, so expected results for fluoride should be low.

Sodium (Na) is another major constituent of groundwater and typically occurs as the ion Na^+. Sodium concentrations ranged from 26.30 ppm in RA-2 and 2.12 ppm in RA-14. The mean sodium concentration was calculated to be 9.25 ppm with a standard deviation of 8.10 ppm.

Magnesium (Mg) occurs in groundwater as the ion Mg^{2+} and is considered another major constituent of groundwater. From the water samples collected during the January 2015 sampling event Mg^{2+} concentrations ranged from 4.67 ppm in well RA-5 and 0.29 ppm in well LH-15. The mean Mg^{2+} concentration was 1.99 ppm with a standard deviation of 1.26 ppm.

Phosphate (PO_4) concentrations in the Lynn Haven Surficial Aquifer occurred at very low concentrations. In all but 2 wells (LH-15 and LH-16), phosphate levels were below the detection limit (0.01 ppm). The relatively low values for this aquifer are expected, since there are no surficial sources of excess nitrate in the area (fertilizers).

Sulfide (S^{2-}) concentrations measured range from 0.01 ppm in several wells to 0.43 ppm in well LH-16. The calculated mean for sulfur concentrations was 0.10 ppm and the standard deviation was 0.12 ppm. High sulfide concentrations in certain locations may be resulting from bacterial sulfate reduction, as indicated by its typical rotten egg smell.

Sulfate (SO_4^{2-}) is a major ion found in surface water, seawater, and groundwater. At the Lynn Haven site, SO_4^{2-} concentrations ranged from below detection (<0.03 ppm) in well LH-2 and LH-19 to 33.7 ppm in well RA-12. The mean sulfate concentration was 8.12 ppm and the standard deviation was 6.98 ppm.

Chlorine is commonly found in water as the ion chloride (Cl^-). The chloride concentration of the Lynn Haven Surficial Aquifer ranged from below detection (<0.03 ppm) in well LH-2 to 50.60 ppm in well RA-12. The mean concentration was 12.74 ppm with a standard deviation of 12.22 ppm.

Potassium found in water exists as the ion K^+. Results from the January 2015 groundwater sampling showed that potassium concentrations ranged from 0.08 ppm in well RA-

13 and 2.21 ppm in well LH-12. The mean concentration of potassium in groundwater samples was 0.74 ppm with a standard deviation of 0.58 ppm.

Calcium occurs in water as the ion Ca^{2+}. The concentration of calcium in the Lynn Haven industrial site samples ranged from 50.00 ppm in well RA-10 and 1.00 ppm in LH-19. The mean concentration was calculated to be 16.48 ppm and the standard deviation was 12.73 ppm.

Iron exists in water as either ferrous (Fe^{2+}) or ferric iron (Fe^{3+}). The iron concentration measured by ICP-MS presented in Table 2 is the total iron concentration including both ferric and ferrous oxidation states. The total iron concentration ranged from 0.05 ppm in well RA-14 and 4.40 ppm in well RA-2. Field measurements of ferrous iron (Fe^{2+}) ranged from 0.08 to 2.74 ppm. The similar range of total iron and ferrous iron suggests that ferrous iron is the dominant iron species at the field site under moderately reducing conditions. The mean concentration of total iron was 0.84 ppm and the standard deviation was 1.04 ppm

The dissolved arsenic concentrations in the surficial aquifer ranged from 0.0002 ppm in well LH-25 and 0.577 ppm in well RA-5. The mean concentration of arsenic was calculated to be 0.15 ppm and the standard deviation was calculated to be 0.22 ppm. The average arsenic concentration is higher than that of EPA drinking water standards (0.01 ppm). When arsenic concentrations are mapped using the collected data from the January 2015 sampling event a residual plume can be seen at the site (Figure 15). The zone of highest concentration occurs in a hot zone between wells RA-4, RA-5, and LH-5 and has a highest concentration of approximately

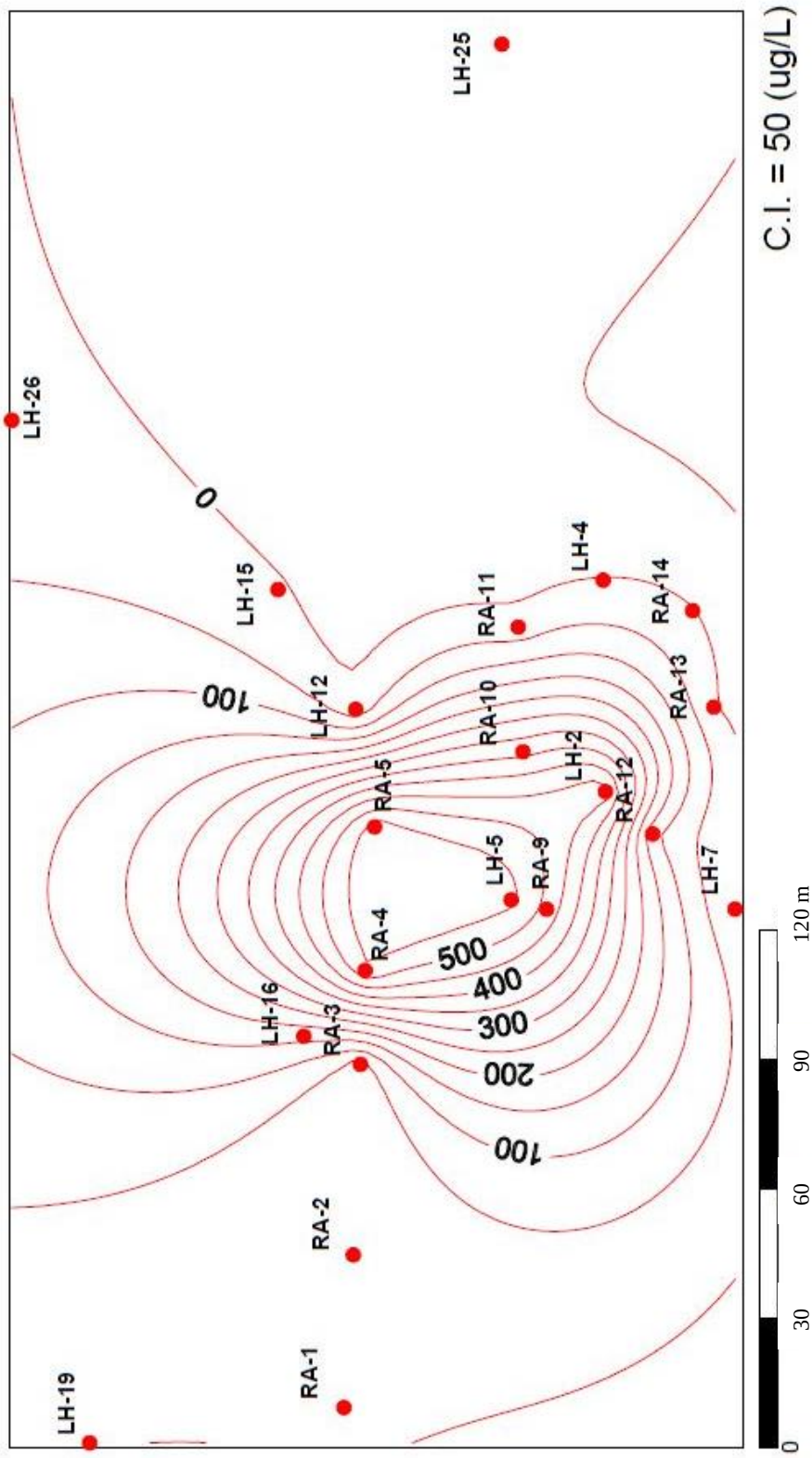

Figure 15. A contour map of arsenic distribution at the Lynn Haven industrial site.

0.550 ppm. Historically, the highest arsenic concentration reached about 4.50 ppm before pump-and-treat remediation (Mintz and Miller, 1993). Results of ICP-MS analysis show that arsenic concentrations of biogenic pyrite at the Macon County site reach approximately 3670 ppm As.

Another major constituent of groundwater is the bromide ion (Br^-). The concentration of bromide in the Lynn Haven wells ranged from below detection (<0.03 ppm) in several wells and 0.23 ppm in well LH-12 and LH-19. The mean bromide concentration was 0.14 ppm and the standard deviation was 0.06 ppm.

The last parameter measured in the Table 2 is that of TDS (total dissolved solids). This value correlates well with conductivity in Table 1. The well with the highest TDS should also have the highest conductivity. TDS in the surficial aquifer groundwater samples ranged from 37.35 ppm in well LH-26 and 187.04 ppm in well RA-12. The mean TDS was calculated to be 81.24 ppm with a standard deviation of 35.65 ppm.

Groundwater Mixing and Water-Rock Interaction

Plots of major ion (Na^+, Ca^{2+}, Mg^{2+}, K^+, SO_4^{2-}) concentrations against chloride concentrations (Figures 16 to 20) relative to the conservative seawater dilution trend, reveal that different water-rock processes (e.g., precipitation, dissolution, and ion exchange) occur to varying extent as well as potential mixing of deep carbonate groundwater (Drever, 1997).

Figure 16 shows the sodium concentration versus the chloride concentration with the conservative mixing line. Most data taken from the well samples falls on or close to the mixing line, suggesting conservative mixing of seawater with freshwater in the surficial aquifer. Points plotted above or below the conservative mixing line may be explained by Na exchange or fixation on clays. Clay-rich Jackson Bluff Formation is present underneath the surficial aquifer.

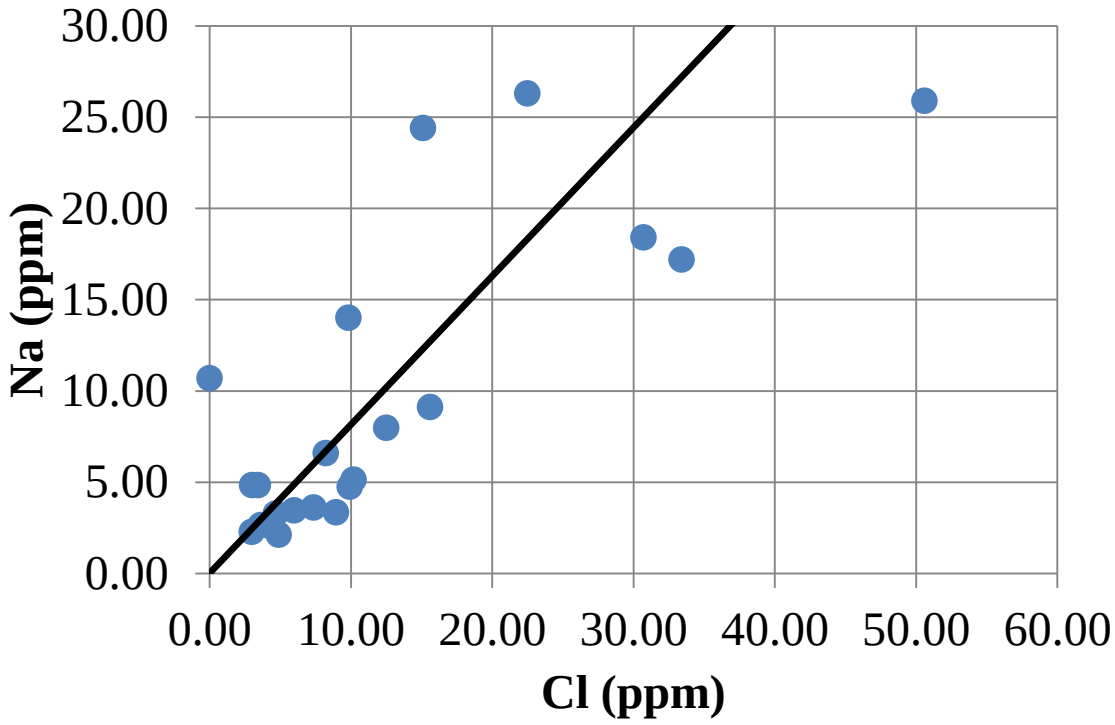

Figure 16. Sodium concentration versus chloride concentration of the surficial aquifer. The bold line represents the conservative mixing of seawater with freshwater.

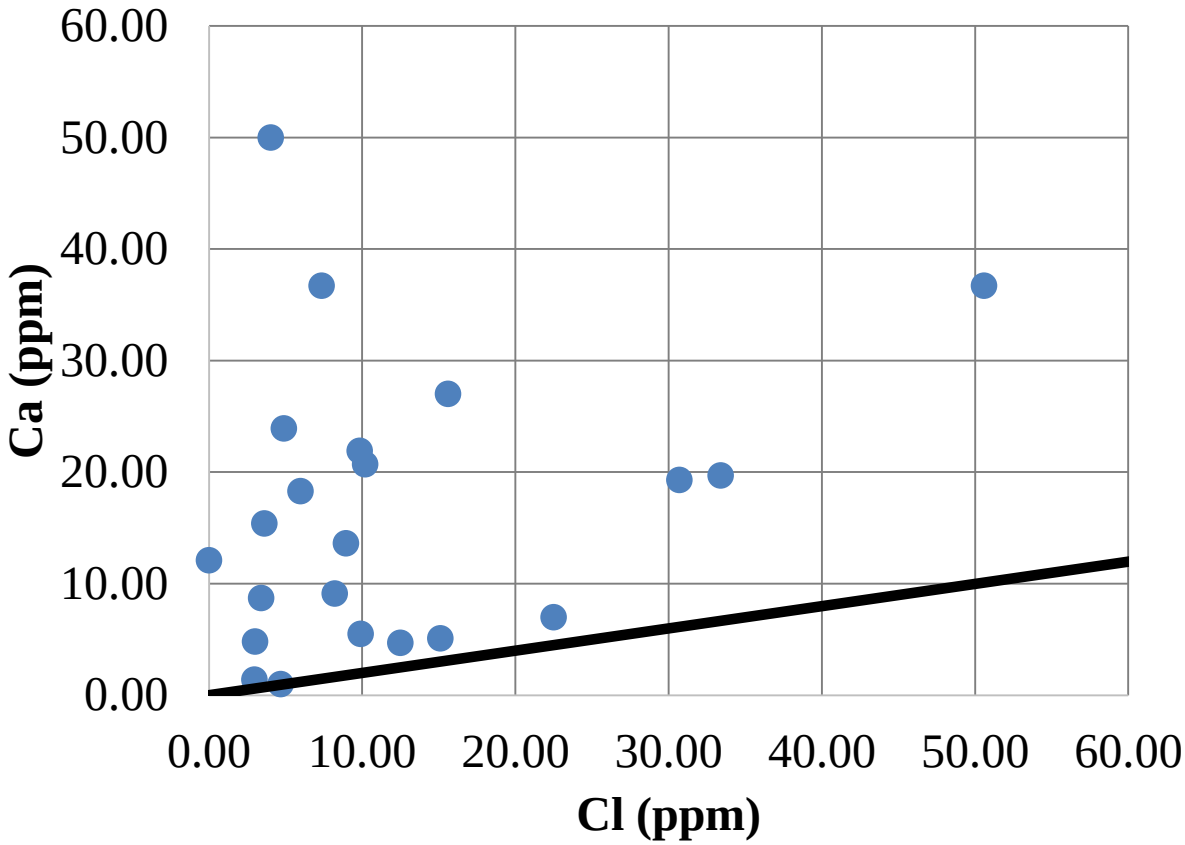

Figure 17. Calcium concentration versus chloride concentration of the surficial aquifer. The bold line represents the conservative mixing of seawater with freshwater.

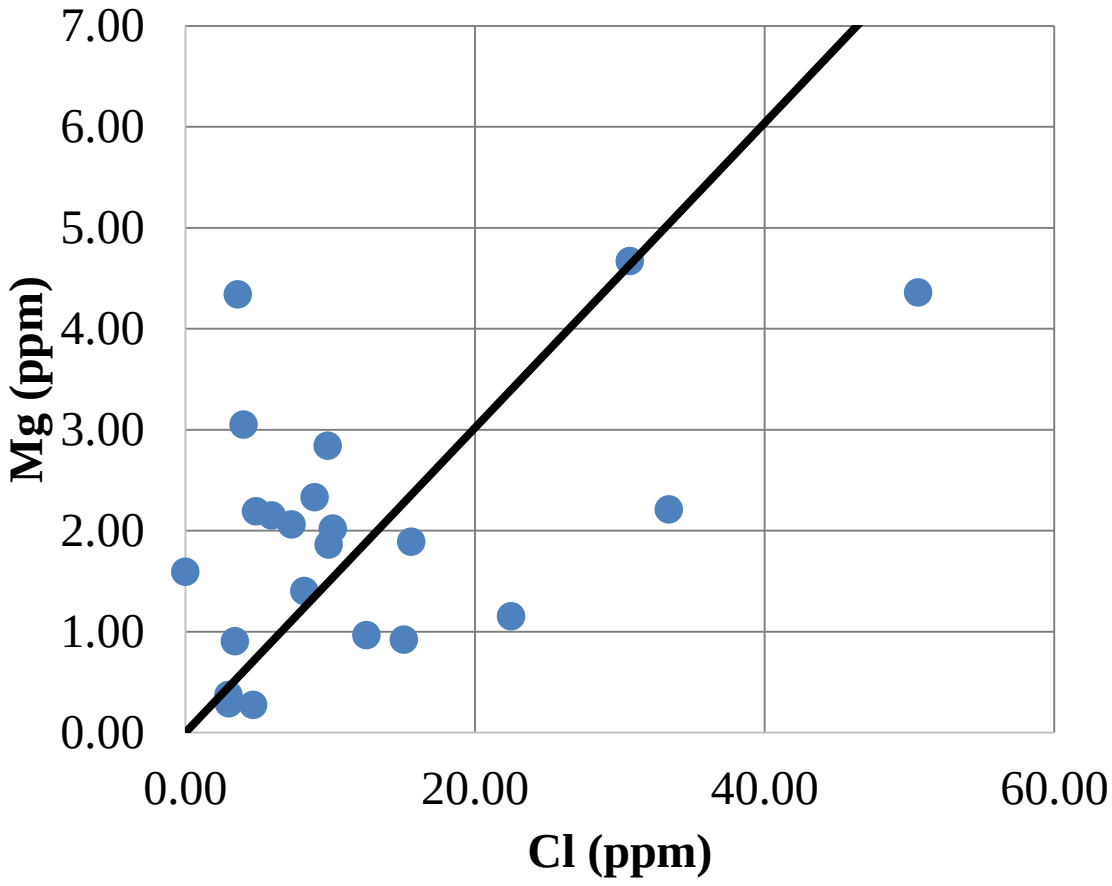

Figure 18. Magnesium concentration versus chloride concentration of the surficial aquifer. The bold line represents the conservative mixing of seawater with freshwater.

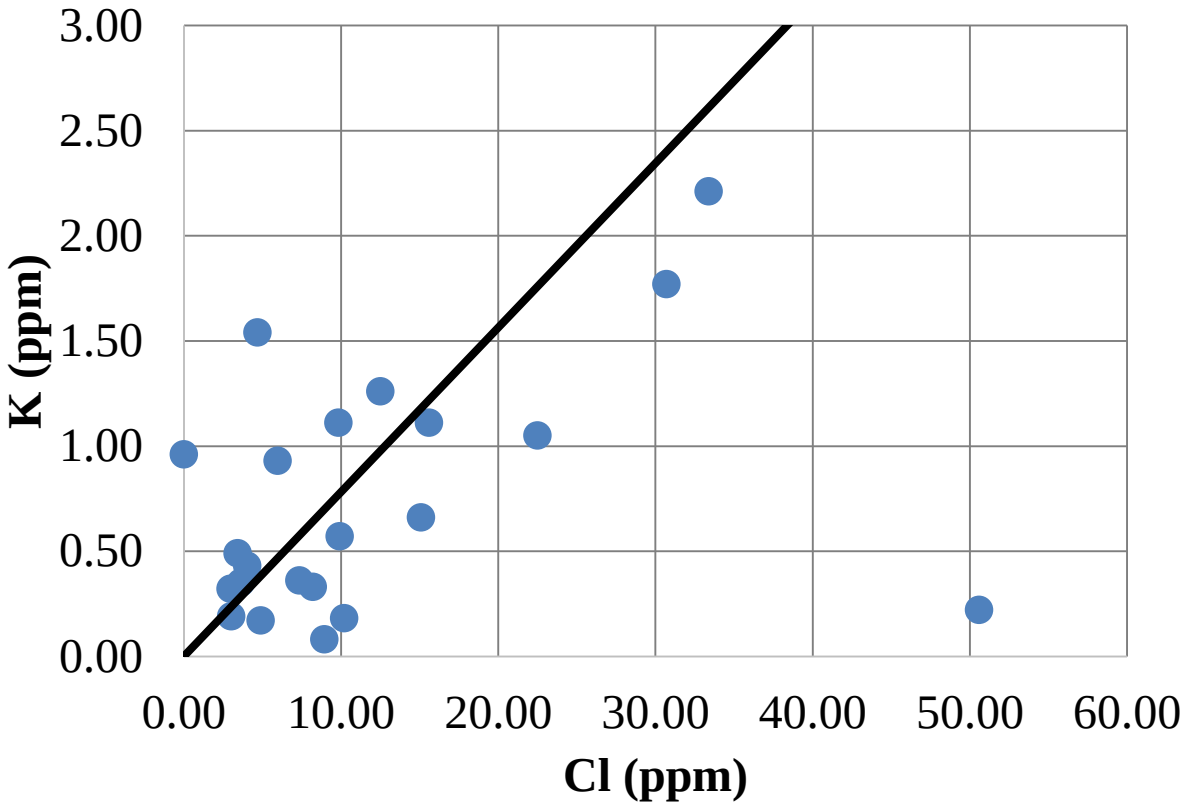

Figure 19. Potassium concentration versus chloride concentration of the surficial aquifer. The bold line represents the conservative mixing of seawater with freshwater.

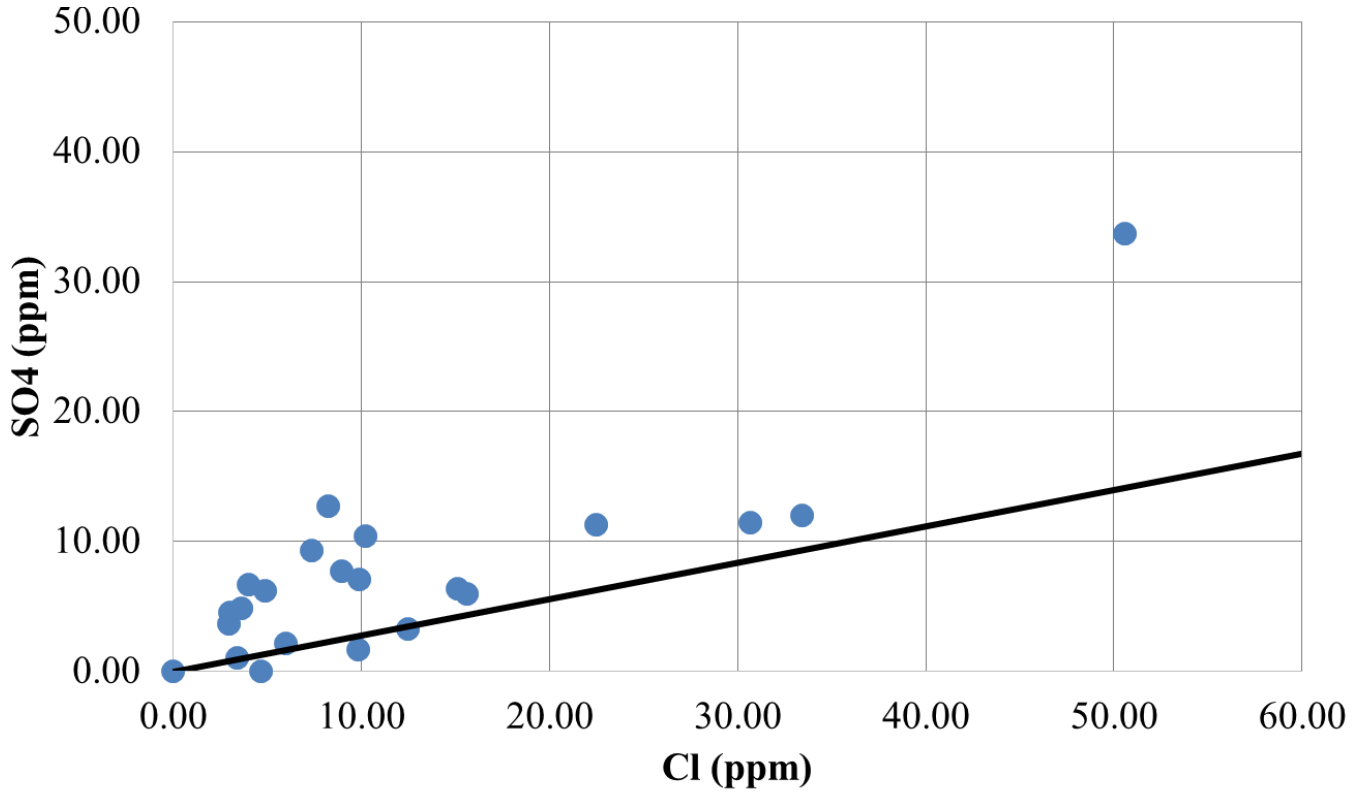

Figure 20. Sulfate concentration versus the chloride concentration of the surficial aquifer. The bold line represents the conservative mixing of seawater with freshwater.

For example, cation exchange reaction of the following equation would produce a $NaHCO_3$ type water with high Na contents (Appelo, 1994: Penny et al., 2003):

$$CaCO_3 + Na_2\text{-clay} + H^+ \rightarrow Ca\text{-clay} + 2\ Na^+ + HCO_3^-$$

Furthermore, ion exchange between Na and a divalent cation such as Ca may be expressed as the following reaction (Drever, 1997):

$$Ca\text{-clay} + Na^+ \Leftrightarrow 2\ Na\text{-Clay} + Ca^{2+}$$

When the aquifer is invaded by saline seawater, the resulting salinization may cause monovalent ions (Na) in groundwater to replace divalent ions (Ca) from the clay. Groundwater affected by saltwater intrusion and subsequent ion exchange thus tends to be depleted in Na^+ with lower Na/Cl molar ratios (Drever, 1997). At the study site, groundwater with higher salinity tends to be slightly depleted in Na^+ (Figure 16).

Figures 17 and 18 plot calcium and magnesium concentration versus chloride concentration of the sampled wells along with the conservative mixing line for seawater and freshwater. The results indicate that there are strong enrichments of both calcium and magnesium in the surficial aquifer. This may be attributed to carbonate stratigraphic units (Bruce Creek Limestone) below the surficial aquifer where the Jackson Bluff confining bed is not present (Schmidt and Clark, 1980). The Jackson Bluff confining unit is locally absent in the eastern part of Bay County (Figure 5), leading to possible sites of calcium enrichment. The enrichments of Ca and Mg may be also attributed to ion exchange processes (see equation above) when the aquifer is diluted by freshwater (Drever, 1997). The dolomitization process, represented by the following reaction:

$$2CaCO_3 + Mg^{2+} \Leftrightarrow MgCa(CO_3)_2 + Ca^{2+}$$

would release Ca but consume Mg in the solution. Thus, dolomitization or de-dolomitization is not likely to cause the simultaneous enrichments of Ca and Mg in solution (Drever, 1997).

Figure 19 show the concentrations of potassium versus chloride concentration. The result also suggests a slight enrichment of potassium. External sources for potassium may be from seawater or saline formation water from the Jackson Bluff confining unit since it is in direct contact with the surficial aquifer (Schmidt and Clark, 1980).

Figure 20 shows the concentrations of sulfate versus chloride relatively to conservative mixing line. Most of the data plots slightly above or along the mixing line. This suggests a slight enrichment of sulfate relative to seawater dilution trend. The result implies that local sulfate reduction has not removed all available sulfate in the aquifer.

Iron and Arsenic Speciation

As stated earlier, the dominant iron species at the Lynn Haven industrial site is ferrous iron (Fe^{2+}). Field measurement of ferrous iron was plotted against the lab measurements of total iron (Figure 21). The plot shows an approximately 1:1 ratio of ferrous and total iron concentration, suggesting that the ferrous iron is the dominant species. However, there were some instances where the ferrous measurements exceeded the total iron measurements. This may be caused by different instrumental methods used in field and laboratory measurements. For arsenic speciation, geochemical modeling results conducted in this study (Figure 22) indicate that arsenite [As(III)] should be the dominated species in the groundwater at the site under moderately reducing conditions. Laboratory measurements of various arsenic species are

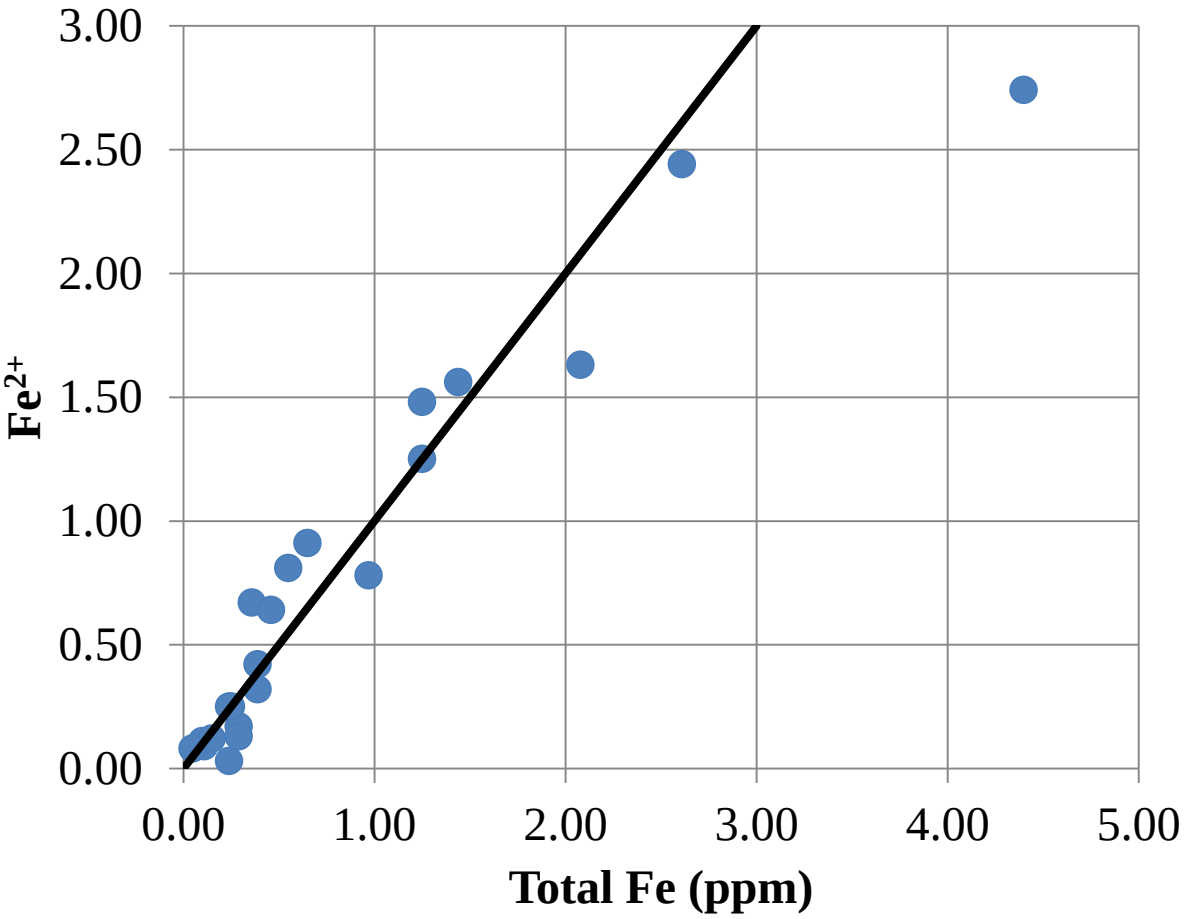

Figure 21. Plot of Ferrous iron concentration versus the total iron concentration of the surficial aquifer. The bold line represents a 1:1 ratio of the two concentrations.

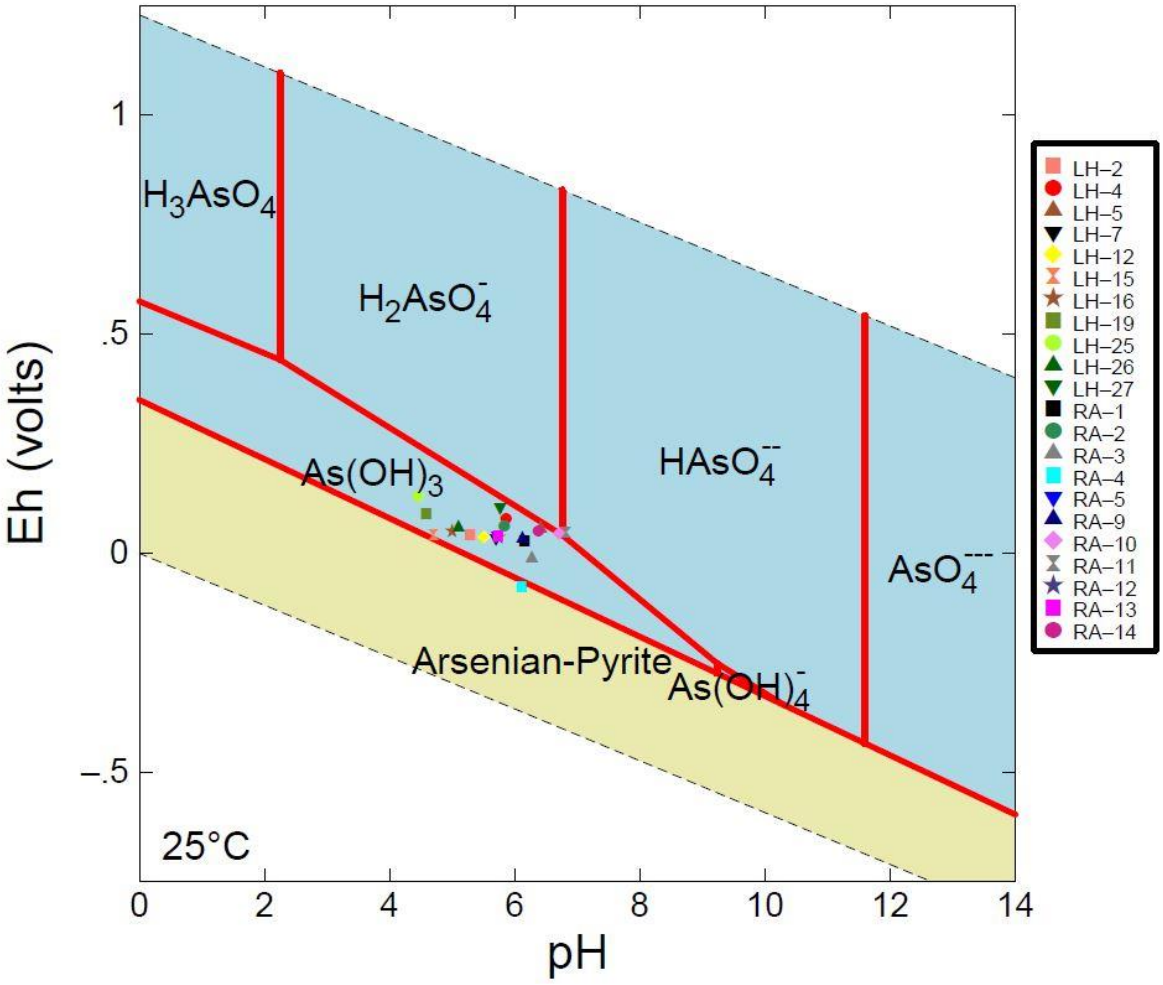

Figure 22. An Eh-pH diagram for the predicted dominant As phases at the Lynn Haven site (blue fields are aqueous phases and tan fields are solid phases). Plotted on the diagram are the redox conditions for each water sample collected.

underway using new ICP-MS facilities at Auburn. The results will be addressed in another study.

XRF and XRD Analysis Results

Selected sediment samples also underwent XRD and XRF analyses (Figures 23 to 30). XRF analyses were used to identify the chemical composition of sediment slurry deposited inside the well casing before remediation. XRF analyses of representative samples consistently resulted in major peaks for Fe, S, and As (Figures 23-27). The spectra were created using the voltage and current settings of 40 KeV and 18 μA (filter #1) without vacuum. This suggests that minor precipitation of pyrite is already taking place in the zones of sulfate reduction. Results of Larger peaks correspond to larger concentrations, but XRF results should only be taken qualitatively. Quantitative ICP-MS analysis shows that arsenic concentrations of biogenic pyrite at the Macon County site reach approximately 3670 ppm As.

Dark sediment slurry samples collected from well RA-5 tested positive for the presence of elements Fe, S, and As. The presence of these elements supports the idea the arsenic bearing pyrite is already be formed locally under reducing conditions. Wells LH-12, LH-19, and LH-26 not only showed positive results for Fe, S, and As, but also showed elevated concentrations of other trace metals that will not be addressed in this study. Interestingly, well LH-25 samples showed a stronger signature for Zn than Fe (Figure 26); this may suggest that sphalerite may also be precipitating if enough zinc is present.

XRD analyses were carried out to show what minerals are present in a given sample. This was done to compliment XRF results and compare dominant minerals to dominant elements to make sure that there is some degree of accordance.

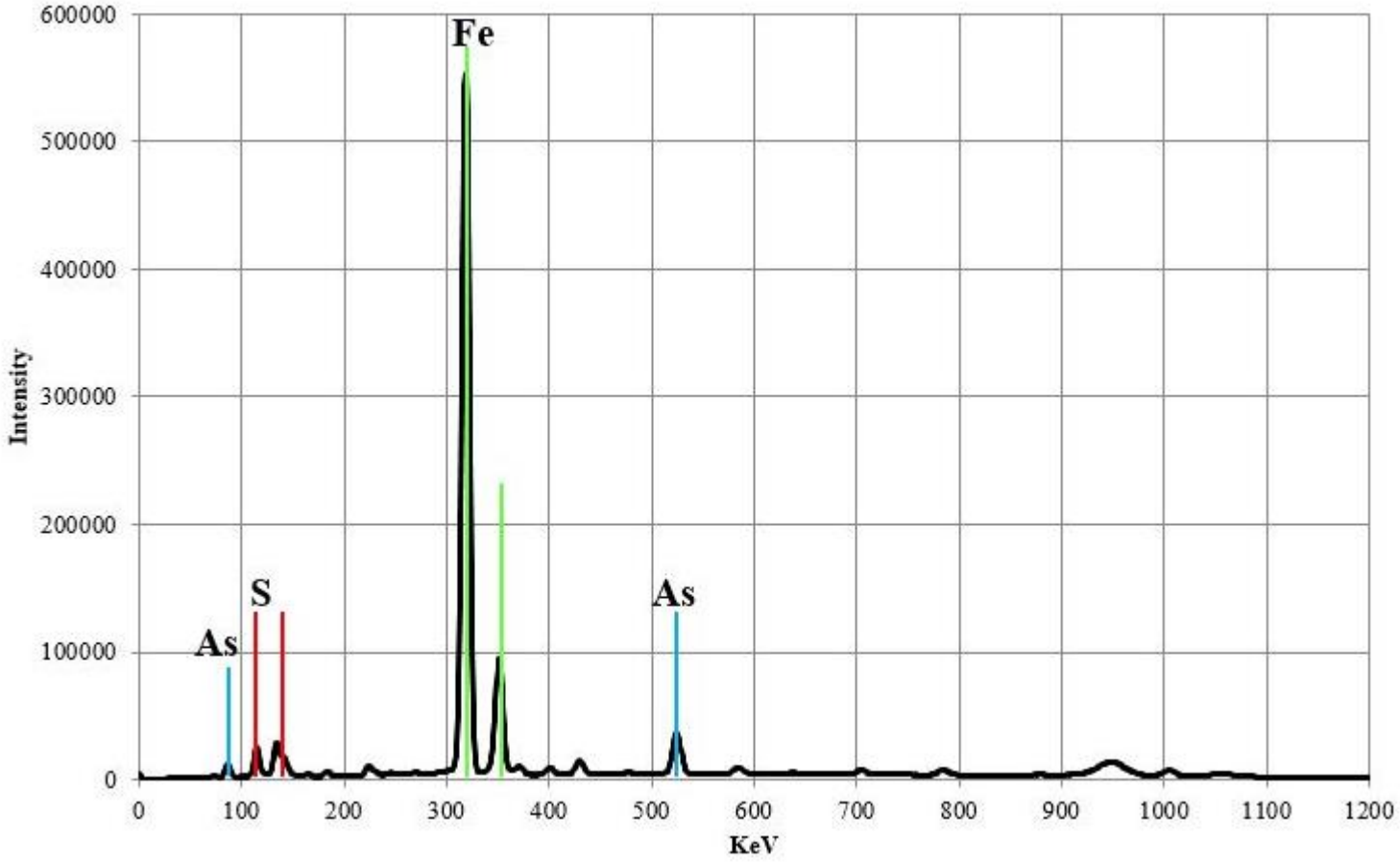

Figure 23. XRF spectra of elements present in the sediment sample of well RA-5. The colored lines represent the peak locations for the labeled elements.

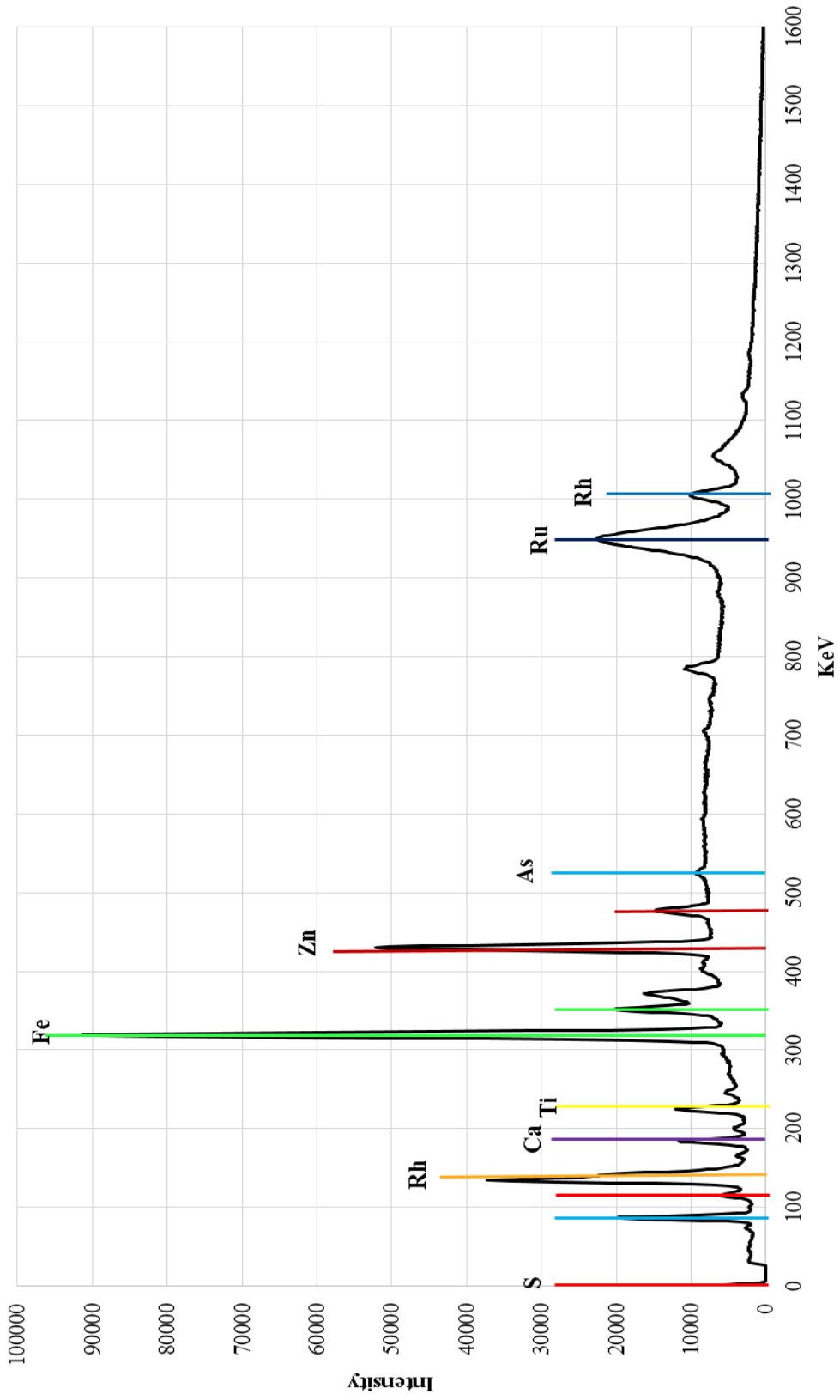

Figure 24. XRF spectra of elements present in the sediment sample of well LH-12. The colored lines represent the peak locations for the labeled elements.

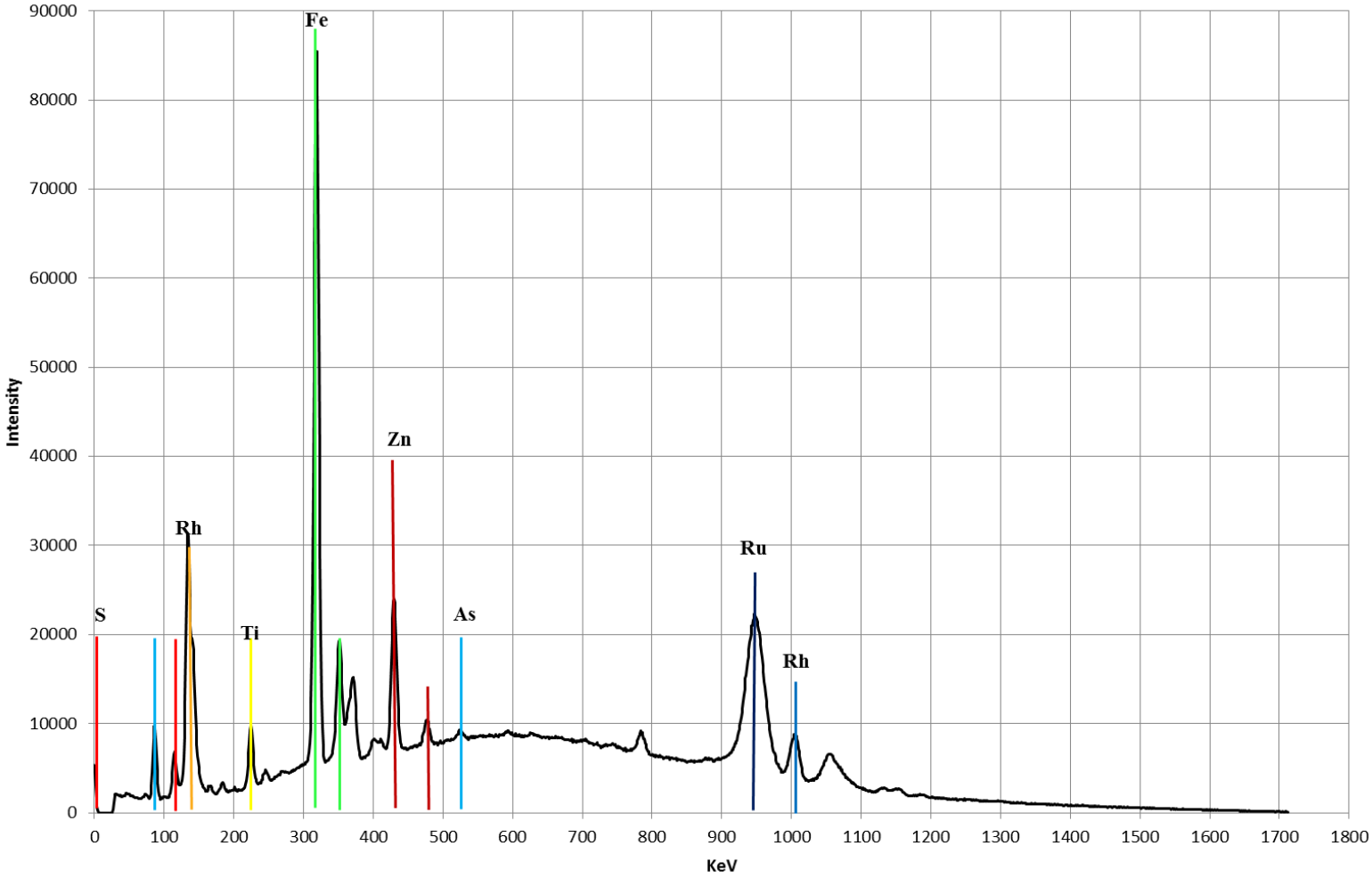

Figure 25. XRF spectra of elements present in the sediment sample of well LH-19. The colored lines represent the peak locations for the labeled elements.

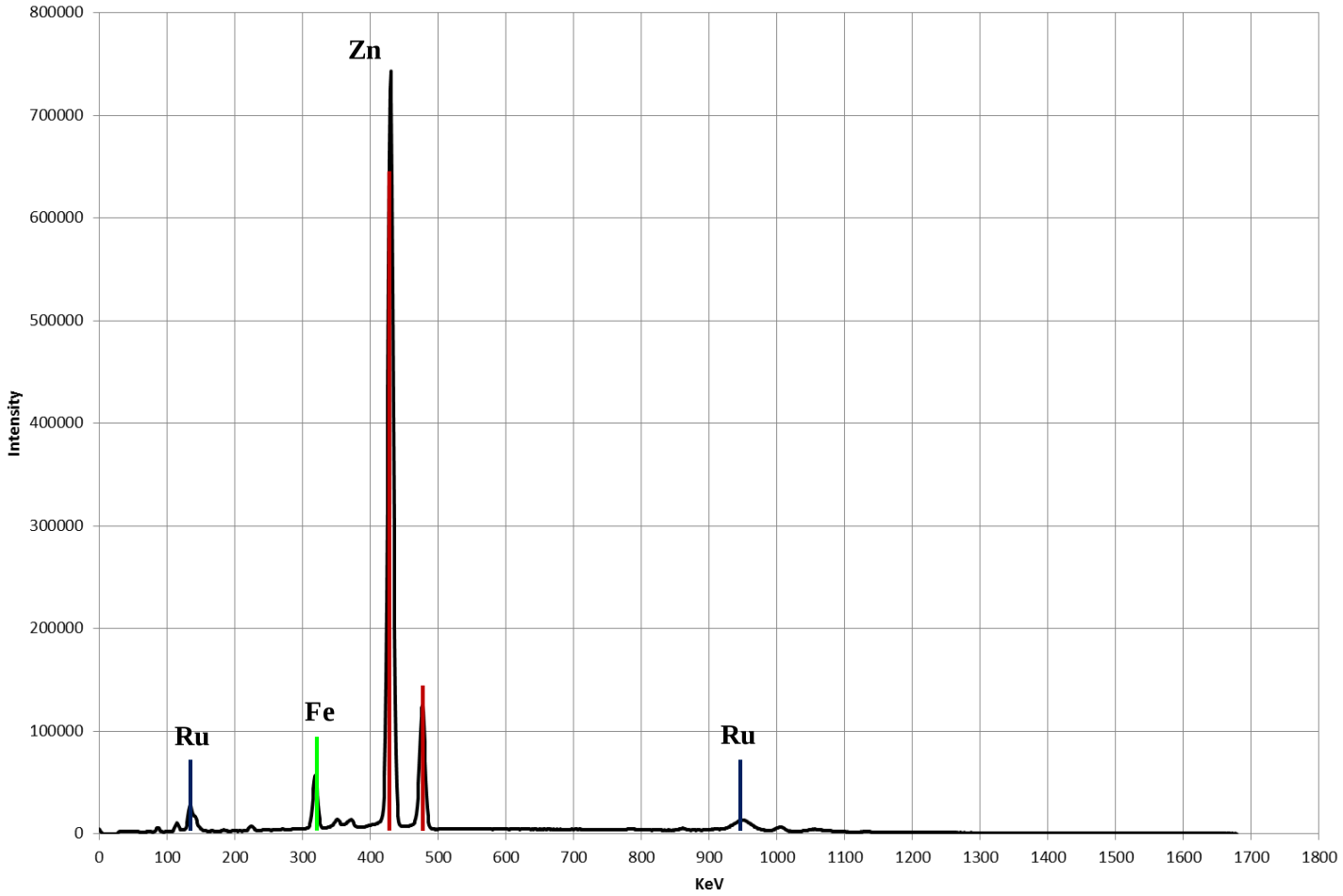

Figure 26. XRF spectra of elements present in the sediment sample of well LH-25. The colored lines represent the peak locations for the labeled elements.

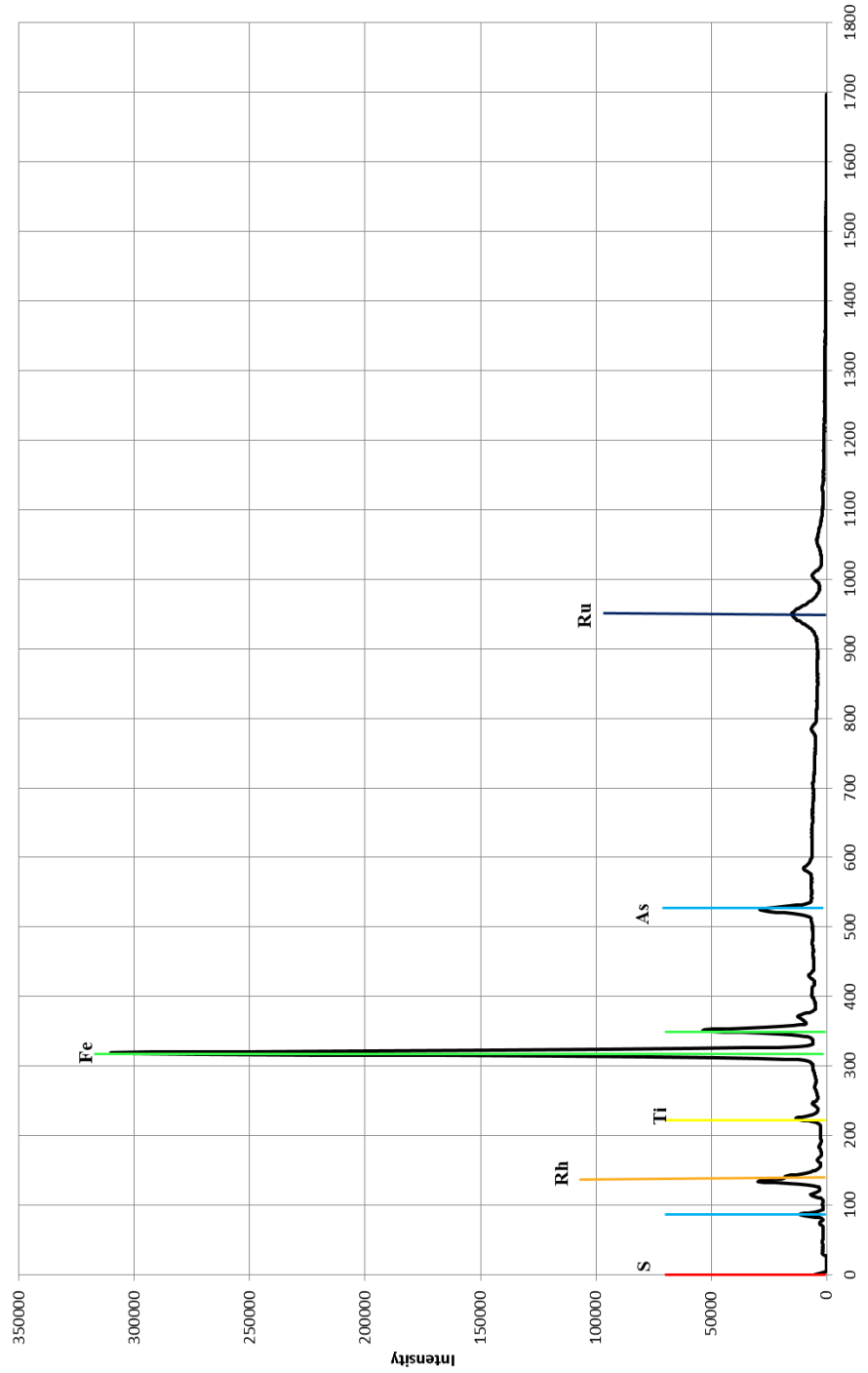

Figure 27. XRF spectra of elements present is the sediment sample of well LH-26. The colored lines represent the peak locations for the labeled elements.

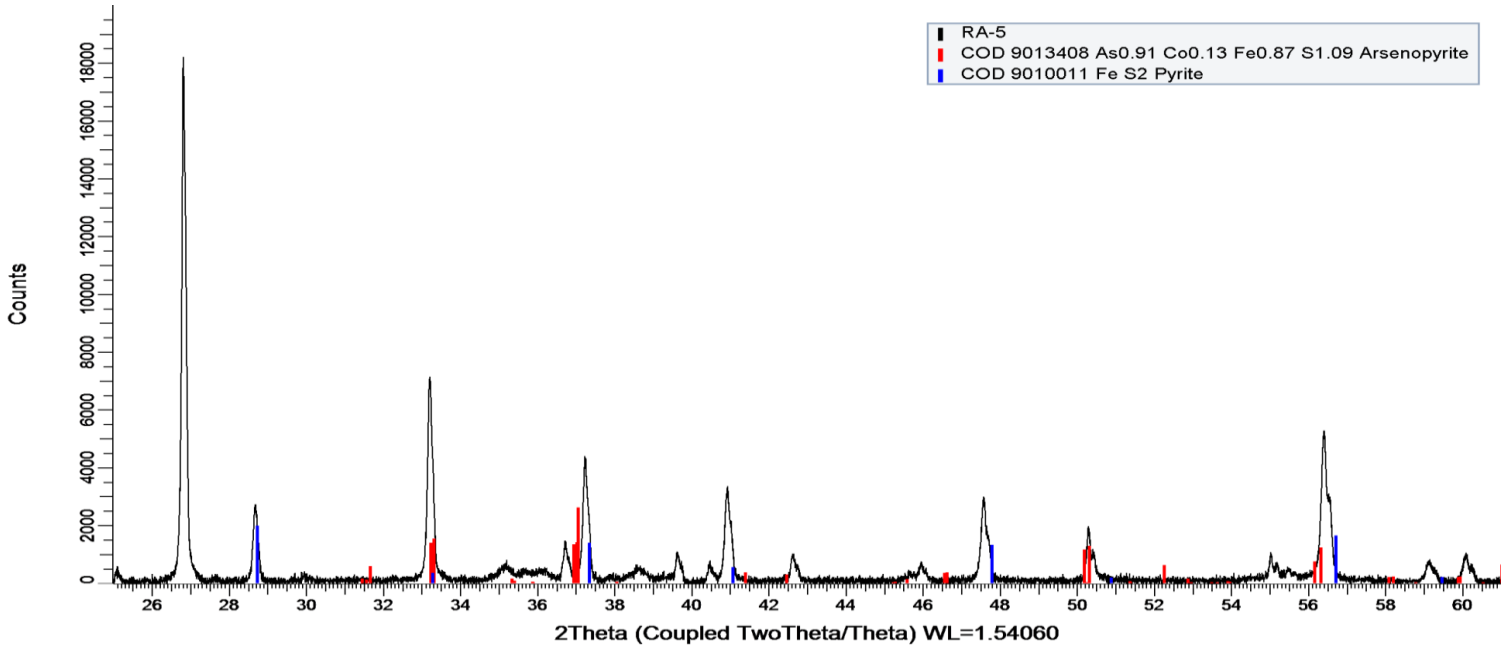

Figure 28. An XRD scan of sediment from well RA-5; Peak lines in blue and red show possible mineral samples. The largest peak of the scan occurring at 26.6 2theta corresponds to quartz that remained in the powdered sediment.

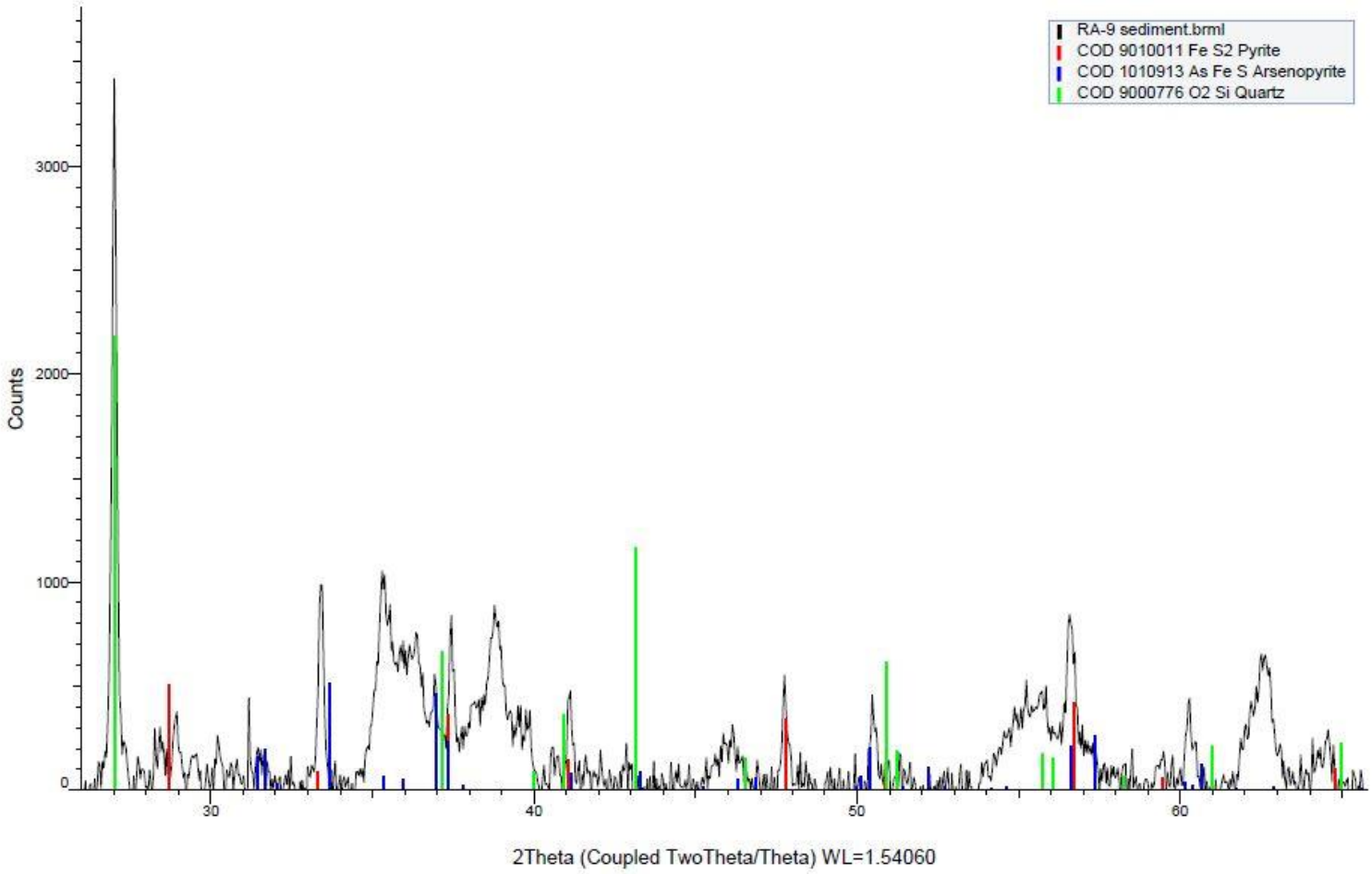

Figure 29. An XRD scan of sediment from well RA-9; Peak lines in blue and red show possible mineral samples The largest peak of the scan occurring at 26.6 2theta corresponds to quartz that remained in the powdered sediment. Geen peaks correspond to quartz, red corresponds to pyrite, and blue corresponds to arsenopyrite.

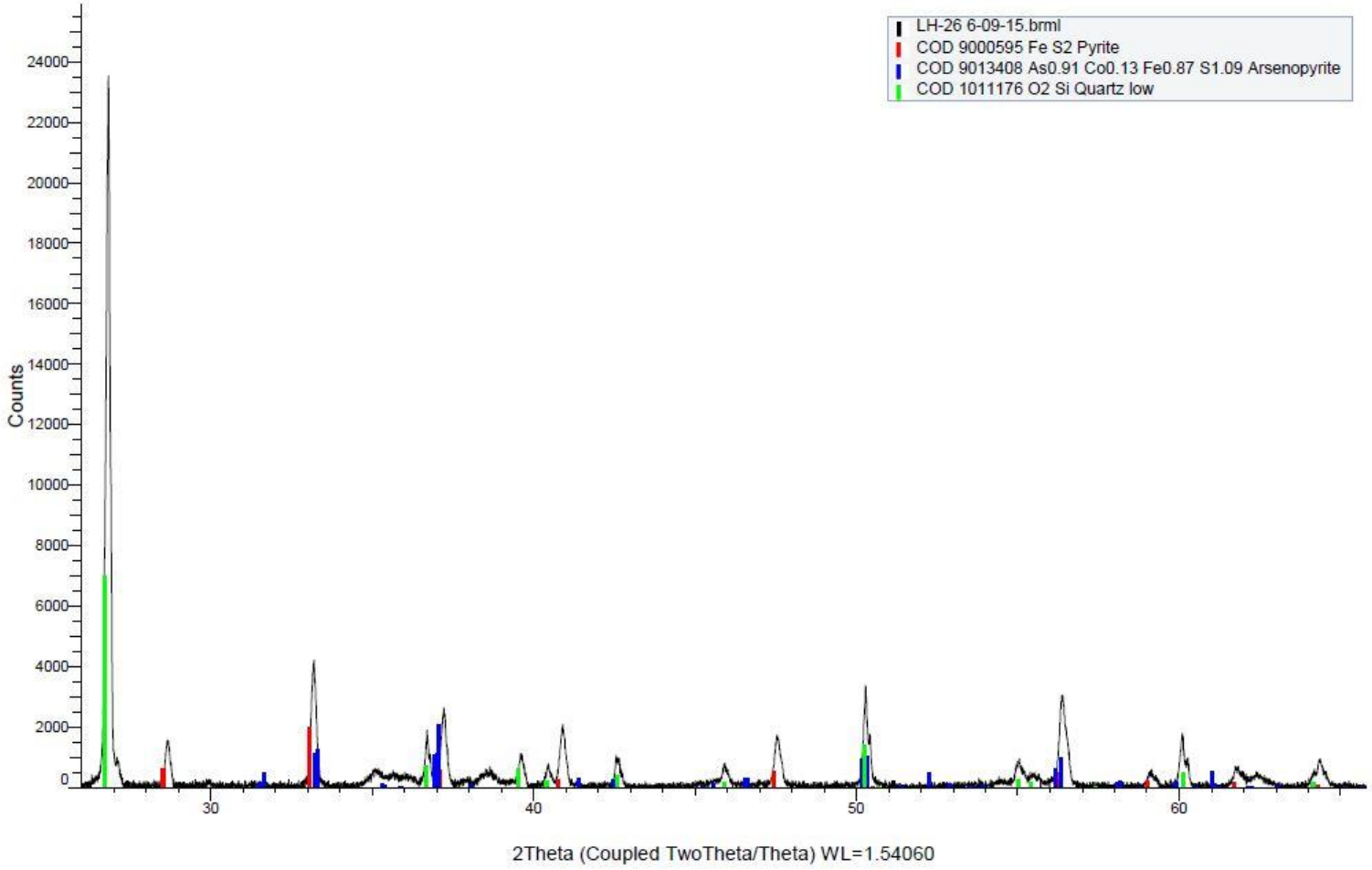

Figure 30. An XRD scan of sediment from well LH-26; Peak lines in blue and red show possible mineral samples. The largest peak of the scan occurring at 26.6 2theta corresponds to quartz that remained in the powdered sediment.

All the sediment samples that underwent XRD analyses showed signatures for the minerals quartz, pyrite, or arsenopyrite (Figures 28-30). Not all wells underwent XRD analyses due to limitations on the amount of sediments collected for each well. The presence of these minerals also supports the idea that current precipitation of arsenic bearing pyrite is taking place. Quartz is common since it represents the main aquifer mineral. Increased flux of organic matter and nutrients amended during proposed biostimulation may fuel bacterial sulfate reduction and formation of sulfide solids at shallower depths than the sediments that were collected.

Geochemical Modeling – Hydrochemical Facies and Speciation

Geochemical modeling was carried out using the computer program Geochemist's Workbench. Results of our field and laboratory analyses of water samples were used to constrain the site geochemistry. Major ion compositions of groundwater samples collected from the January 2015 sampling event were plotted in a piper diagram (Figure 31) to characterize the hydrochemical facies of groundwater in the surficial aquifer. This type of diagram allows for anion and cation compositions of many water analyses to be plotted on a single graph showing possible mixing or water-rock interaction trends (Freeze and Cherry, 1979; Nesbitt, 1980; Stueber, 1993).

Figure 31 shows that the samples fell in a wide range of hydrochemical facies. Samples (8) that plot near the far left portion of the graph represent groundwater enriched in Ca and bicarbonate. The far right side of the piper diagram represents waters that have similar compositions to seawater. A significant number of samples (14) fall within the middle portion of the graph that represents meteoric mixing composition. It is important to note that, although the site is close to the coast, none of the Lynn Haven aquifer samples plotted near seawater

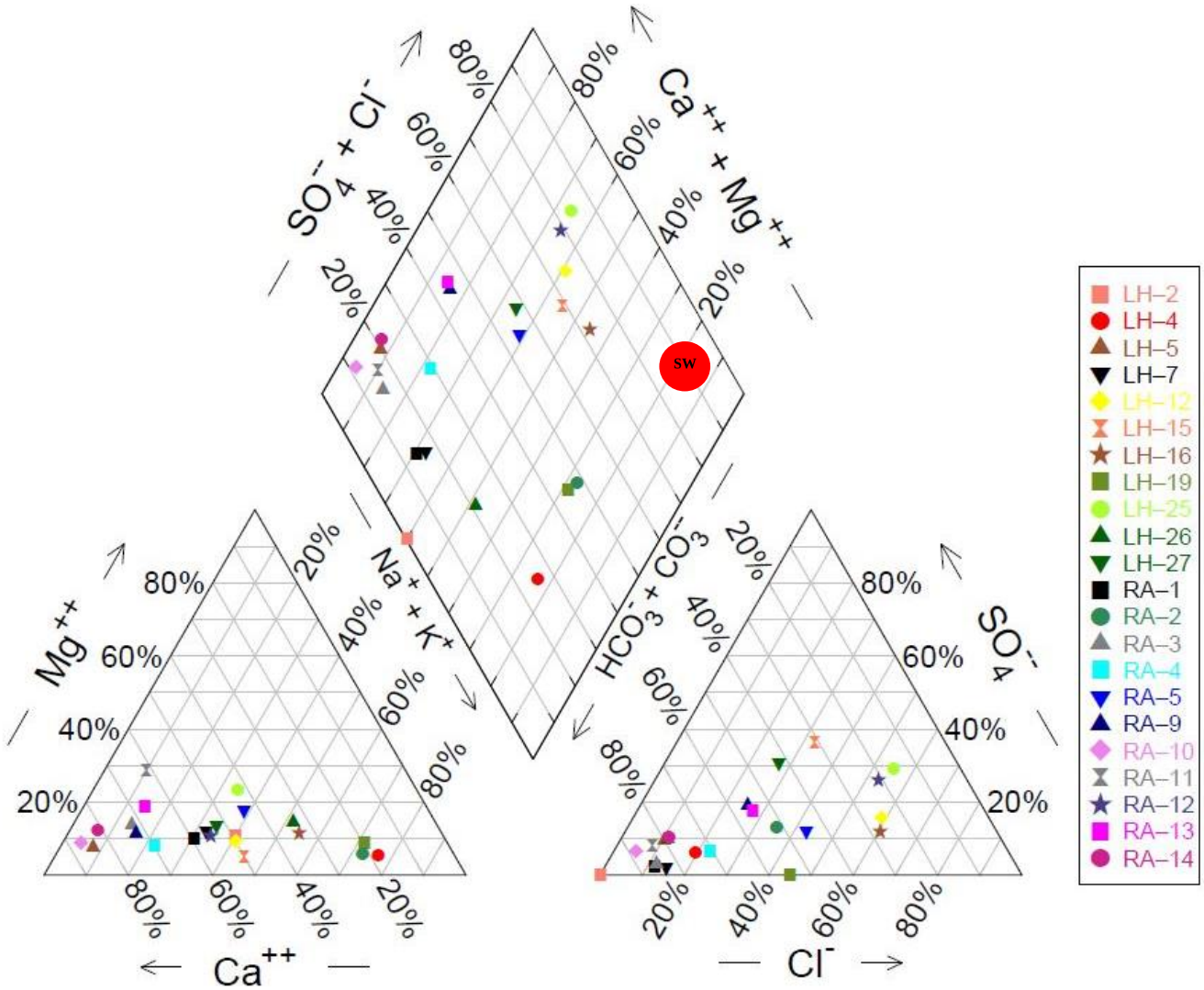

Figure 31. A Piper diagram with all water samples taken from the Lynn Haven industrial site showing major ion concentrations in percent.

composition. Based on Figure 31 the most dominant cations of the groundwater samples were Ca^{2+} and Na^{+}. The most dominant anions were HCO_3^{-} and Cl^{-}. The main hydrochemical facies in the aquifer can thus be characterized as a Ca-HCO_3-Na-Cl type.

Activity diagrams were generated to characterize the speciation and stability fields of various aqueous and solid phases of iron, arsenic, and sulfur in the aquifer under different pH-Eh conditions.

All samples showed a similar trend for moderately reducing conditions in the surficial aquifer (Figures 22 and 32). The Eh values cluster between 0 to 0.25 volts and pH between 5 and 7. This data is consistent with previous groundwater studies conducted at the site (Saunders, 2005). The field Eh-pH diagram of 22 samples indicate that As(III) (i.e., H_3AsO_3) is the dominant arsenic species at the field site under moderately reducing conditions. Figure 22 shows that by forcing a drop in the redox potential (Eh) of the groundwater would result in the sequestration of arsenic into a solid phase of arsenian pyrite (as a solid solution $FeS_{1.99}As_{0.01}$) under sulfate reducing conditions (Saunders et al., 2008). This will be a key process to lower the dissolved arsenic concentrations of this site.

Figure 32 shows the groundwater Fe speciation at the Lynn Haven industrial site. Similar to Figure 22, all samples clustered from an Eh of 0 to 0.25 volts and a pH of 5 to 7. This also provided evidence that the surficial aquifer is in a moderately reducing environment with near neutral pH. The modeling results show that the dominant Fe species is ferrous iron (Fe^{2+}), this result is consistent with measurements of ferrous vs. total iron concentrations (Figure 21). The modeling results also show that reduced ferrous iron may react with bicarbonate in the aquifer to form iron carbonate (siderite). Figure 32 also shows that by forcing a drop in the redox potential

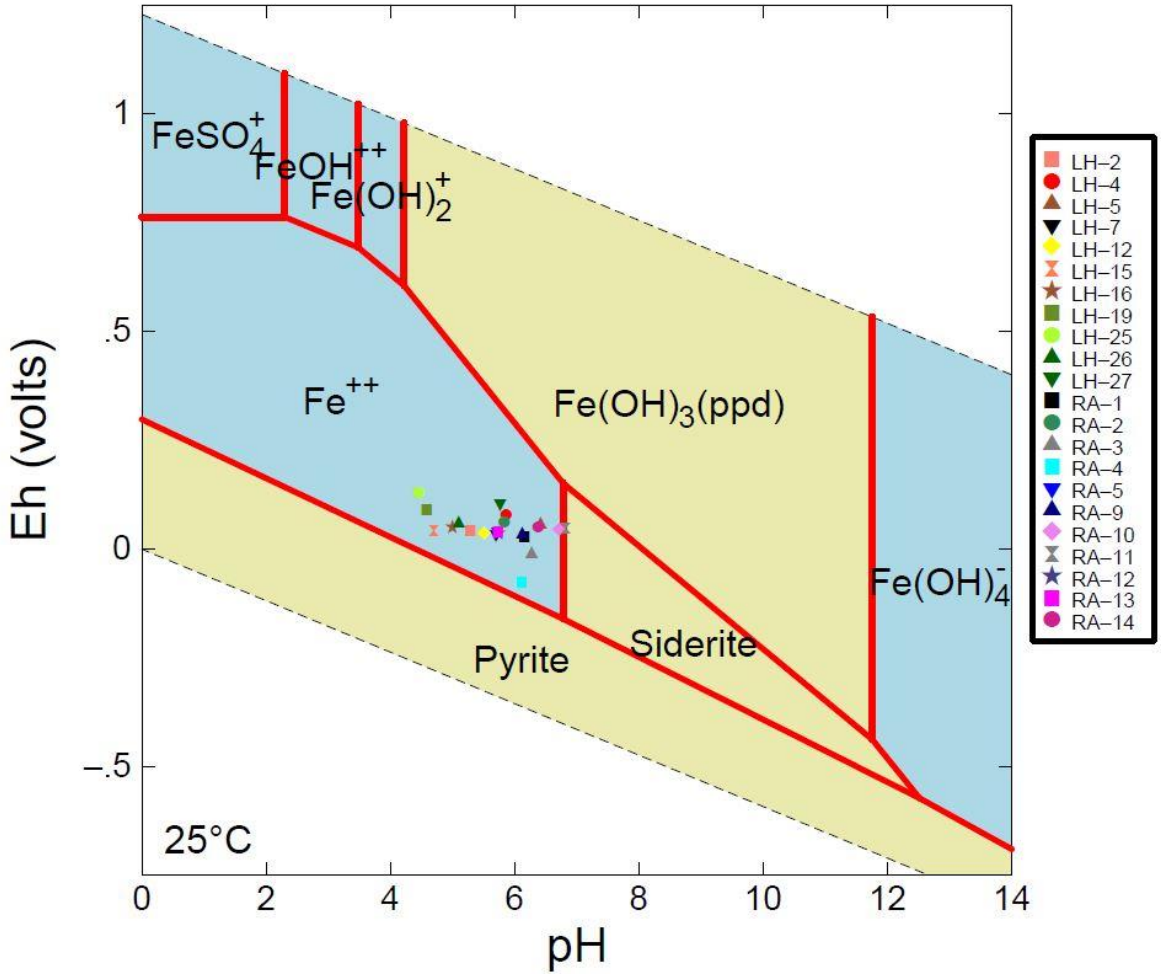

Figure 32. An Eh-pH diagram showing stable Fe species under various redox conditions (blue fields are aqueous phase and tan fields are solid phases). Plotted on the diagram are the redox conditions for each water sample collected.

(Eh) of the groundwater would result in the sequestration of iron, along with arsenic into a solid phase of pyrite.

Geochemical Modeling – Reaction Path Model

The subprogram React within the Geochemist's Workbench software was used to trace the sequence of mineralogical reactions associated with the proposed bio-stimulated bacterial sulfate reduction. React can be used to calculate the equilibrium distribution of different aqueous species in a fluid, saturation states with respect to minerals, and fugacity of dissolved gases (Bethke, 2008). The program traces the geochemical evolution of a system (including both fluids and mineral phases) as it undergoes a reaction path in which the initial system is open to mass transfer at a given temperature.

The React model has two components: the initial geochemical system and the processes of mass transfer and Eh-pH changes that alter it. React will first determine the system's equilibrium state and then the program will change the system by adding (titrating) or removing the reactants (Bethke, 2008). This process is called the reaction path. Another feature of the reaction path model used in this study will be sliding the Eh. This means that the Eh of the system is increased or decreased linearly over a reaction path; such as those occur from iron reducing to sulfate reducing conditions.

The model first equilibrates a typical groundwater sample at the site under moderately reducing conditions at measured field temperature. The calculation uses the water chemical data collected from well RA-5 presented in Tables 1 and 2. Because the reaction that is being modeled involves the reduction of redox conditions, sliding the Eh was enabled and the value was decreased from +0.2 to -0.2V over the course of the reaction. The model also simulates the

geochemical effects of titration of $FeSO_4$ (1 mmol) into the system as proposed amendments of iron sulfate during biostimulation (Figure 33).

As the reaction starts, ferrous iron (Fe^{2+}) dominated in the initial system. Next the reaction proceeds to precipitate realgar (AsS) a pure As-sulfide species when more iron sulfate is titrated into the system. In this reaction, realgar is a thermodynamically stable species, but not likely to form in natural aquifers as its precipitation is probably kinetically inhibited at low temperatures. The formation of realgar may require higher temperatures to achieve a kinetically favorable environment. As the reaction progresses and the Eh decreases below -0.08V, pyrite is the next mineral to precipitate. This can be explained by imposing an Eh-pH diagram on top of the reaction path (Figure 34). From the start of the reaction, decreasing redox conditions move the reaction path from into the stability field of Fe^{2+} into that of pyrite; available Fe^{2+} ions (from initial solution and $FeSO_4$ amendments) react with H_2S produced from sulfate reduction to facilitate pyrite precipitation. The reaction path in Figure 34 also shows an increase in pH values because H^+ is consumed in H_2S production during bacterial sulfate reduction. As this trend continues and the pH-Eh conditions follow the boundary of siderite and pyrite stability fields and it is also possible to precipitate siderite. Siderite forms from Fe^{2+} ions reacting with HCO_3^- from the initial system or breakdown of organic matter.

The modeling results suggest that under highly reducing conditions, reduced aqueous Fe^{2+} reacts with H_2S to form pyrite, which can remove trace elements such as As, Co, Ni, and others from groundwater by co-precipitation or adsorption processes (Saunders et al., 1997, 2008; Lehner et al., 2006). This biogeochemical reaction forms the basis for the proposed in-situ bioremediation strategies at this site.

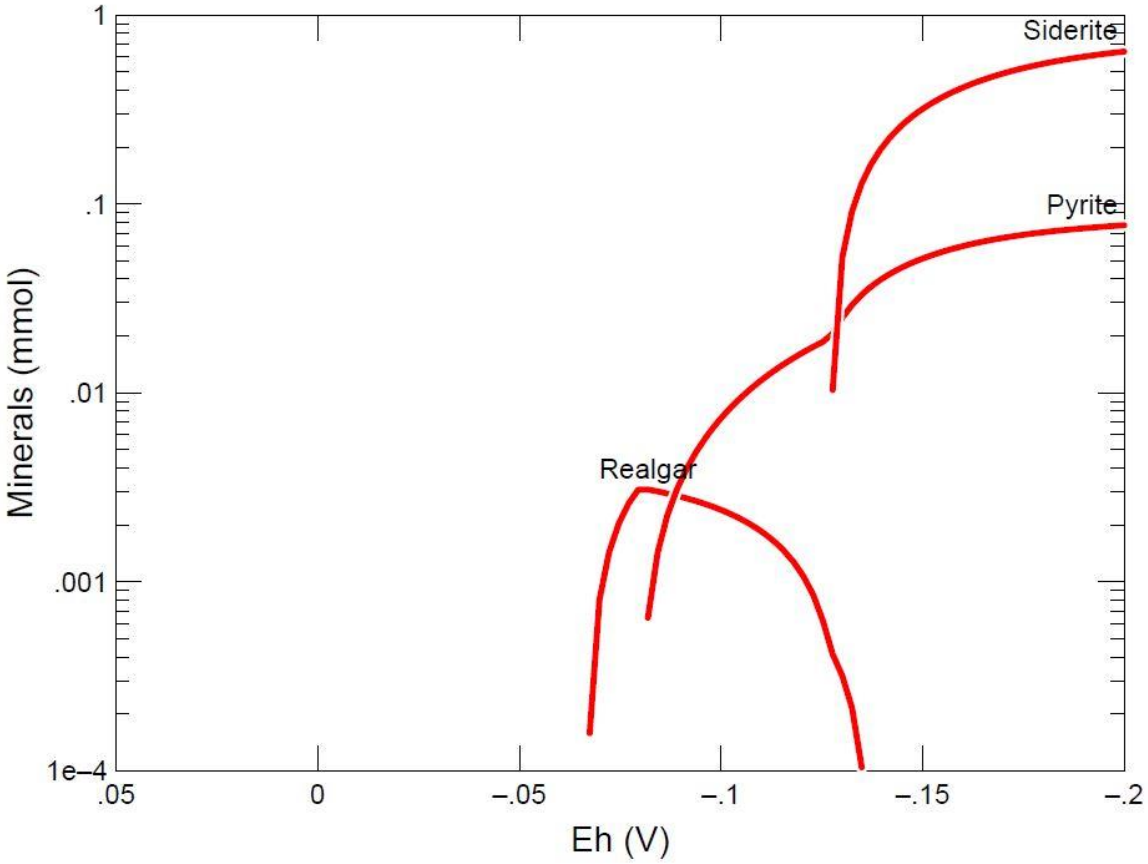

Figure 33. Plot of results of the reaction path model created with Geochemist's Workbench. The plot shows the sequence and amounts of minerals precipitated as a function of biogenic sulfate reduction using RA-5 groundwater as the starting aqueous composition. Reaction progress traces mineralogical changes from left to right (Eh decreasing) as a result of biogenic sulfate reduction.

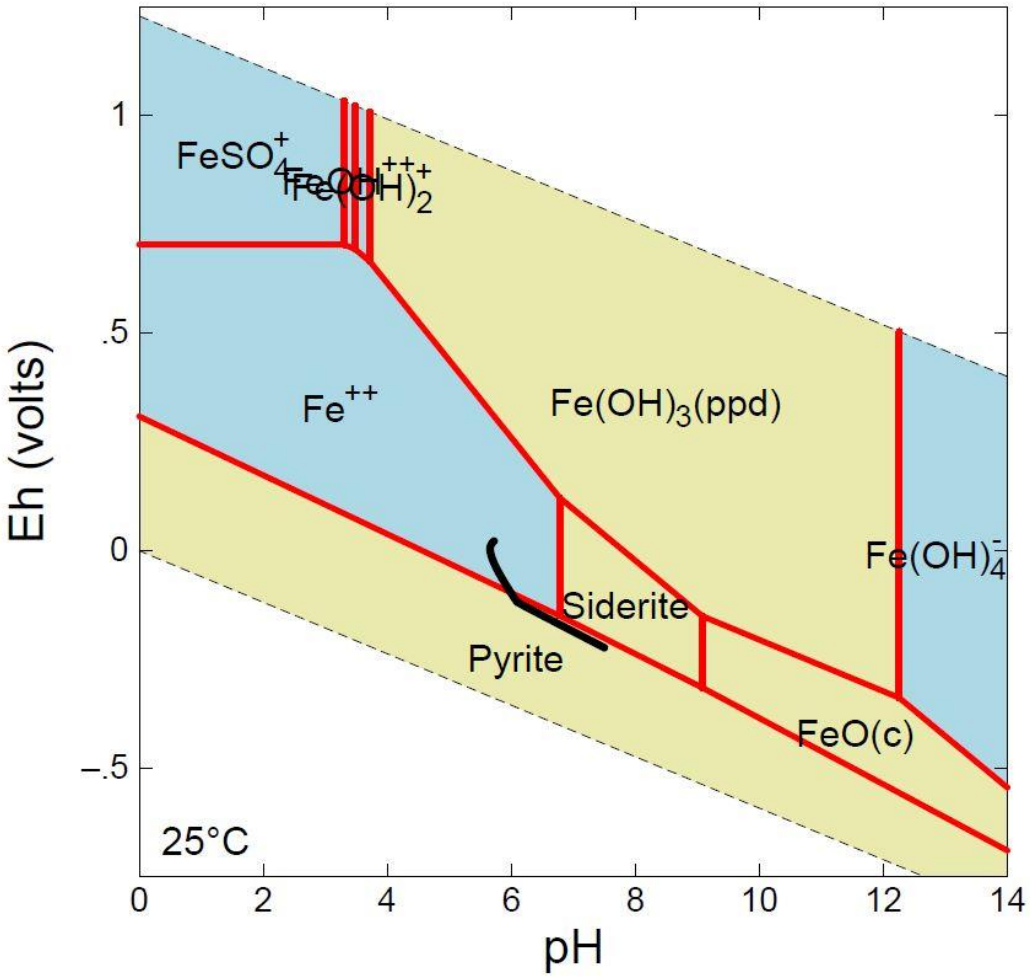

Figure 34. Reaction path model created with Geochemist's Workbench imposed on an Eh-pH diagram showing the relationship between the path of the reaction and the stable mineral precipitates of the Lynn Haven industrial site.

Hydrogeologic Framework and Modeling

Regional Groundwater Model

Regional groundwater flow across the Bay County was modeled using Basin2 (Bethke et al; 2003). Data from Schmidt and Clark (1980) were used to reconstruct the hydrostratigraphy in the cross section. The sides and bottom of the cross section are set to be no flow boundary conditions. The simulation models the regional groundwater flow in response in regional topography and water table along this east-west cross section. The transect of the model domain (Figure 35) is interpreted to cross the Lynn Haven industrial site in the vicinity of well 6 (Figure 35). The model predicts that shallow groundwater flow in the basin is controlled by local topography; groundwater recharges in local topographically high areas and discharges toward local topographically low areas. A general westward groundwater flow is predicted near the vicinity of well 6 at the Lynn Haven site. The predicted east-west direction of groundwater flow near the well 6 location is consistent with water table data and westward hydraulic gradients observed at the Lynn Haven site (see section below).

Hydrogeologic Framework

Results of three-dimensional, numerical groundwater modeling at the Lynn Haven site are presented in this section. The flow boundary of the study area was set to be a constant head boundary using historical water table data. The modeled area is too small to contain any real hydrologic boundaries such as rivers or lakes (Figure 36). Four continuous contaminant transport models and two discontinuous contaminant transport models were developed to show the effects of the distribution coefficient (K_d) has on reactive transport of arsenic.

The first step in building flow and contaminant transport models is to create the initial conditions. This serves as a basis for all transient models that will be run. First, a base site map (Figure 2) was imported into Visual MODFLOW. This base map was then portioned into a grid consisting of 100 columns and 37 rows (Figures 36 and 37) with 3700 total cells for the surficial aquifer. Each cell is then assigned specific hydrologic parameters. Since historical arsenic contamination is only found in the surficial aquifer and hydrologic data are only available in the surficial aquifer, deeper geologic layers are not considered in the numerical simulations.

Topography for the surface (Figure 38) and initial heads of groundwater table (Figure 39) were the first parameters imported into the model. The head values were calculated by subtracting water table depths from the land surface elevations for each well.

Most groundwater flow models have complex constant-head or no-flow boundaries for different geologic units. For the model presented in this study, the boundary conditions are relatively simple because no physical groundwater boundaries such as rivers or lakes are present at the site. Due to the small area simulated one constant head boundary away from the main model domain was created to maintain flow regimes consistent with historical water level data. A constant head boundary (Figure 40) of approximately 200 feet away from the worst contaminated zone was selected during the course of simulations.

After initial and boundary conditions are defined other hydrologic parameters including hydraulic conductivity, storage, dispersion, distribution coefficient of arsenic between sediments and water, and recharge (from surface precipitation) were also assigned. Since the surficial aquifer is composed of relatively homogeneous silty sands most of these parameters remained

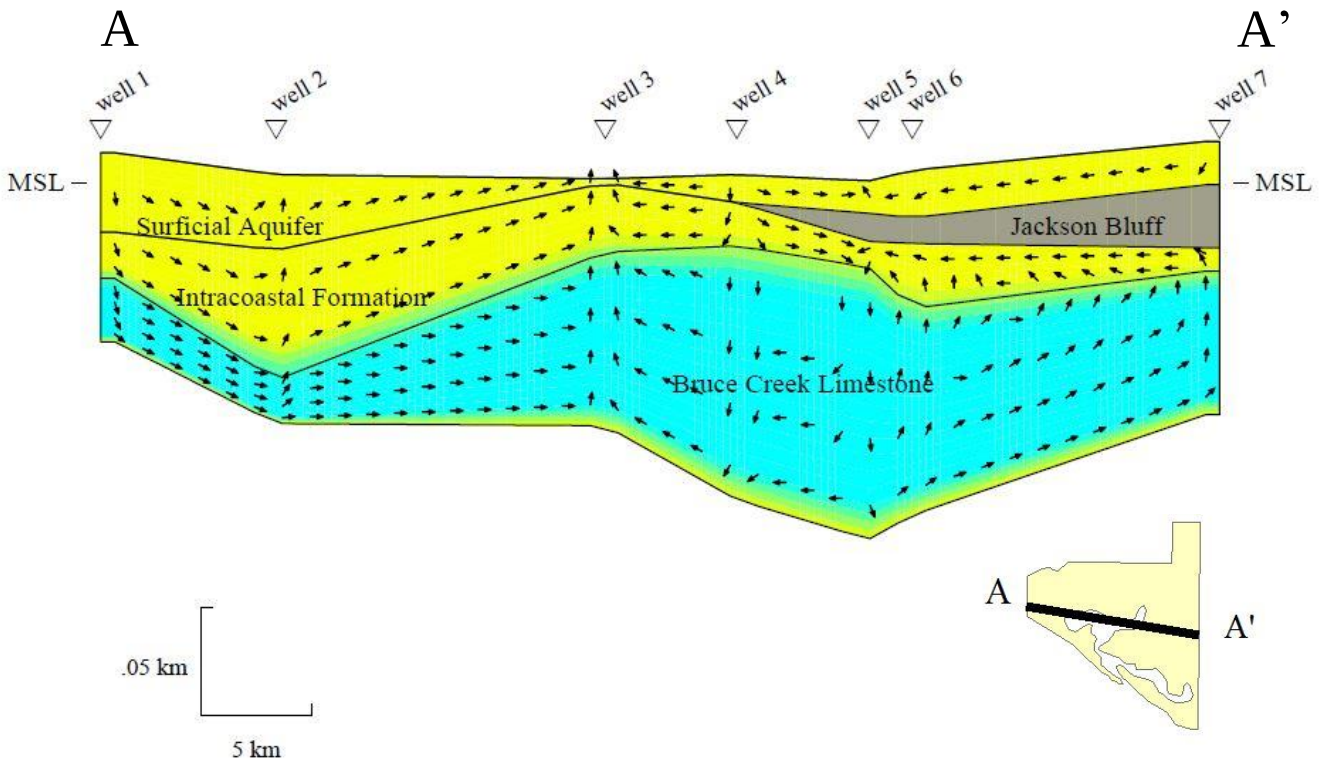

Figure 35. A cross-section showing calculated regional groundwater flow regime in a of Bay County from west to east. Flow was calculated from the 2D groundwater flow model Basin2. Hydrostratigraphic framework was from data presented in Schmidt and Clark (1980).

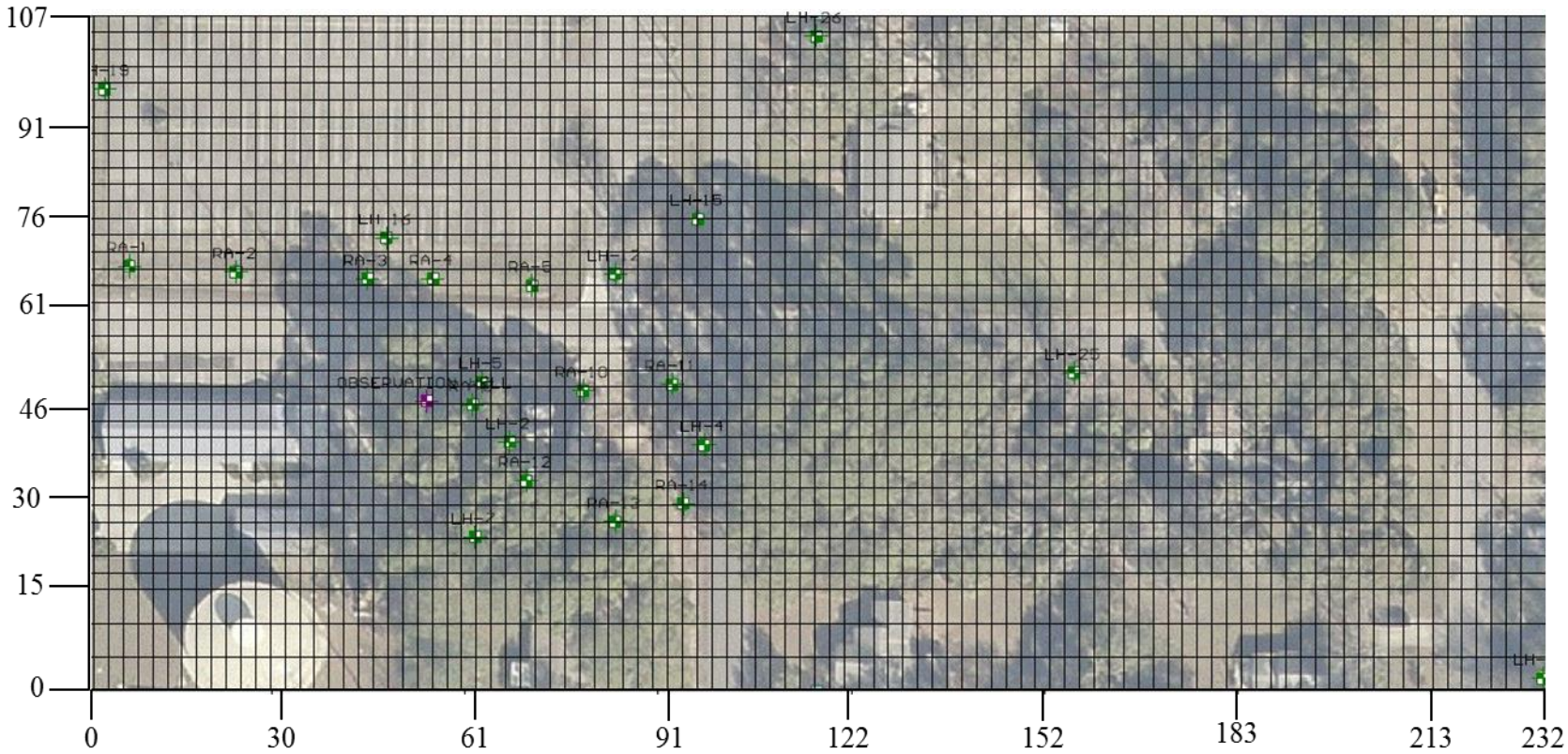

Figure 36. The Visual MODFLOW grid developed for the Lynn Haven Industrial site. Both the x and y coordinates are in meters. Also plotted are locations of sampled wells.

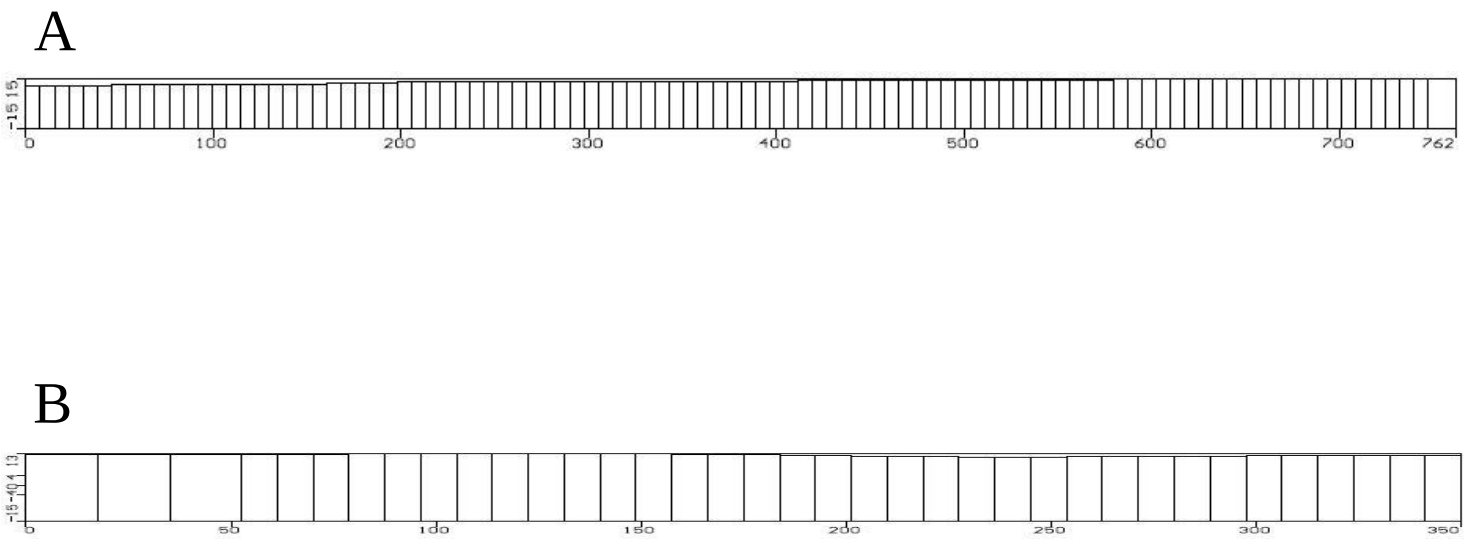

Figure 37. A horizontal transect (A) showing each cell across the model from west to east. A vertical transect (B) showing each cell from north to south.

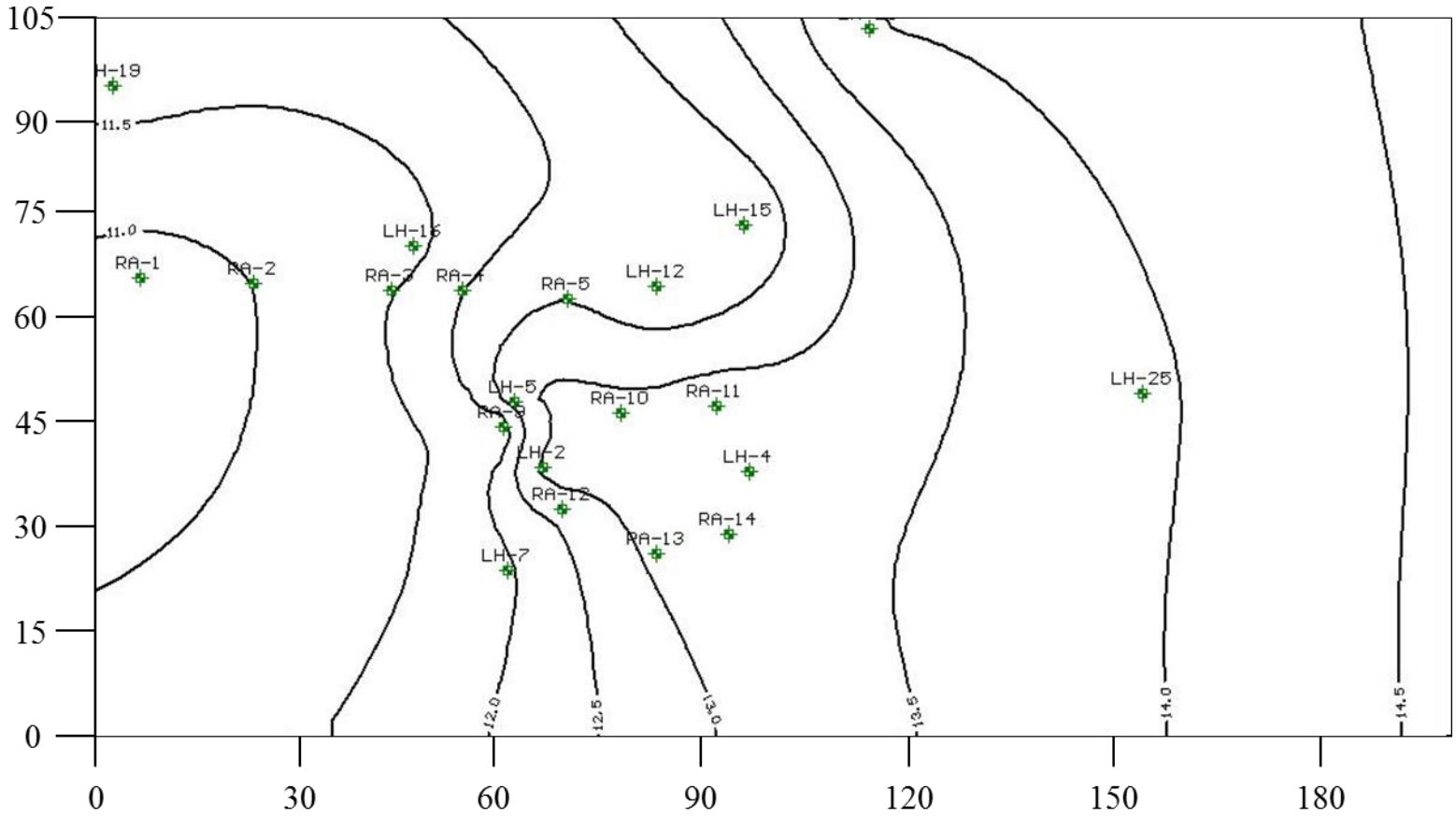

Figure 38. Imported surface elevations for the groundwater model. Axes are in meters.

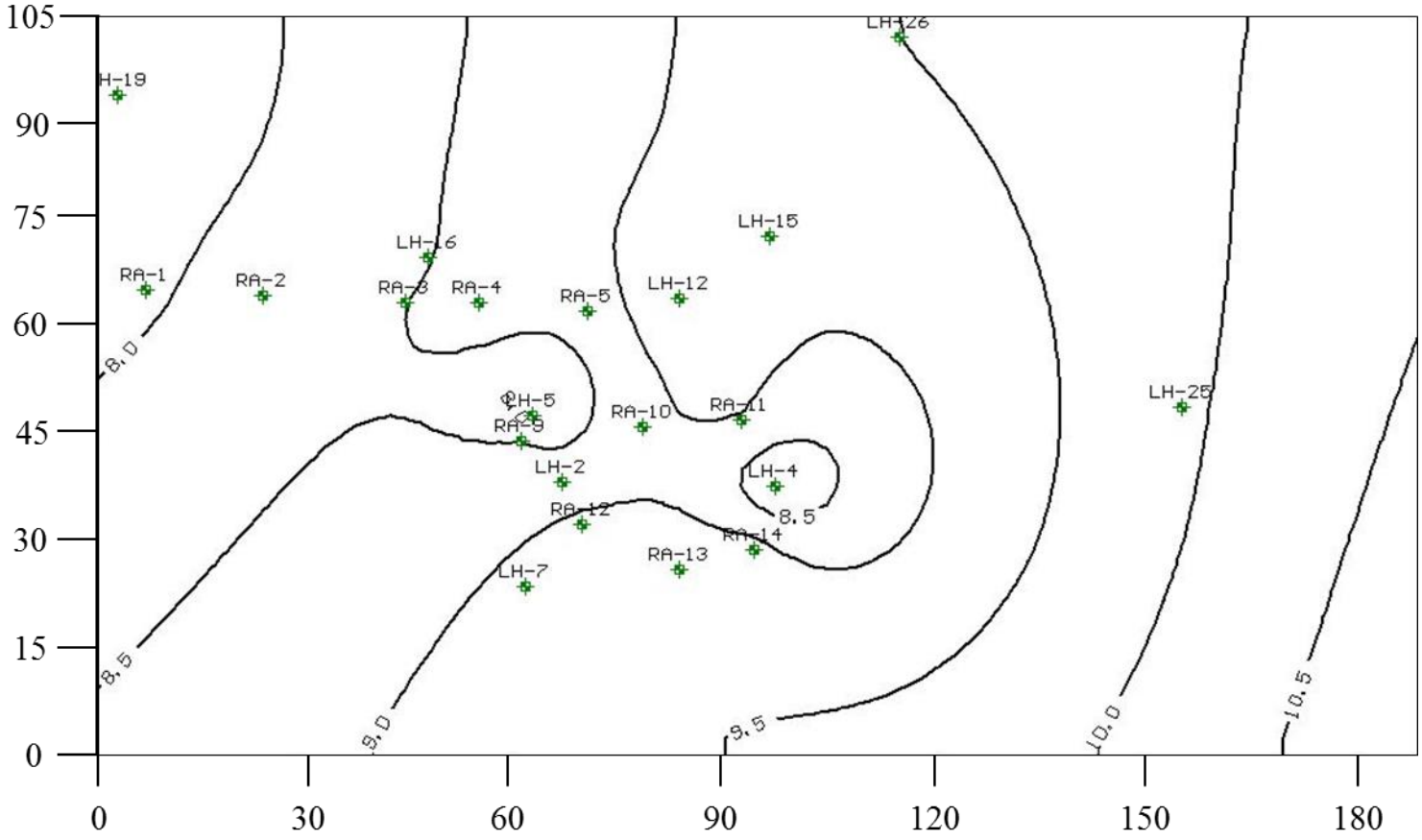

Figure 39. The imported initial heads of the water table for the groundwater model. Axes are in meters.

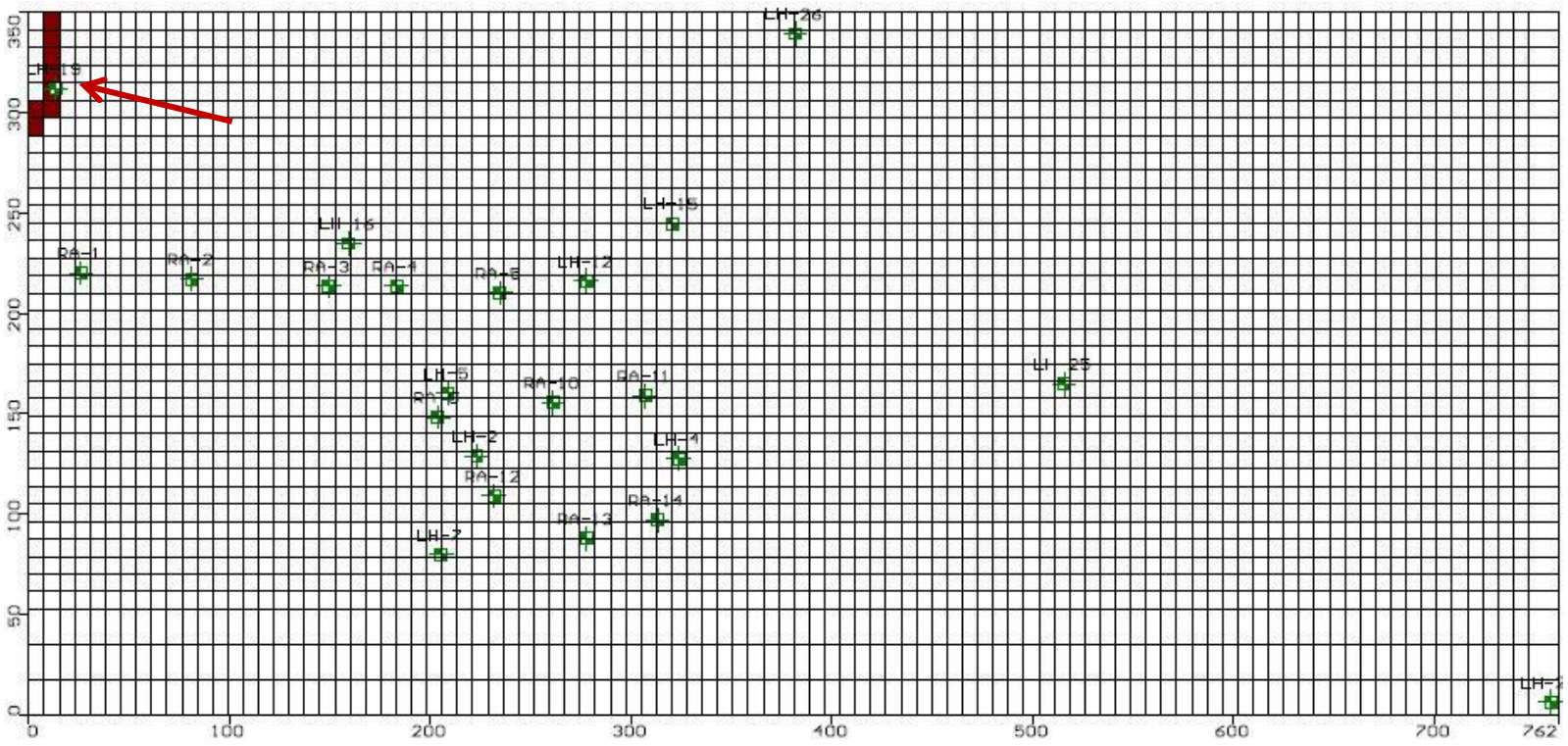

Figure 40. The constant head boundary within the model domain is colored in maroon and is approximately 200 feet away from the site, which was selected not to interfere with hydrologic stress (pumping and injection) employed near the major arsenic plume at site.

constant throughout the grid. Values for input parameters (Table 3) were taken from historical data collected on the site (Mintz and Miller, 1993) or from values recorded during the January 2015 sampling event.

Input Parameter	**Value**
Hydraulic Conductivity	0.0014 cm/s
Specific Storage	9.3×10^{-7} 1/m.
Storativity	0.01
Effective Porosity	0.35
Total Porosity	0.35
Dispersivity	10.4 meters
Recharge	66 cm/year
Distribution Coefficient	0; 1; 4; 10 mL/g

Table 3. Values of various hydrologic parameters assigned to the model domain.

Hydraulic conductivity can be defined as the rate of flow of a volume of groundwater through a cross section of rock and has dimensions of length/time (Bates and Jackson, 1984). It is used to show how much water can move through a certain aquifer type per unit time.

Normally, the hydraulic conductivity may vary in different directions. For relatively isotropic media present at the Lynn Haven industrial site, the geometry of void spaces is assumed

to be near isotropic and equal in three dimensions (x,y, and z). The hydraulic conductivity for the surficial aquifer was determined with previous slug testing and was calculated to be 0.0014 cm/s in all directions (Mintz and Miller, 1993).

The Visual MODFLOW model allows for the use three types of storage parameters: specific storage (Ss), storativity (S), and porosity (n). Specific storage (Ss) is defined as the volume of water a unit of volume of aquifer releases from storage under a unit decline in hydraulic head (Freeze and Cherry, 1979). The unit of specific storage is 1/length.

Storativity (S) is a dimensionless quantity defined as the water released from the saturated interval of aquifers under per unit decline in hydraulic head, it is calculated by multiplying an aquifer's saturated thickness, b, by its specific storage Ss:

S = Ss*b; where

S = storativity
Ss = specific storage
b = thickness of the aquifer

A value of 0.01 was used (Freeze and Cherry, 1979) to specify the storativity of the unconfined aquifer at the site. The specific storage value of 9.3×10^{-7} 1/m was used for the model (Freeze and Cherry, 1979). Porosity is a measure of percentage of the amount of void space with a unit volume of aquifer. Effective porosity and total porosity for the surficial aquifer are assumed to be equal at 0.35 or 35 percent.

Recharge can be defined as the volume of surface water introduced per unit of surface area of an aquifer through surface infiltration per unit of time. The units for recharge are

length/time. For this model cm/year were used from previously published data (Mintz and Miller, 1993) and recharge for the site is approximately 66 cm/year.

The distribution coefficient K_d can be defined as ratio of sorbed concentration C* of a contaminant on solids to dissolved contaminant concentration C:

$$K_d = \frac{C^*}{C}$$

Thus, larger K_d values indicate that the sorbed concentration of a given contaminant is larger than the dissolved concentration and vice versa. This parameter controls the extent to which a dissolved ion can be adsorbed by sediments, which causes the retardation of the solute front as it travels through an aquifer. The retardation factor R_f is calculated as:

$$R_f = 1 + \frac{\rho_b}{\varphi} K_d$$

Where is ρ_b the dry bulk density of the sediment (gm/cm^3) and ϕ is the porosity of the sediments. The K_d values for arsenic transport in an aquifer typically range from 1 to 10 mL/g (Allison and Allison, 2005). If the average linear groundwater flow velocity is v, the average velocity of the plume v_c is given by

$$v_c = \frac{v}{R_f}$$

The average velocity of a given contaminant plume is lower than that of groundwater because the value of retardation factor R_f is greater than one. This study used the range of reported K_d

values (Allison and Allison, 2005) to assess the impact of adsorption on the movement of arsenic at the study site.

Groundwater Flow Model

MODFLOW was used to predict changes in hydraulic heads and flow velocities in the unconfined aquifer at the study site. Water levels measured in all the sampled wells were selected as the initial condition. Hydrologic parameters used in simulations are shown in Table 3. Figures 41 through 51 show the calculated hydraulic head distribution and flow direction from the simulations over a period of 10 years. The first time output results presented was 1 day after the start of the simulation, and then each successive step was one year for 10 years. There are variations in hydraulic head values of time in the model from the constant recharge that is added to each cell for each time step. However, the models show that groundwater flows in a general direction along an east to west-northwest trend over the 10 year simulation span. The predicted flow direction at local scale is consistent with those predicted in the large regional scale model near the Lynn Haven site (Figure 35). The predicted flow velocity is on the order of a few to tens of m per year depending on the local hydraulic gradients.

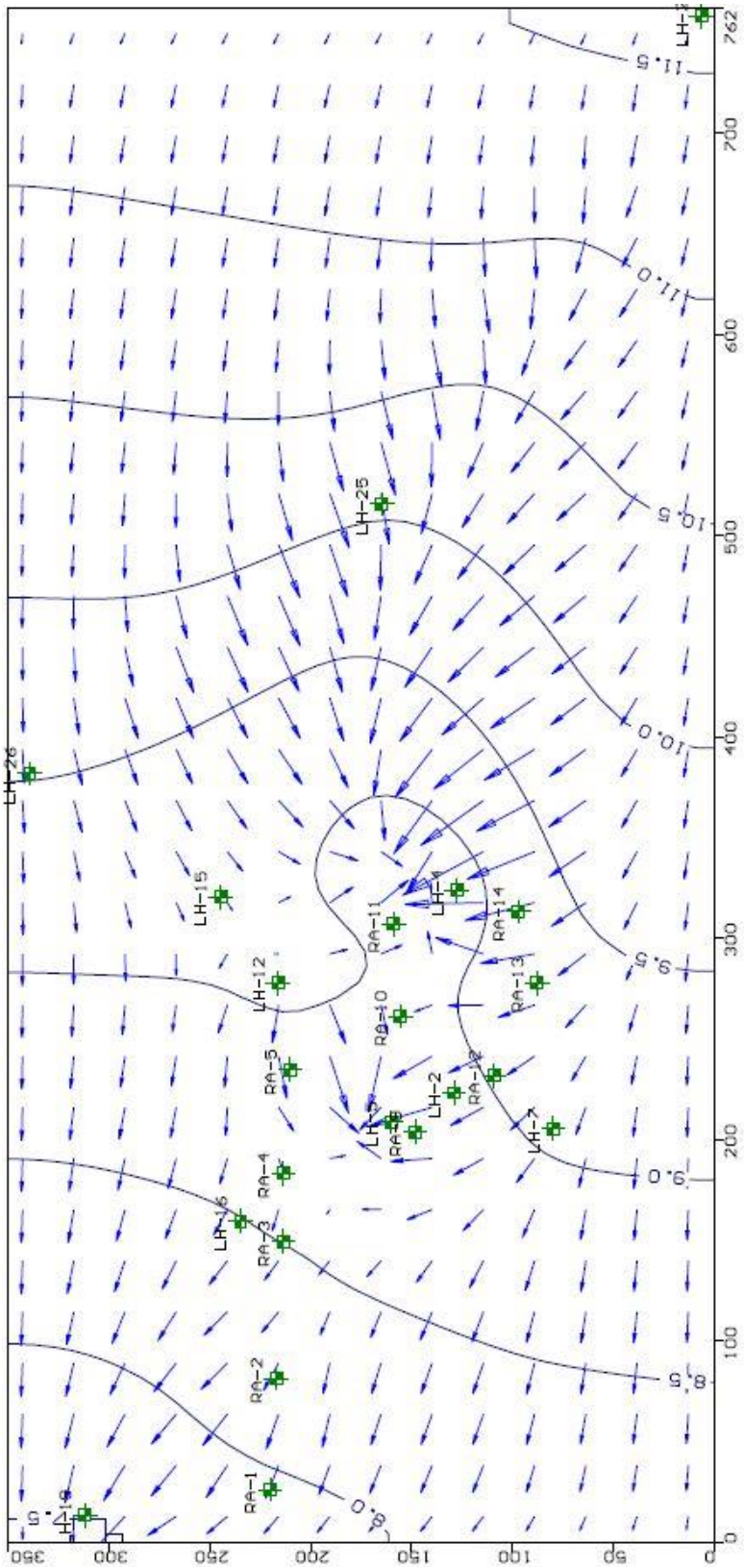

Figure 41. The simulated hydraulic head contours and velocity arrows for 1 day after the start of the model.

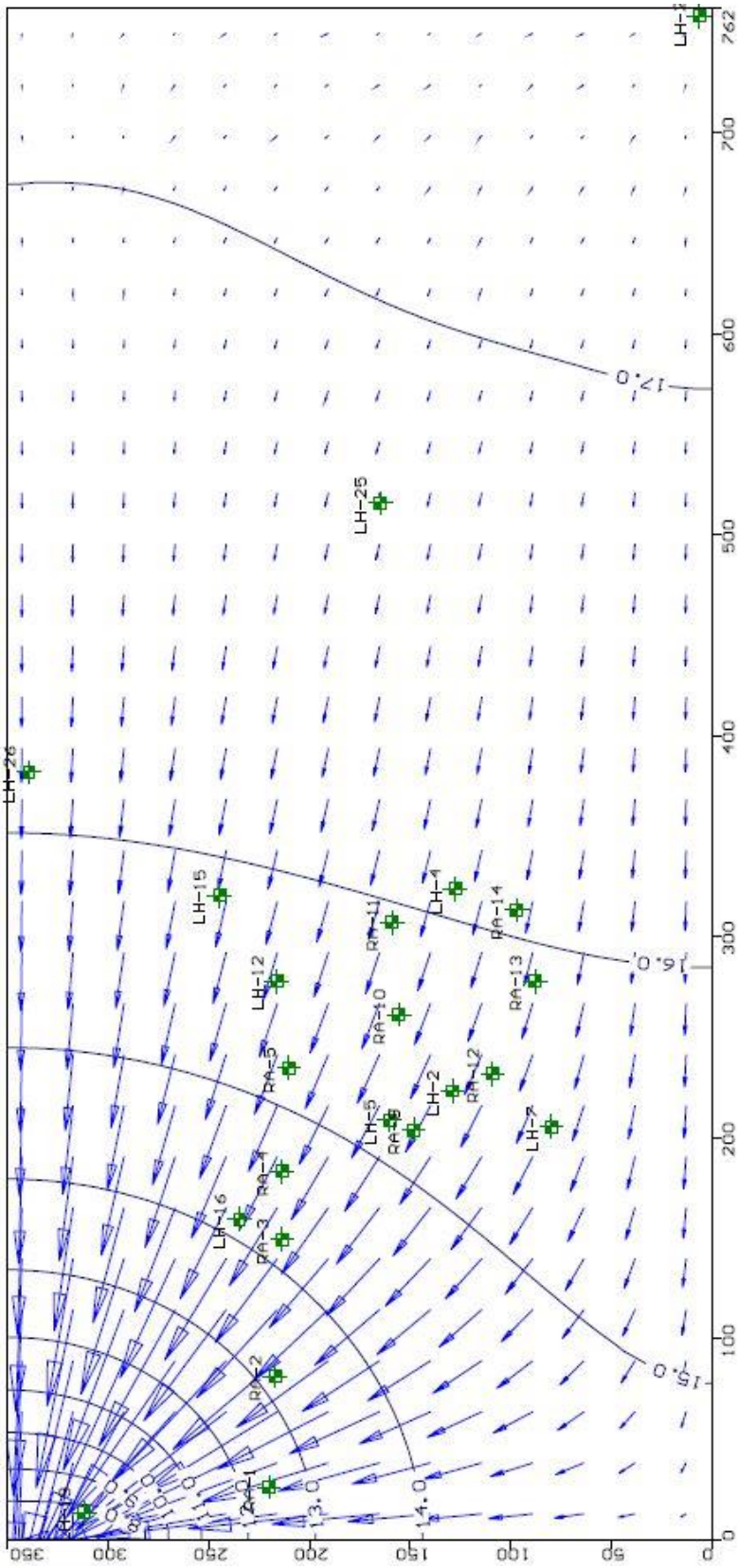

Figure 42. The simulated hydraulic head contours and velocity arrows for 1 year after the start of the model.

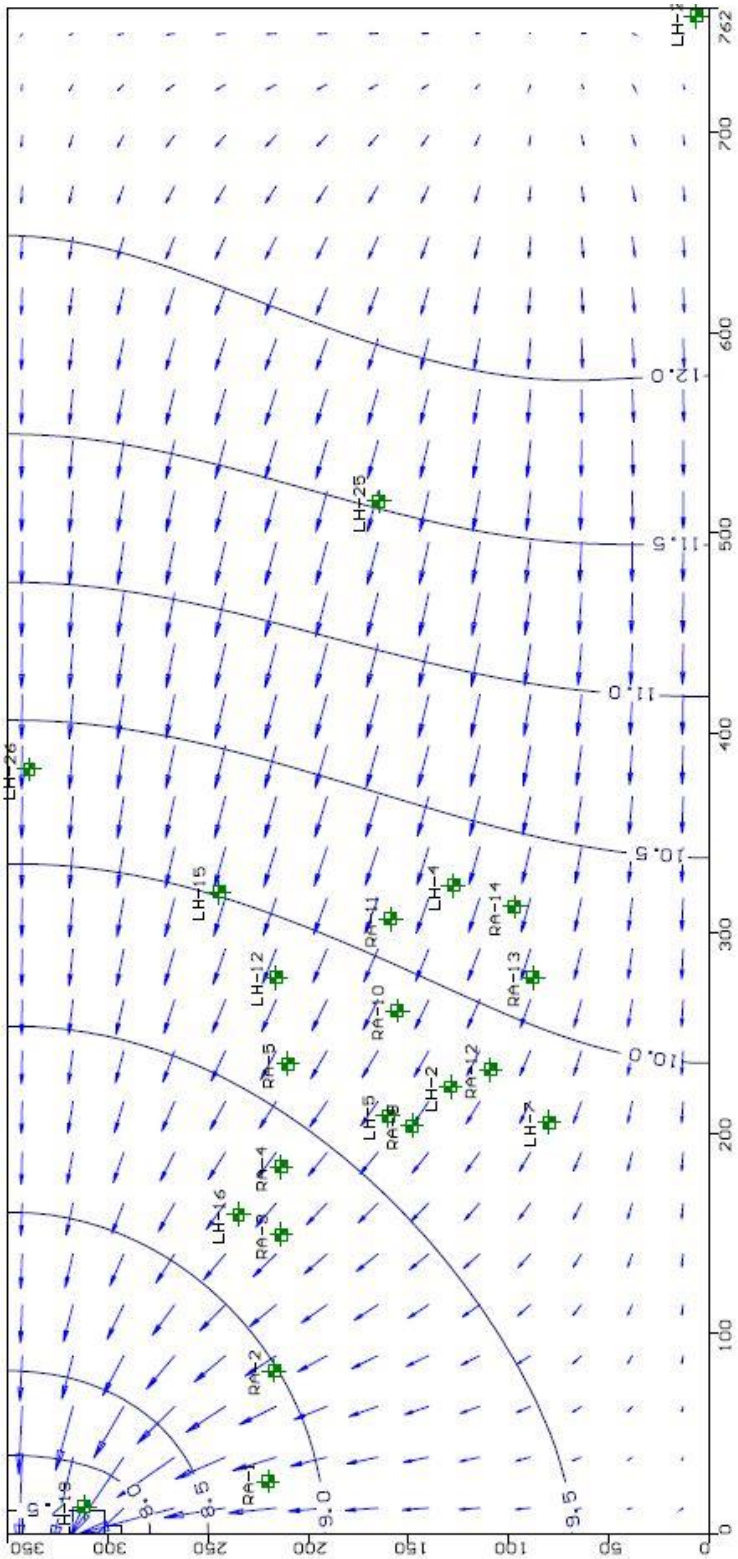

Figure 43. The simulated hydraulic head contours and velocity arrows for 2 years after the start of the model.

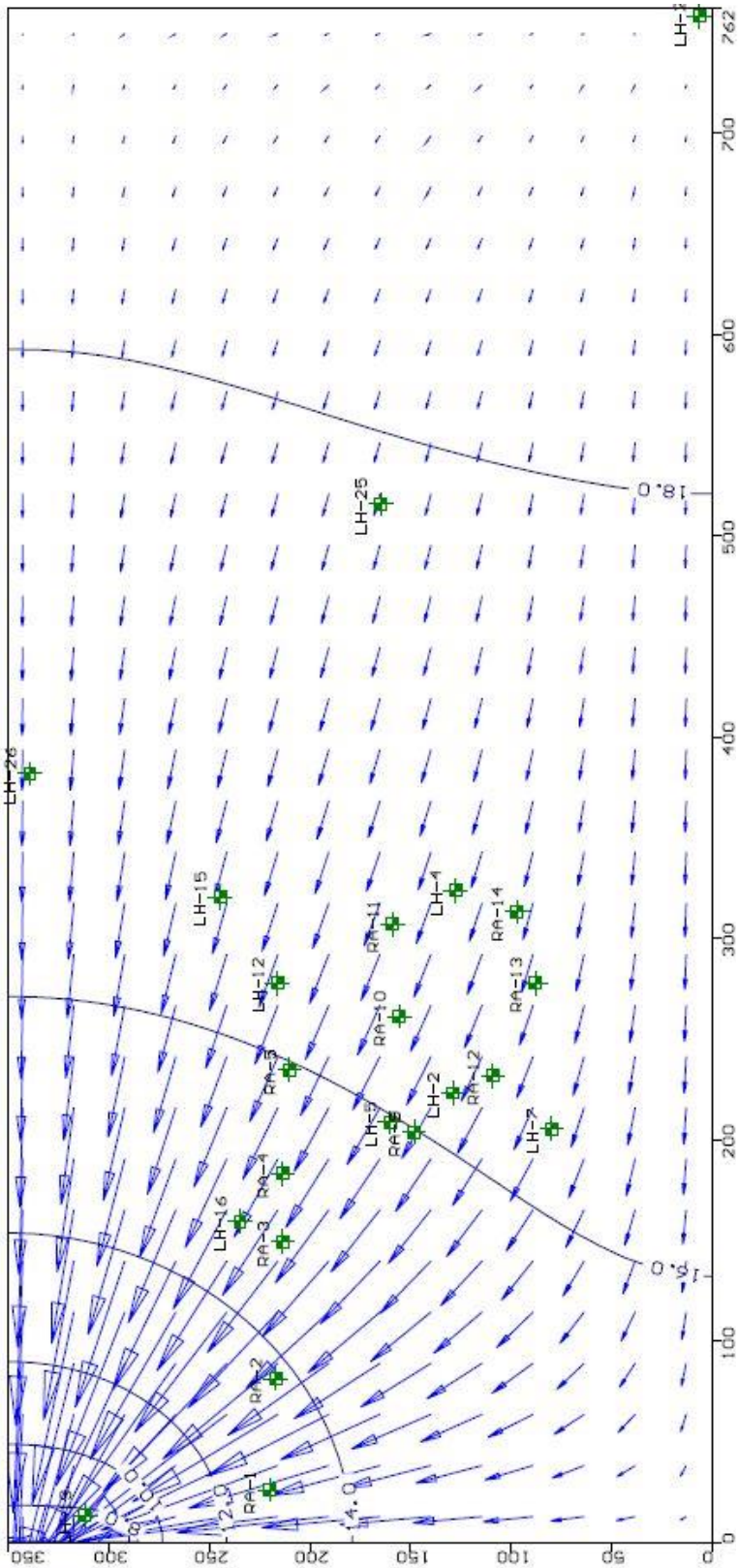

Figure 44. The simulated hydraulic head contours and velocity arrows for 3 years after the start of the model.

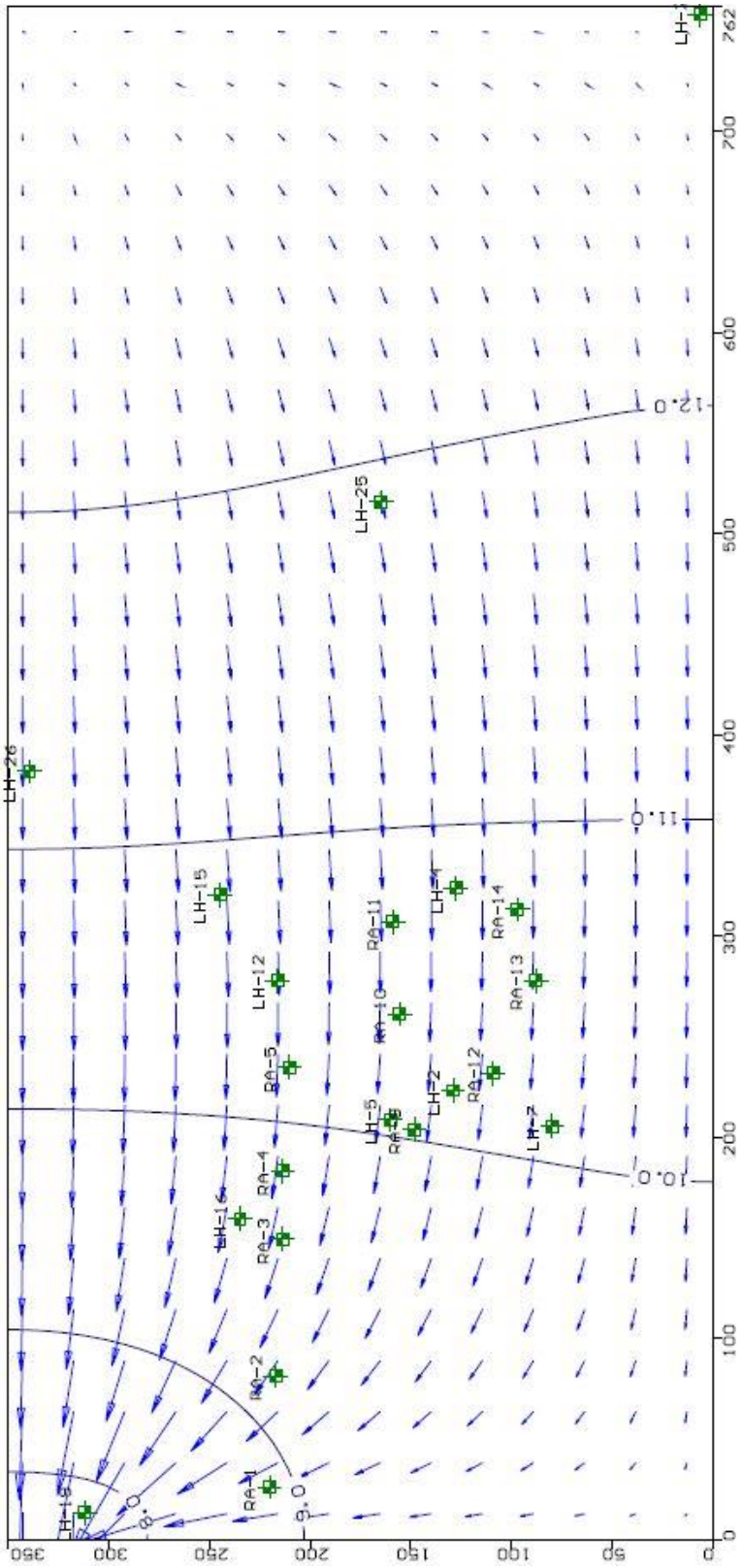

Figure 45. The simulated hydraulic head contours and velocity arrows for 4 years after the start of the model.

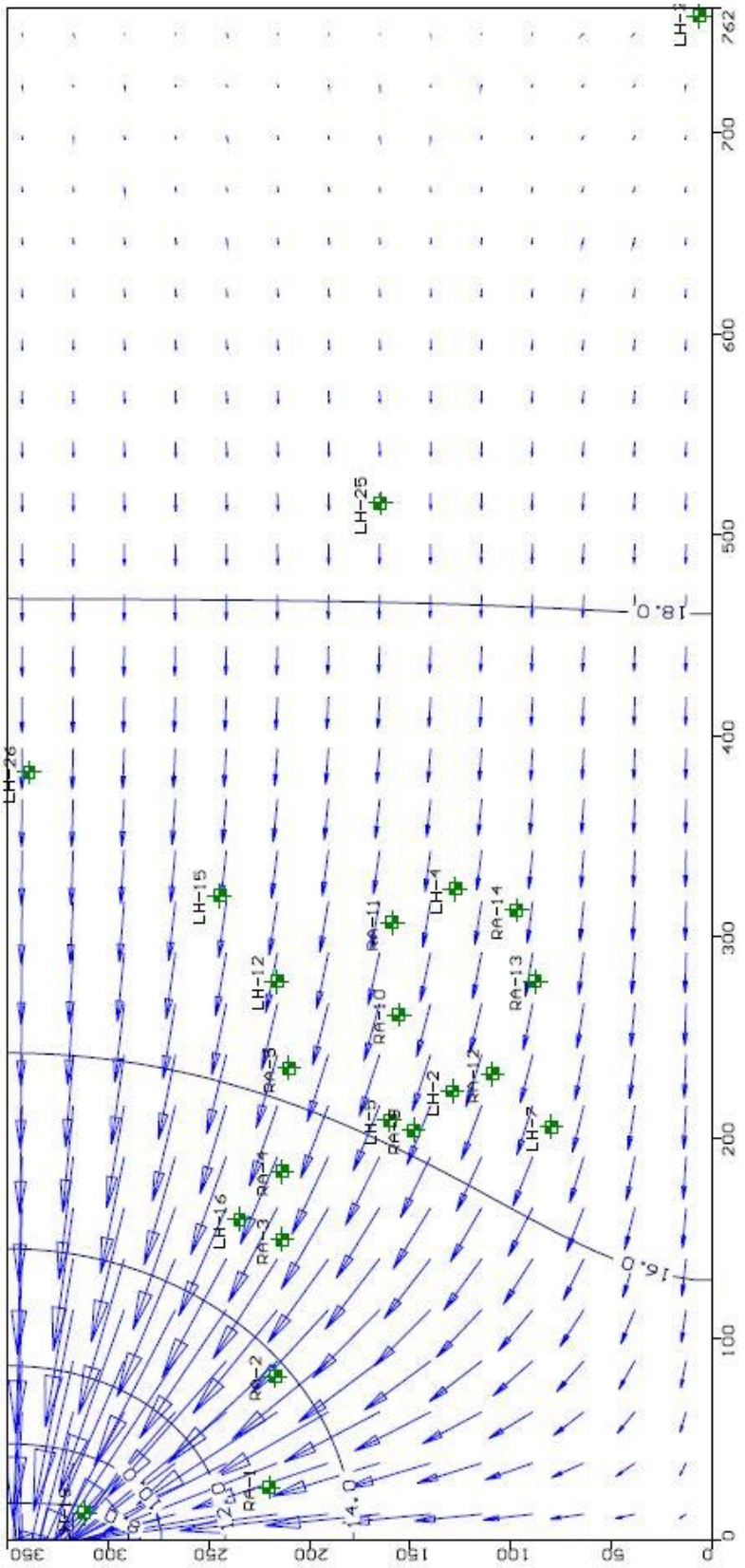

Figure 46. The simulated hydraulic head contours and velocity arrows for 5 years after the start of the model.

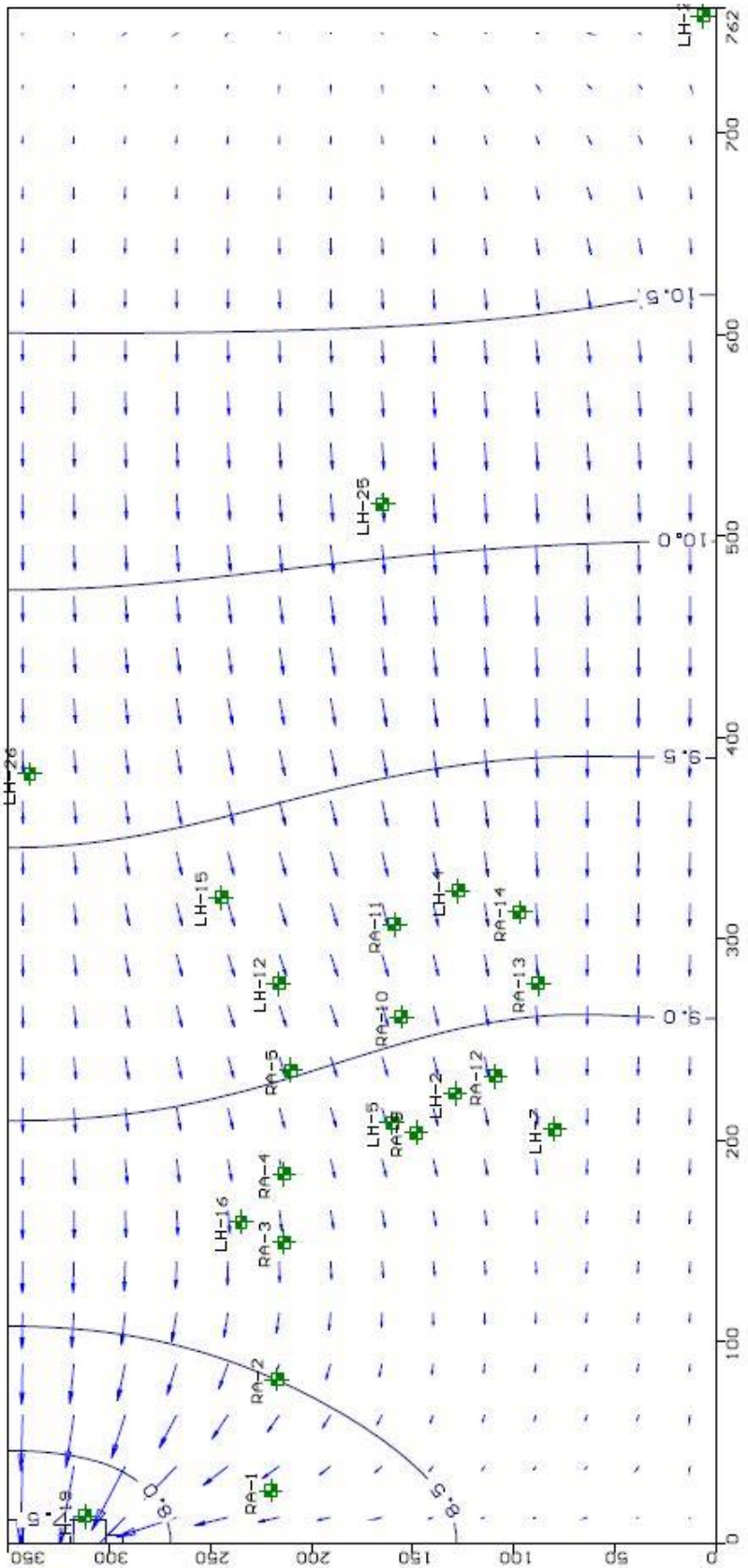

Figure 47. The simulated hydraulic head contours and velocity arrows for 6 years after the start of the model.

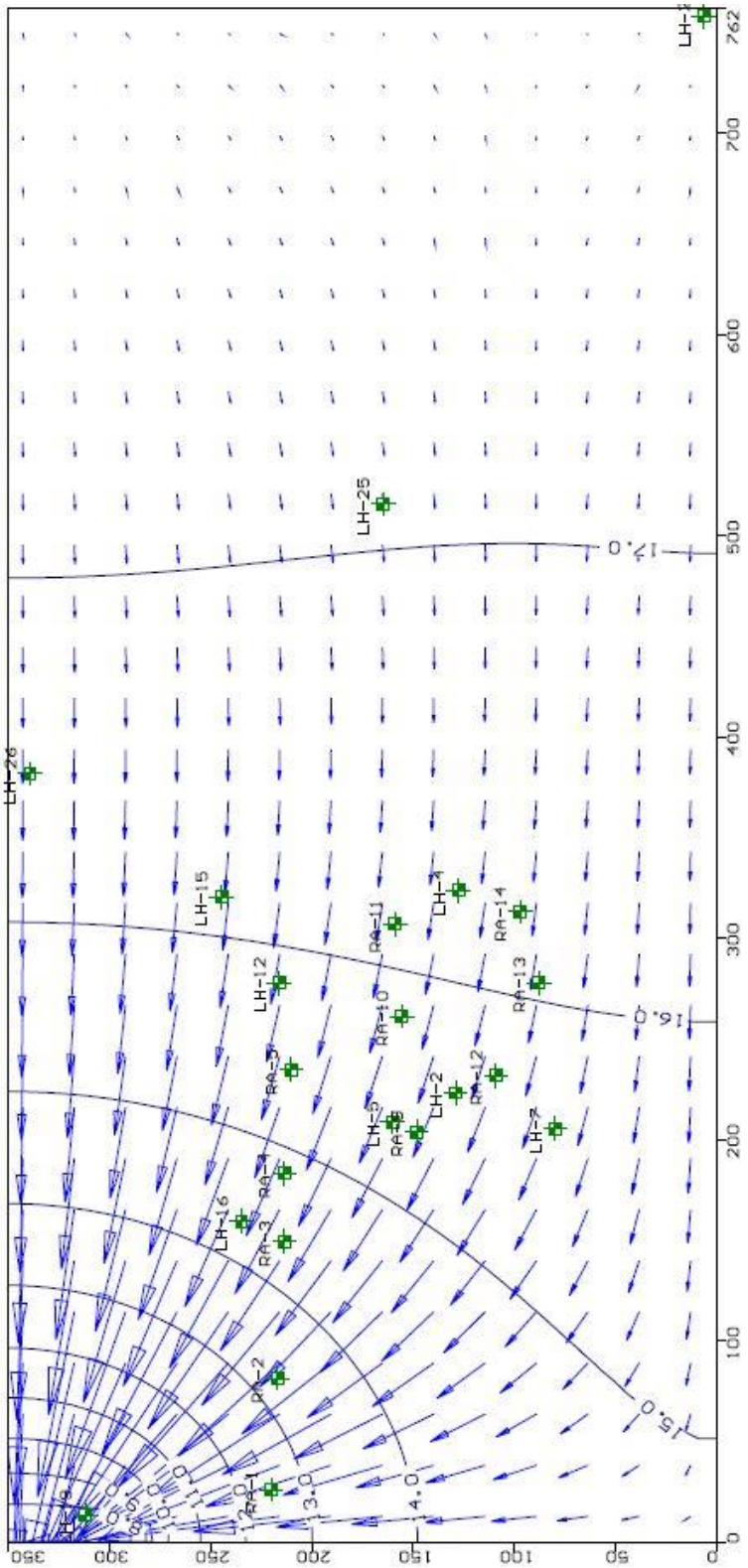

Figure 48. The simulated hydraulic head contours and velocity arrows for 7 years after the start of the model.

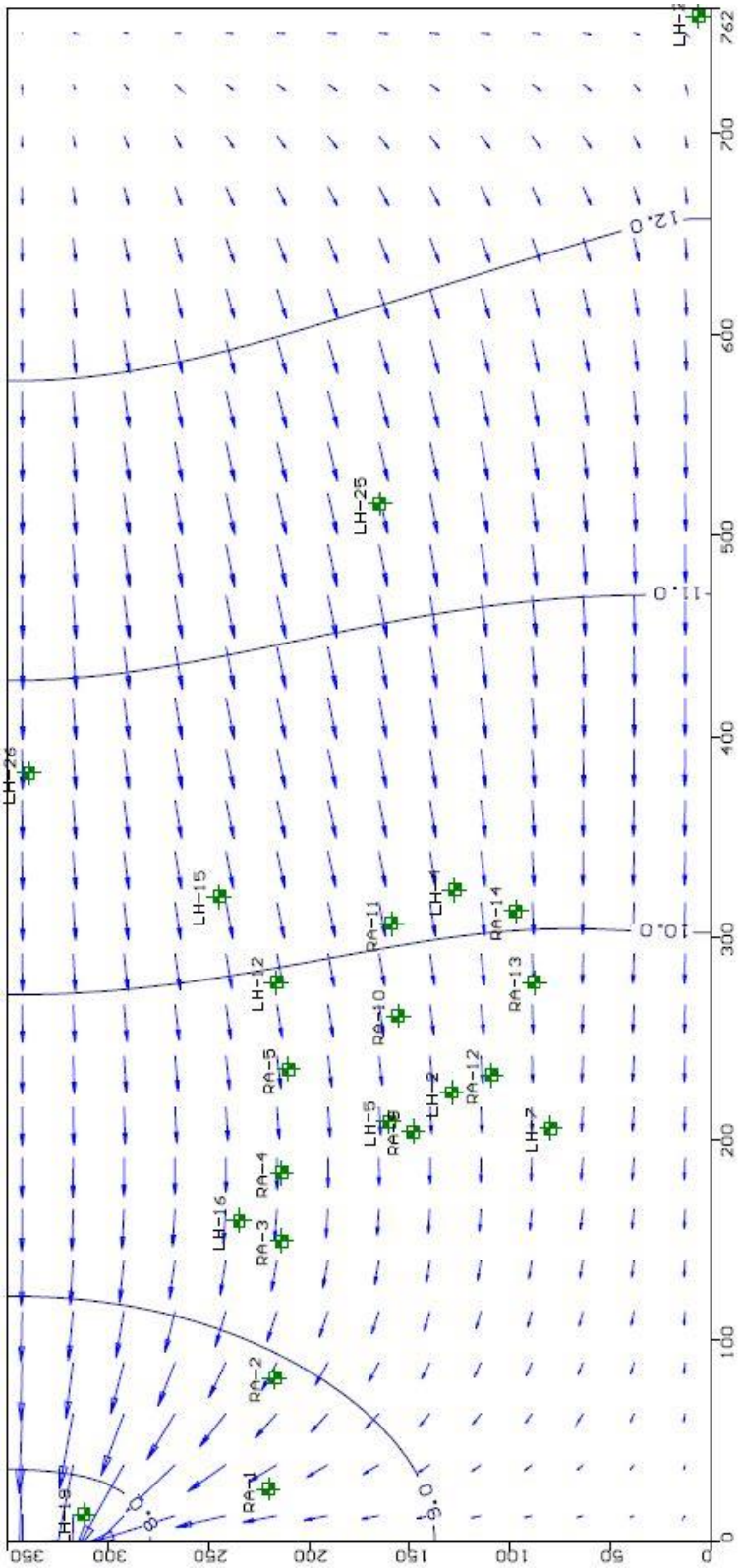

Figure 49. The simulated hydraulic head contours and velocity arrow for 8 years after the start of the model.

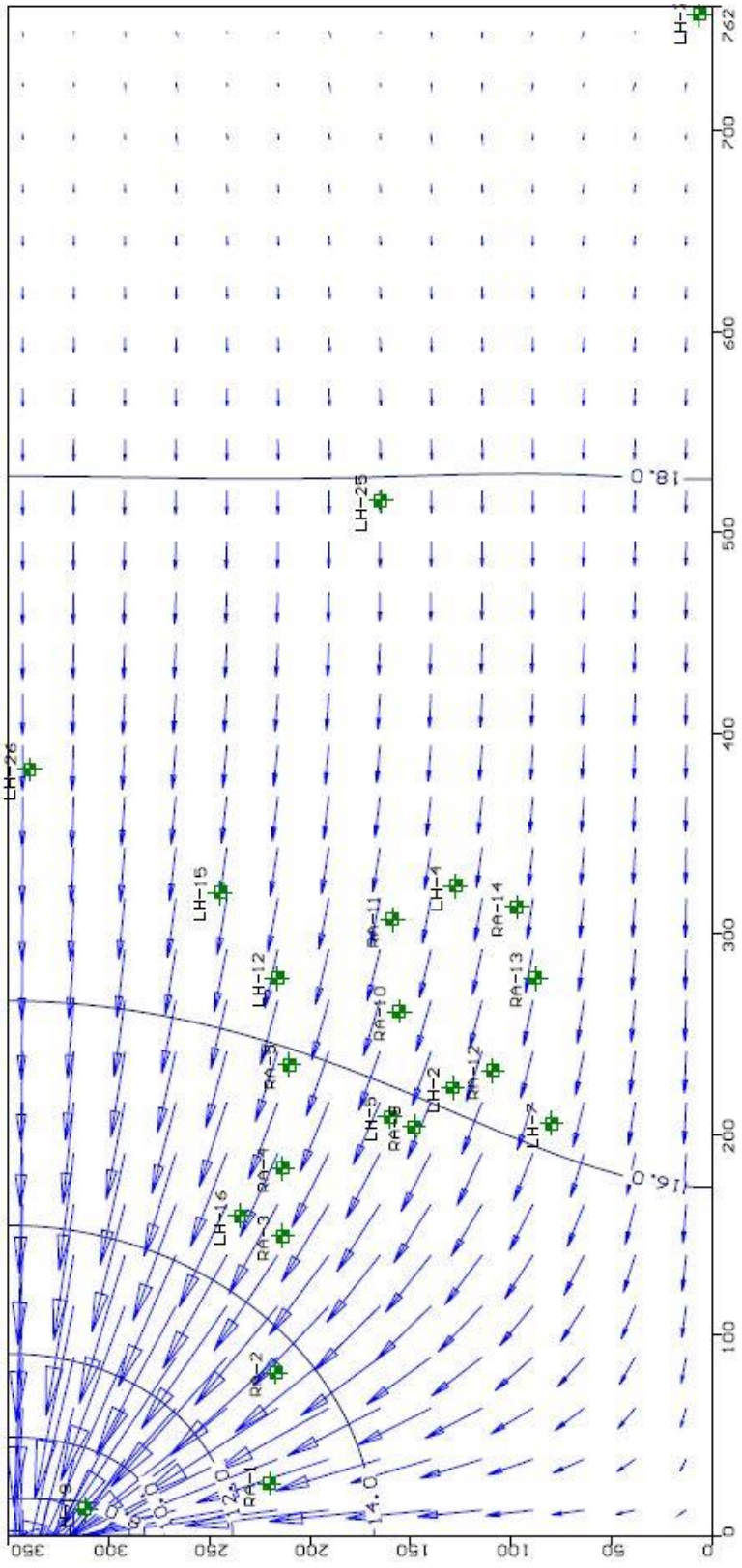

Figure 50. The simulated hydraulic head contours and velocity arrows for 9 years after the start of the model.

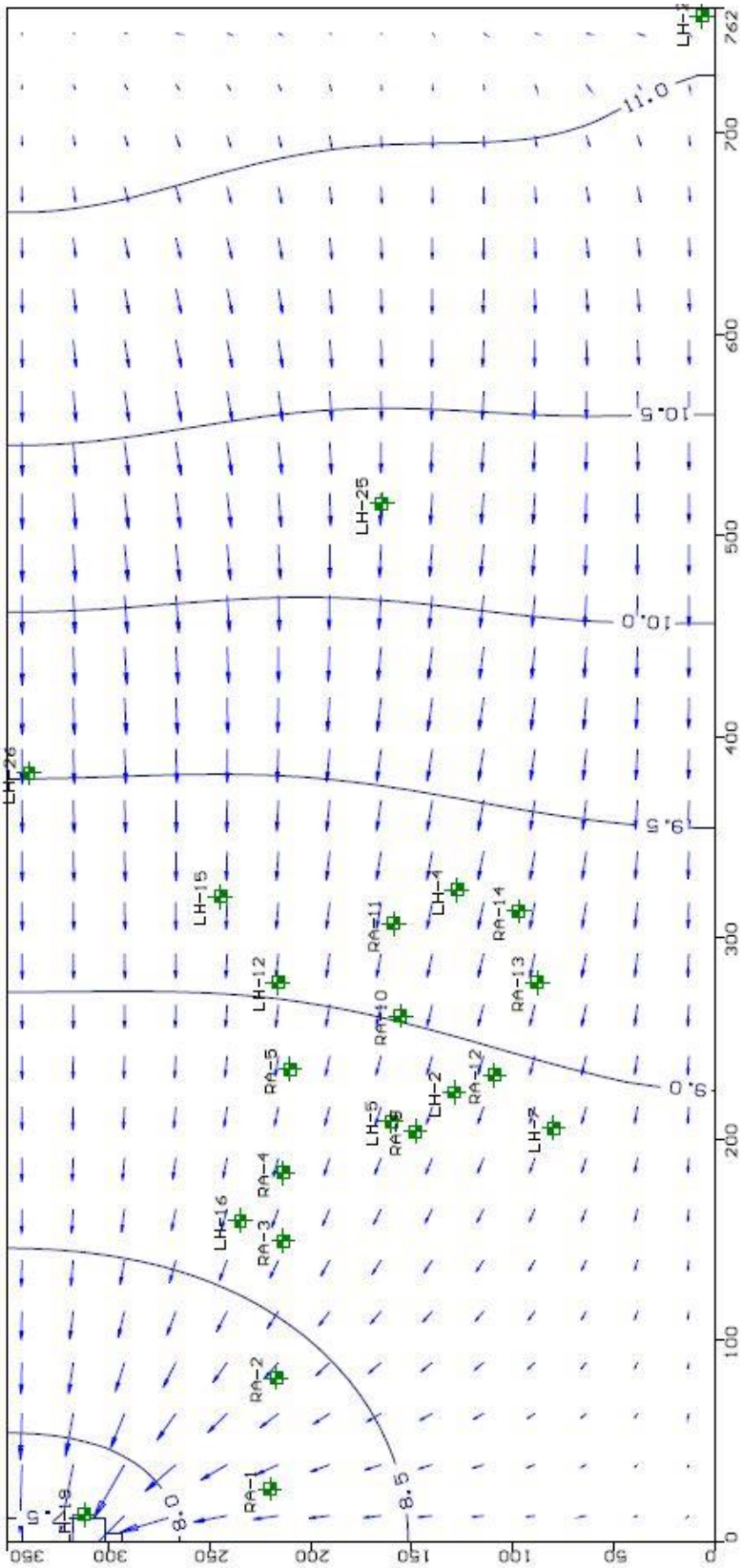

Figure 51. The simulated hydraulic head contours and velocity arrows for 10 years after the start of the model.

Particle Tracking Analysis

Velocity fields calculated from simulated groundwater flow were used in conjunction with a particle tracking program (MODPATH) to delineate advective transport of contaminants. Particle tracking simulations predicted flow paths and advective travel distances for specified periods of time by tracing particle movements through a computed flow field. In this study, a number of particles were released from two contaminated locations and the advective advance of those particles through the aquifer was calculated from the simulated flow field over a 10 year span (Figure 52). The computed flow path of a particle was displayed graphically as a line connecting trace of discrete points (Figure 52). Results indicate that contaminants such as arsenic released from the site travel to west or northwest on an average rate of 13 m/year.

MT3DMS (Zheng, 1990) was used to simulate the reactive transport of arsenic at the site based on flow field and advection process predicted by MODFLOW. Specifically, the model was used to examine the effect of advection, hydrodynamic dispersion, and adsorption on the migration of arsenic plumes released from specified locations at the site. The main parameters influencing solute transport used in simulations are shown in Table 3. The main parameter that controls the adsorption and retardation of arsenic transport is the distribution coefficient or K_d. As stated earlier the purpose of these models is to examine the different scenarios of adsorption for arsenic transportation.

Continuous Contaminant Transport Models

Four continuous contaminant transport models were developed to examine the reactive transport of arsenic and how the distribution coefficient may affect the spreading of a plume in the aquifer. All contaminant transport models were run in the groundwater flow fields computed

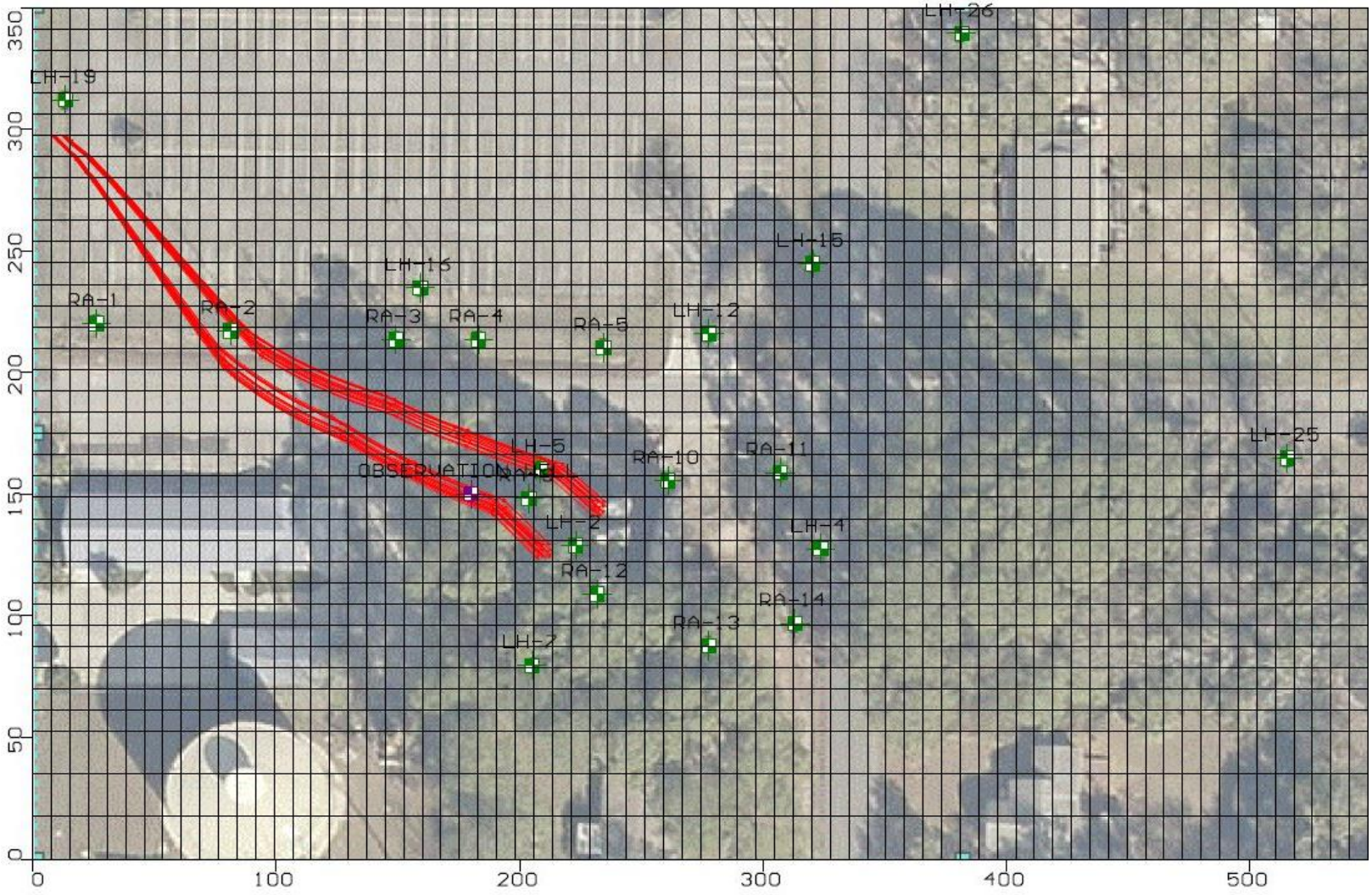

Figure 52. Results of particle tracking in Visual MODFLOW. Particles were released from two possible injection sites and tracked as they migrate over a 10 year of simulation period.

from transient, three-dimensional numerical models shown in the previous section. For the simulations, concentration of 4 mg/L of arsenic was specified at a couple cells near its initial source derived from As-rich pesticides at the site. Sensitivity analyses were conducted to explore how variations in distribution coefficient K_d values may affect arsenic transport in the aquifer. In four sets of numerical experiments, the aquifer had constant K_d values of 0, 1, 4, and 10 mL/g, respectively, close to the range of values reported in literature (Allison and Allison, 2005). The dispersivity, α, was held constant at 10.4 m (about 10% of the dimension of model domain, Gelhar et al., 1992) in these simulations. An increase in distribution coefficient would decrease the extent of arsenic spreading by increasing its sorption on sediments.

This first contaminant model with the K_d value equal to zero mL/g (i.e., no sorption of the contaminant solution) yielded the greatest degree of spreading and highest arsenic concentrations downstream, where arsenic is transported at the same rate as groundwater. Figures 53, 54, and 55 show the movement, size and spreading of the plume 1 day, 1 year, and 10 years after arsenic was released from the source. The size of the initial plume is very small and restricted to the source area after 1 day due to very limited advection and spreading (Figure 53). After 1 year the zone of maximum contamination or the center of mass of the plume has started to travel down gradient with the groundwater flow and the overall area of the plume has grown noticeably by dispersion and spreading (Figure 54). The front of the plume (defined as 0.01 mg/L of concentration) has traveled about 36 meters down gradient. Lastly, after 10 years the size of the plume has increased significantly and the zone of maximum concentration has traveled

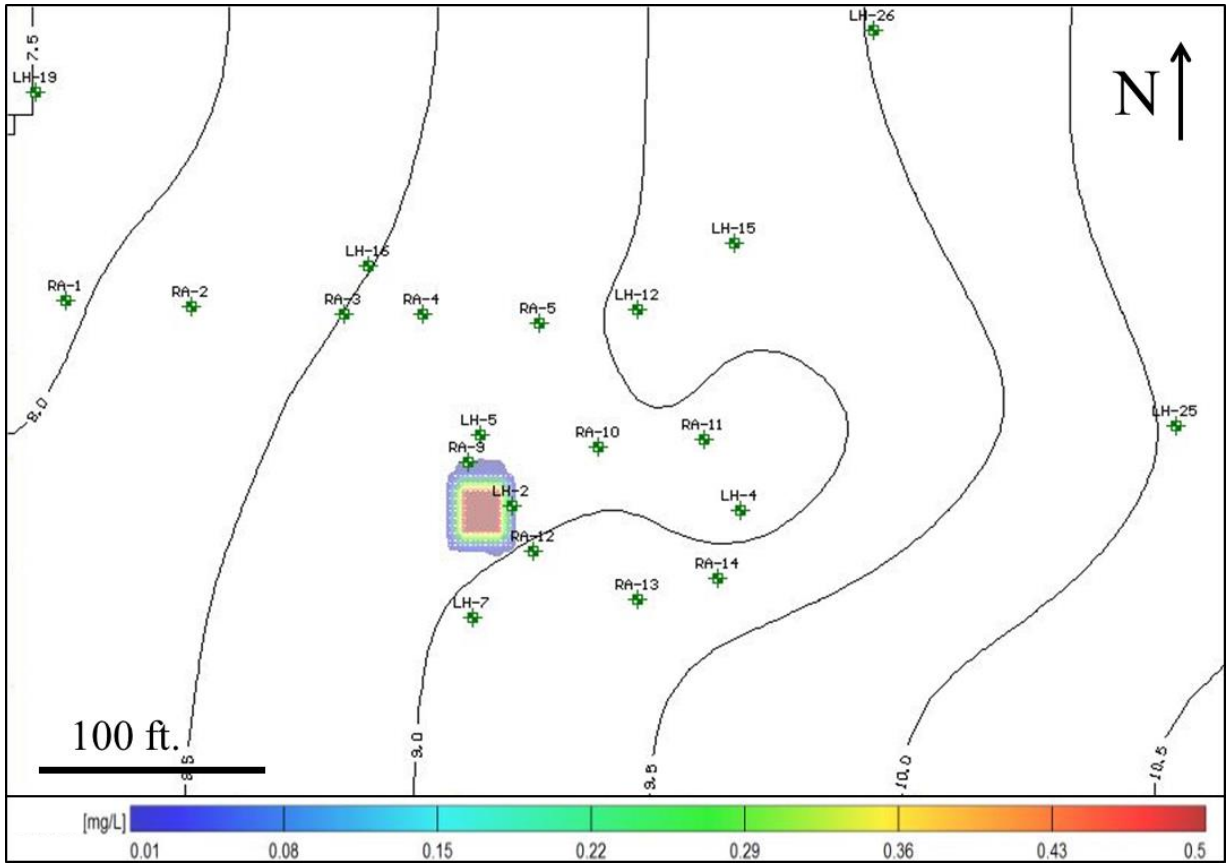

Figure 53. The distribution of arsenic 1 day after injection and $K_d = 0$. The contours are values of the simulated hydraulic heads.

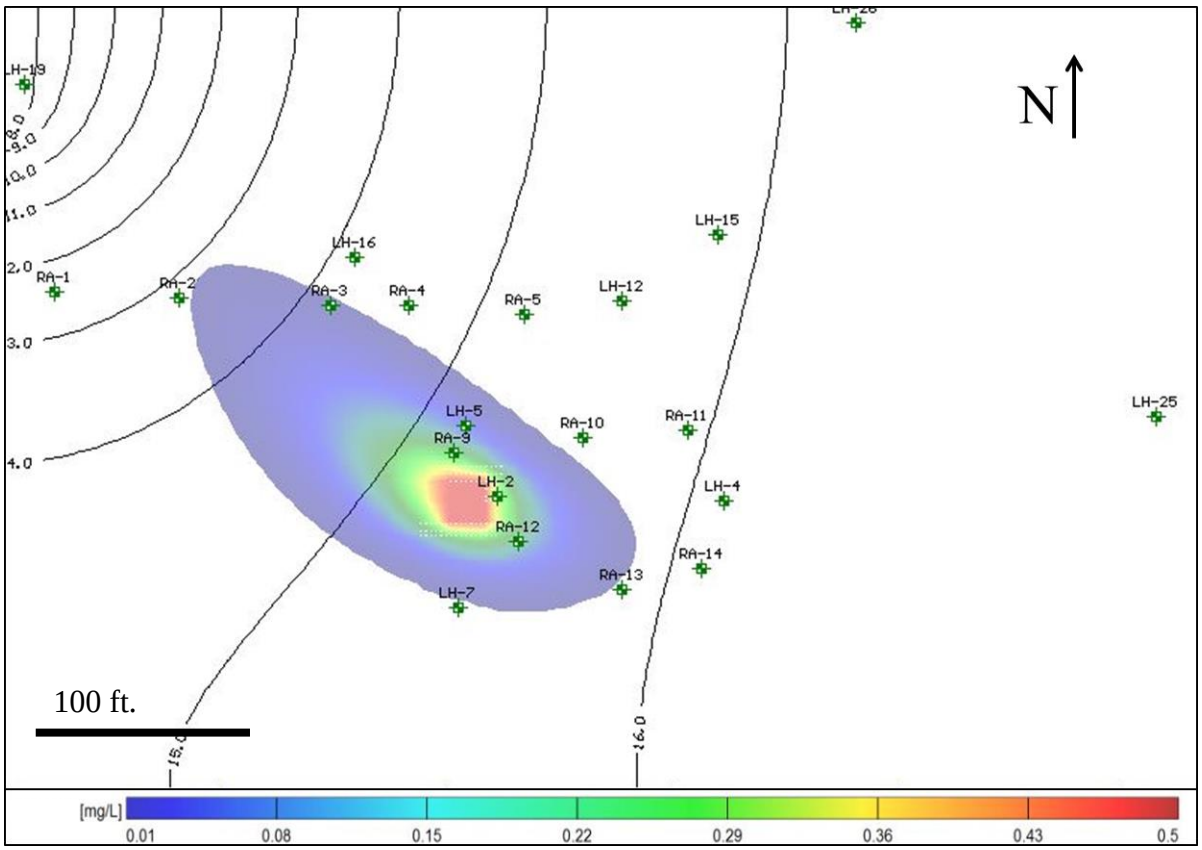

Figure 54. Distribution of arsenic after 1 year with $K_d = 0$. The contours are the simulated hydraulic head values.

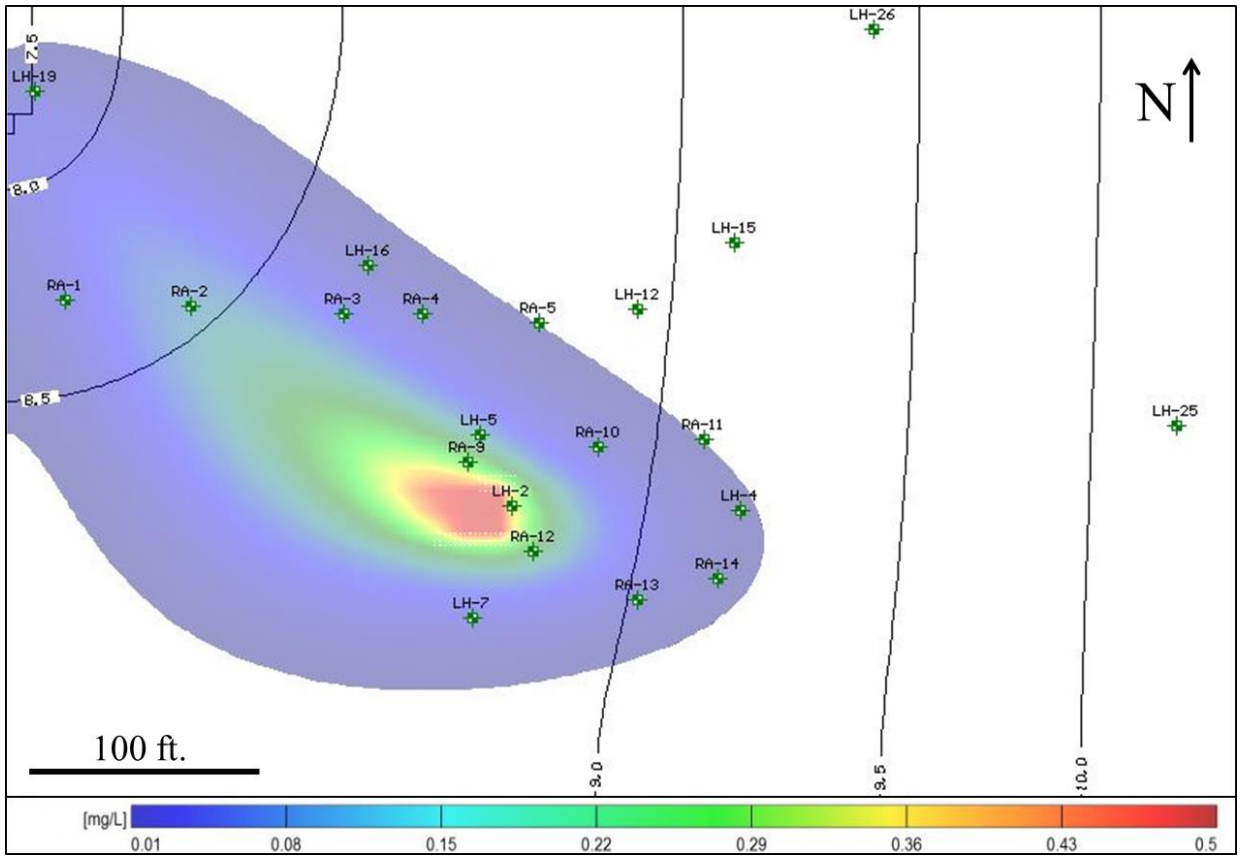

Figure 55. Distribution of arsenic after 10 years with $K_d = 0$. The contours are the simulated hydraulic head values.

significantly beyond the site toward the west-northwest (Figure 55). The front of the plume has traveled about 61 meters down gradient.

The second contaminant transport model was run with same parameters as the first. It contained the same location of injection, but had a larger K_d value of 1 mL/g. The distribution coefficient used in this model simulated a small amount of arsenic that is being sorbed by the aquifer sediments. Initially, one day after an injection the plume of contaminant remains close to the injection location and the zone of maximum contamination is small and restricted to the source (Figure 56). After 1 year the size of the plume has grown by advection and dispersion (Figure 57), however it is still smaller than the corresponding plume with K_d equal to zero (Figure 54). The front of the plume has traveled about 12 meters down gradient, shorter than the no-adsorption case. After the 10 year simulation the plume is at its largest and is moving in the north-northwest direction (Figure 58). The size of the plume is still relatively smaller than the corresponding plume with the K_d equal to zero (Figure 55). The front of the plume has traveled about 45 meters down gradient after 10 years.

The third contaminant transport model was set up with a higher distribution coefficient value of 4 mL/g. This value represents stronger adsorption that limits the spreading of the arsenic plume. Thus, the modeling results show that the plume grows and advances slowly with time compared to the previous models. The size and distribution of the plume after 1 day is similar to that of the simulations with lower K_d values. The size and distribution of the plume after 1 year (Figure 60) has grown little due to strong adsorption and retardation effects. Lastly, after 10 years the plume is at its largest size and has transported to the west-northwest (Figure 61), but its spreading is very limited compared to other simulations with smaller K_d values. The front of the plume has traveled about 25 meters down gradient after 10 years.

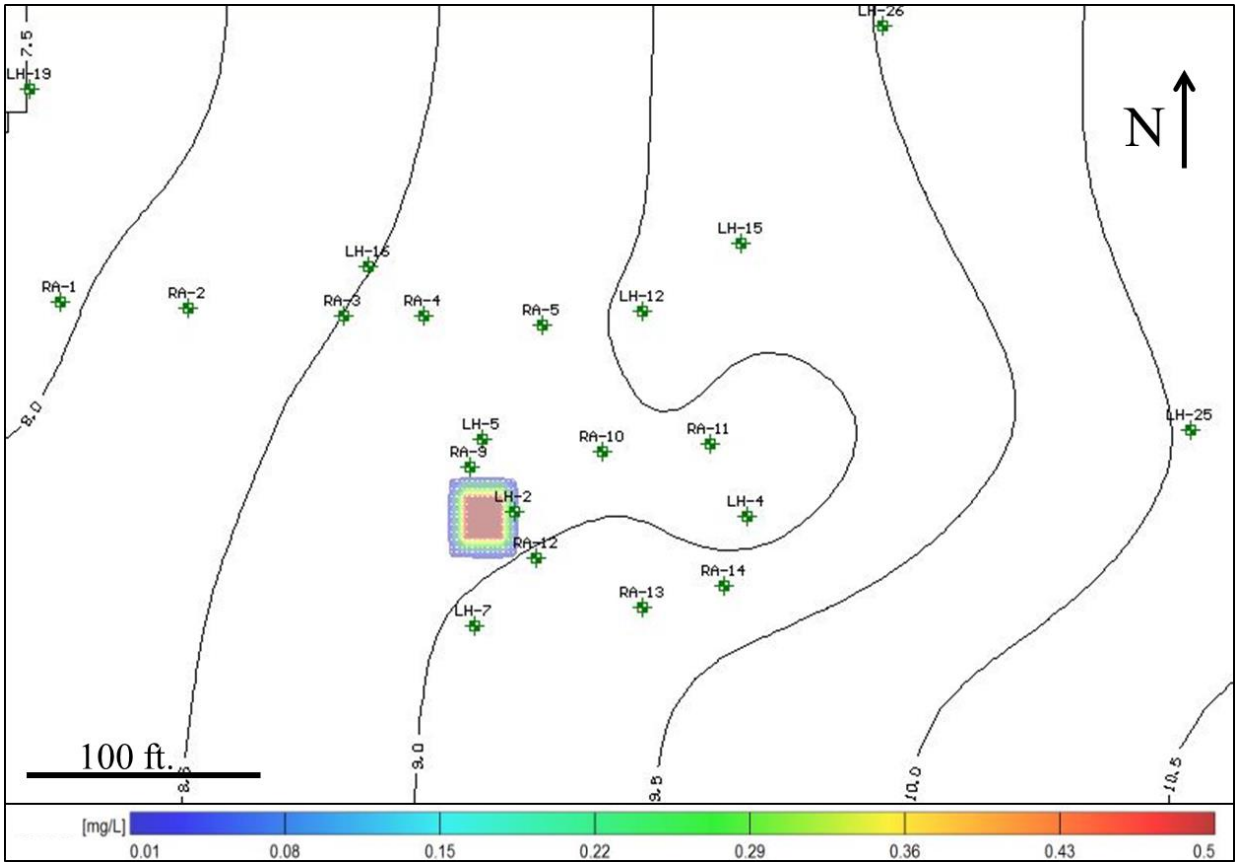

Figure 56. The distribution of arsenic after 1 day with $K_d = 1$. The contours are the simulated hydraulic head values.

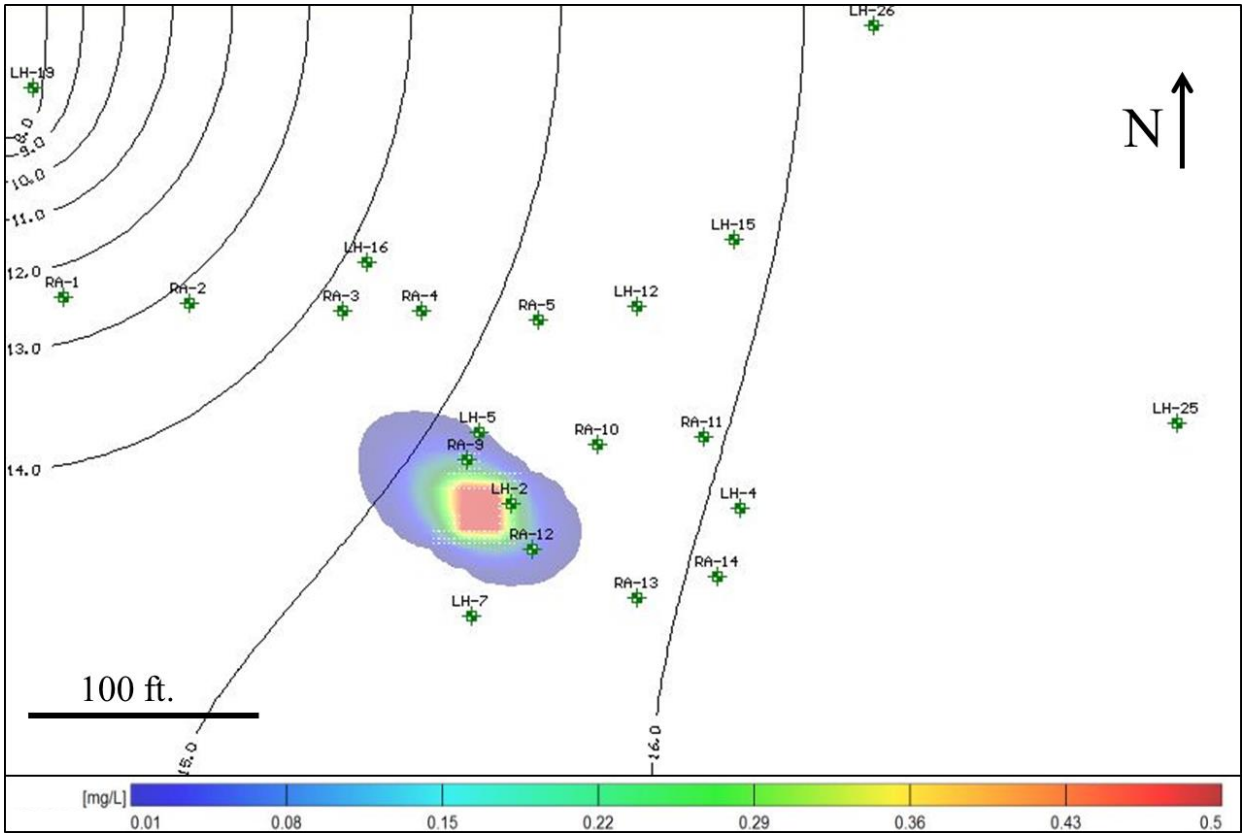

Figure 57. The distribution of arsenic after 1 year with $K_d = 1$. The contours are the simulated hydraulic head values.

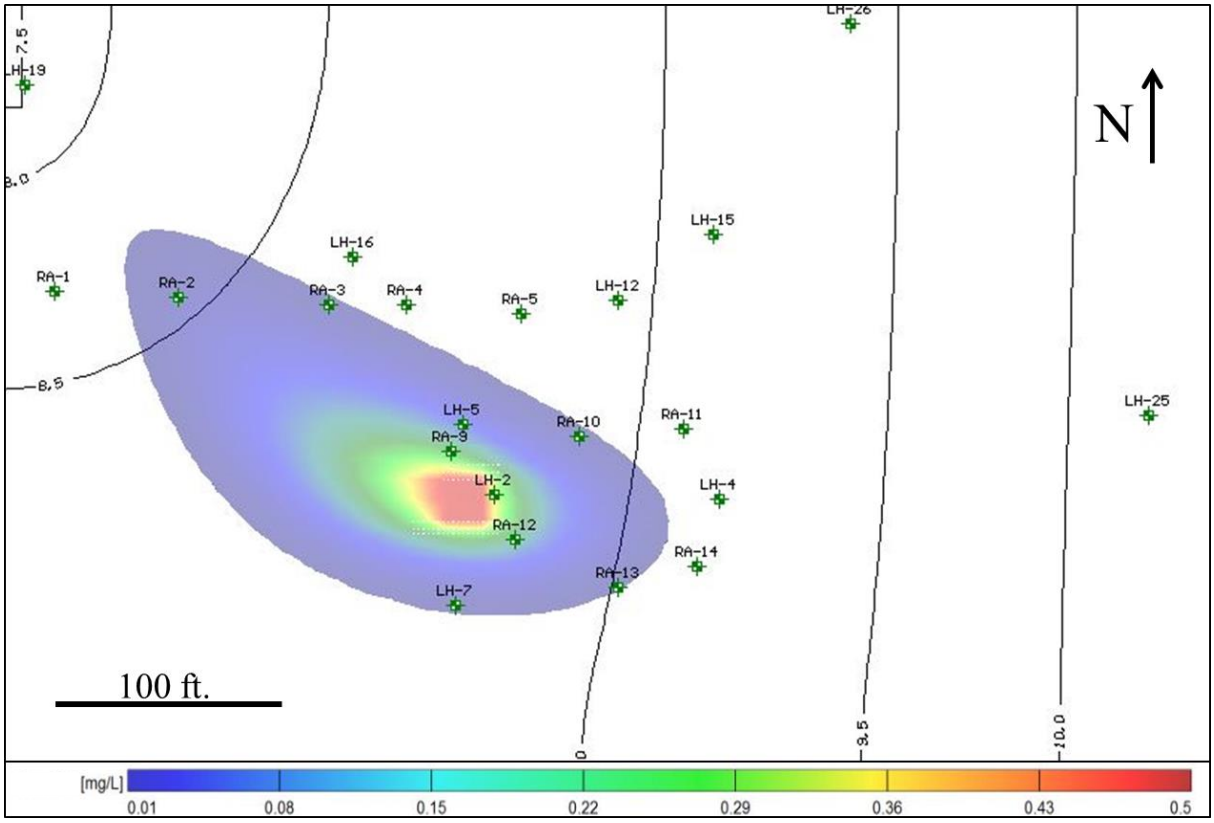

Figure 58. The distribution arsenic after 10 years with $K_d = 1$. The contours are the simulated hydraulic head values.

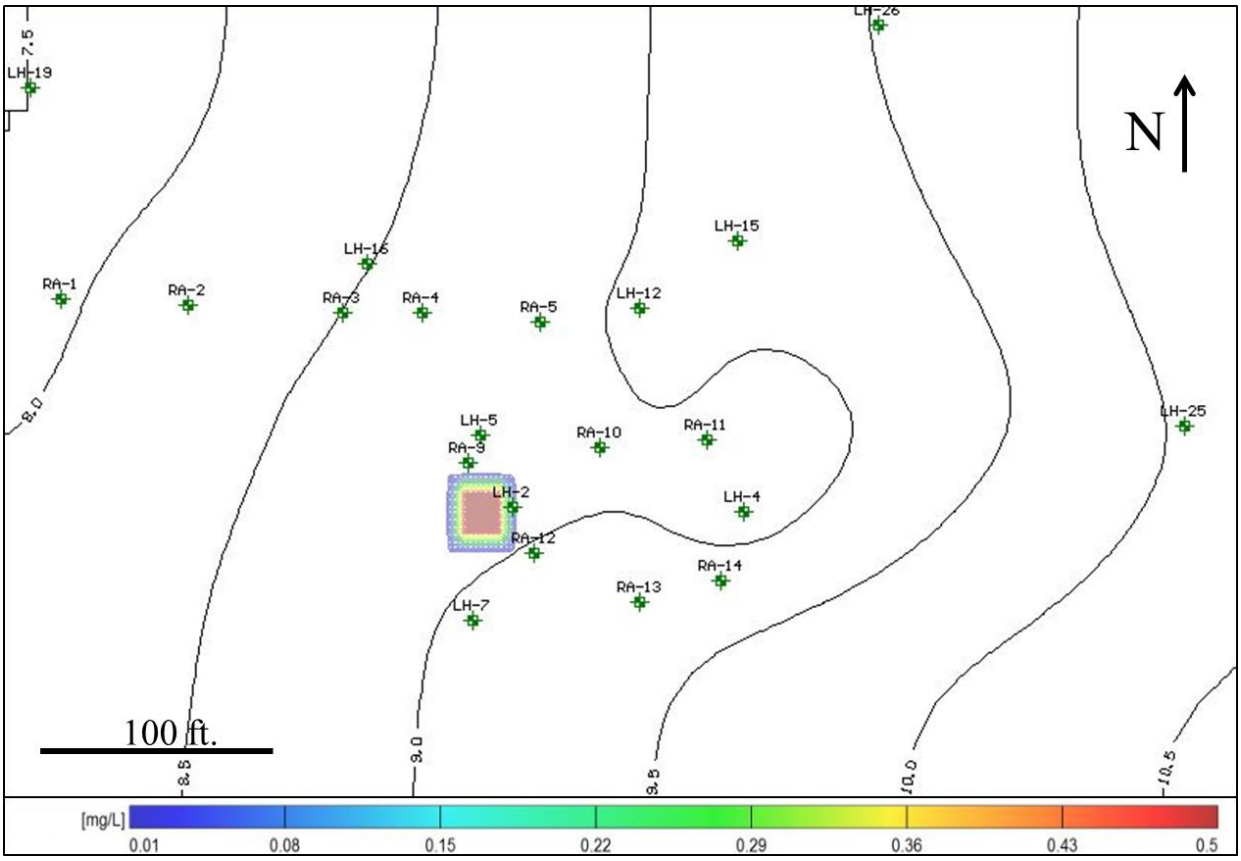

Figure 59. The distribution arsenic after 1 day with $K_d = 4$. The contours are the simulated hydraulic head values.

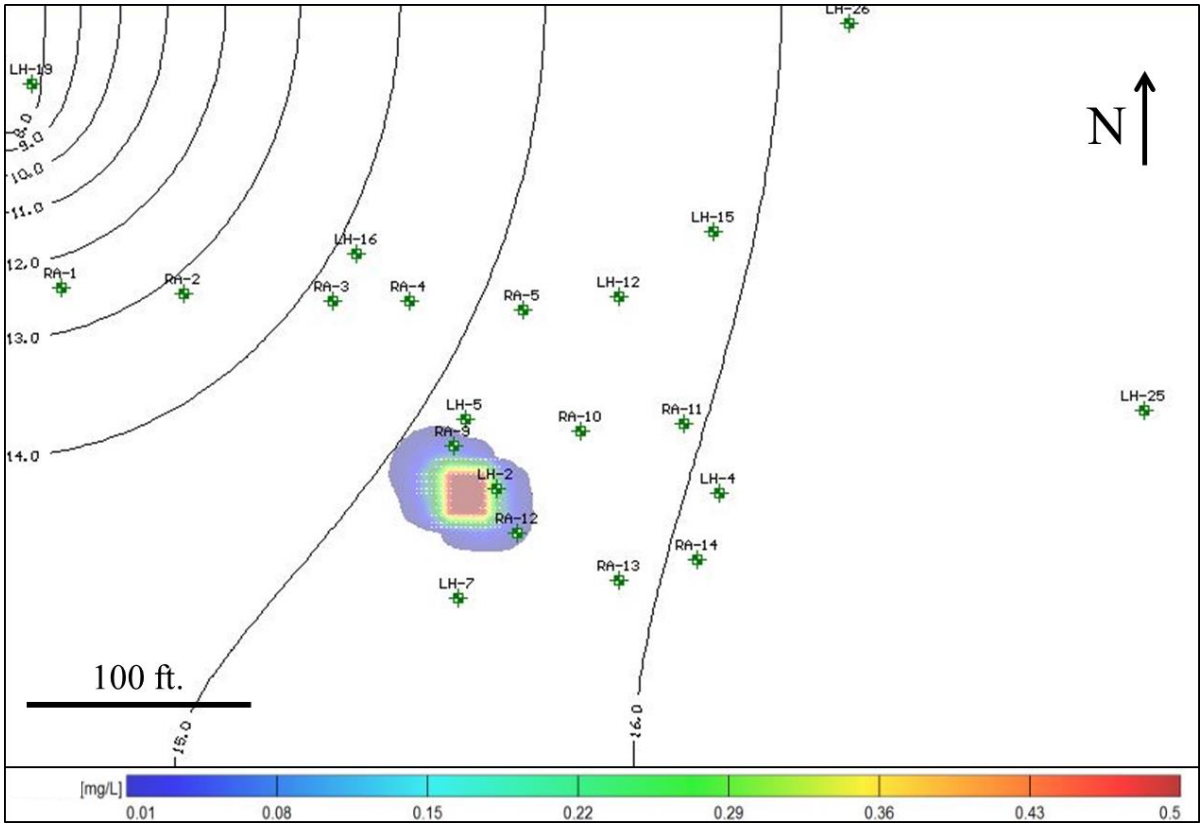

Figure 60. The distribution arsenic after 1 year with $K_d = 4$. The contours are the simulated hydraulic head values.

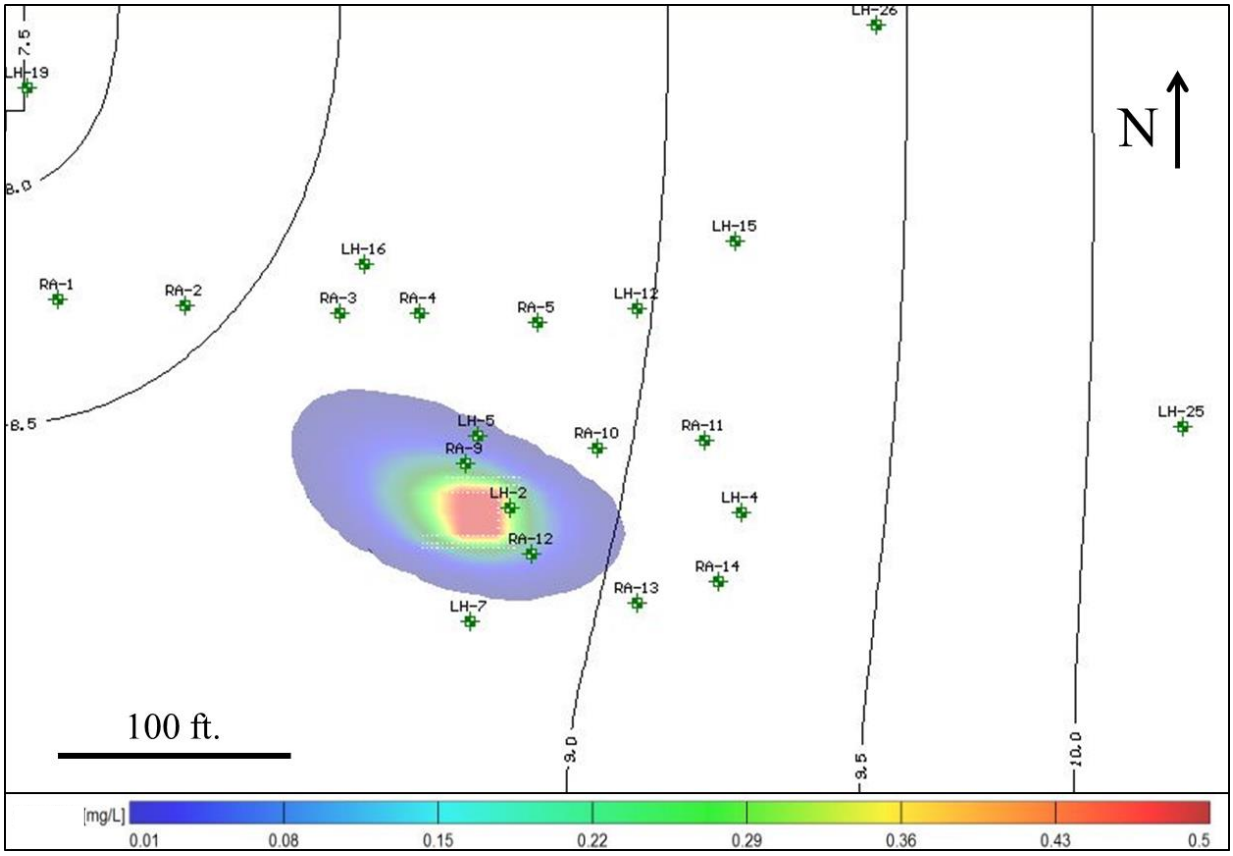

Figure 61. The distribution arsenic after 10 years with $K_d = 4$. The contours are the simulated hydraulic head values.

In the last model the distribution coefficient was set to a value of 10 mL/g, which is at the higher end of the spectrum for distribution coefficients expected for arsenic (Figures 62, 63, and 64). The modeling results show the most restricted contaminant transport of among the four continuous contaminant models. The front of plume has only migrated approximately 15 meters toward the west from the injection location after 10 years (Figure 64). The advection of the plume is significantly retarded by strong adsorption and only dispersion leads to limited spreading from the center of the mass.

Discontinuous Contaminant Transport Models

The discontinuous contaminant transport models were set up in the same manner and with the same flow parameters as the previous continuous contaminant transport models. However, the timing of the contaminant injection was reduced from 3650 days (10 years) to just 1 day. This was done to see arsenic transport in the same flow field where the contamination is an isolated incident that occurs for a very short time period. An observation well located about 12 meters down-gradient from the source was also added to record the breakthrough and calculated concentration of the traveling plume over time. The distribution coefficients of arsenic used in the models were 0, 0.5, and 1 mL/g (Figures 65-70).

The first discontinuous transport model was run with a K_d of 0 mL/g. This model represents how arsenic distribution is affected by an isolated exposure of arsenic without sorption. In the first year of the simulation the leading edge of the arsenic plume (with As concentration = 0.01) traveled approximately 24 meters from the source (Figure 65). After 10 years of groundwater flow and recharge, the plume continued to follow the regional flow direction to the northwest approximately 60 meters offsite (Figure 66).

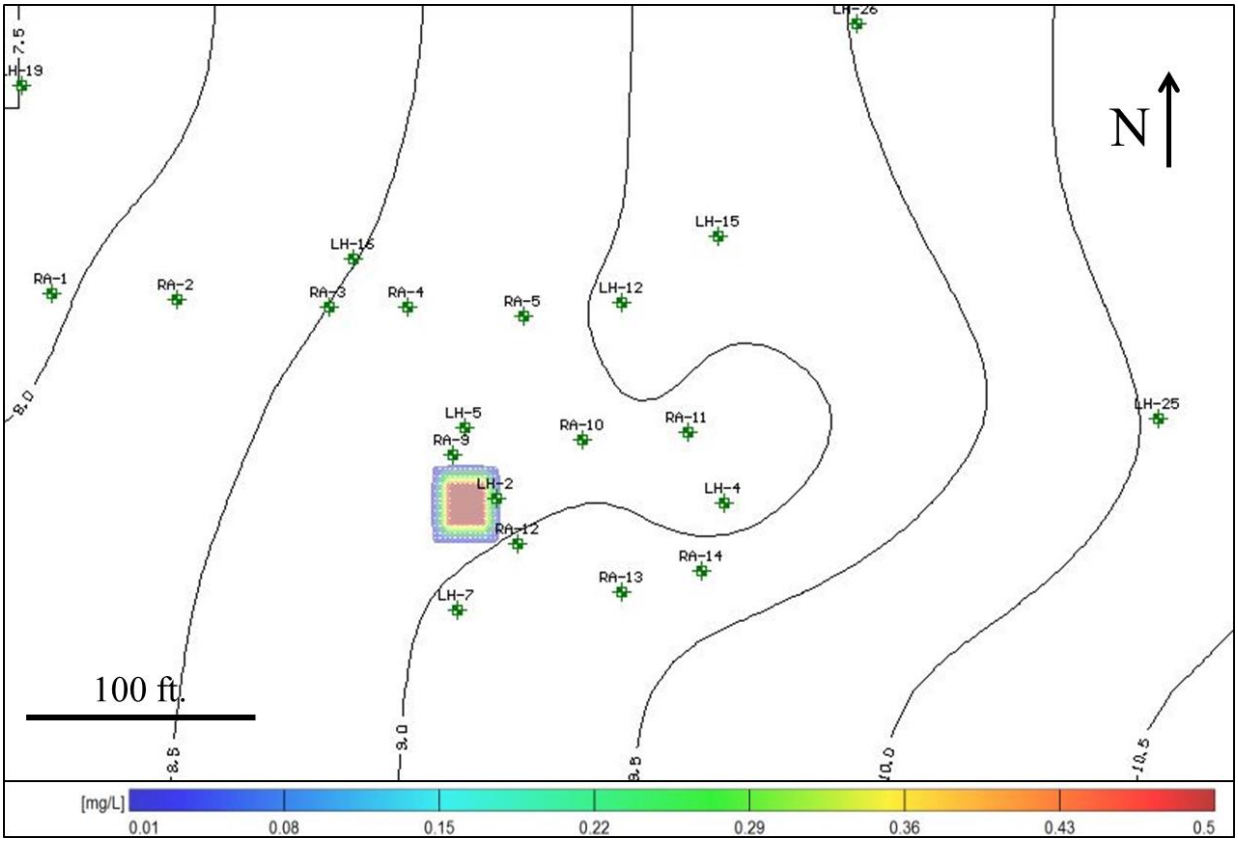

Figure 62. The distribution arsenic after 1 day with K_d = 10. The contours are the simulated hydraulic head values.

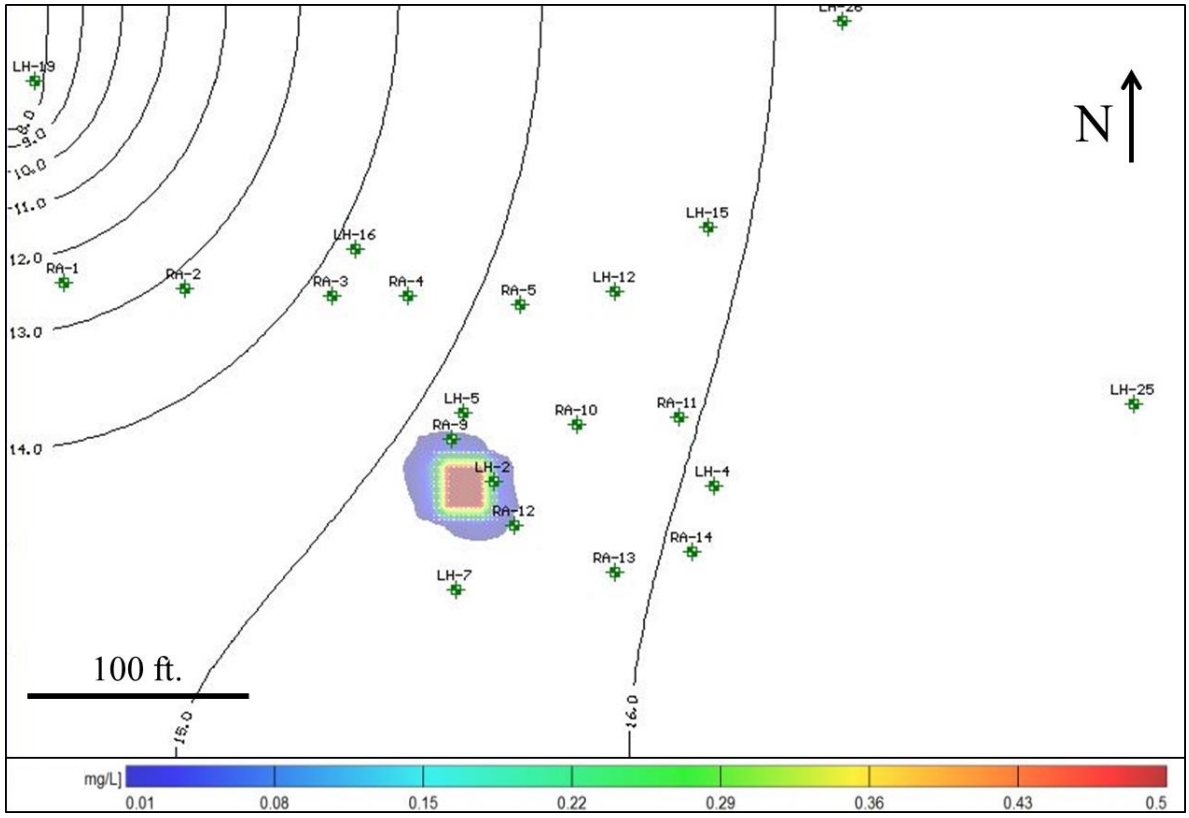

Figure 63. The distribution arsenic after 1 year with K_d = 10. The contours are the simulated hydraulic head values.

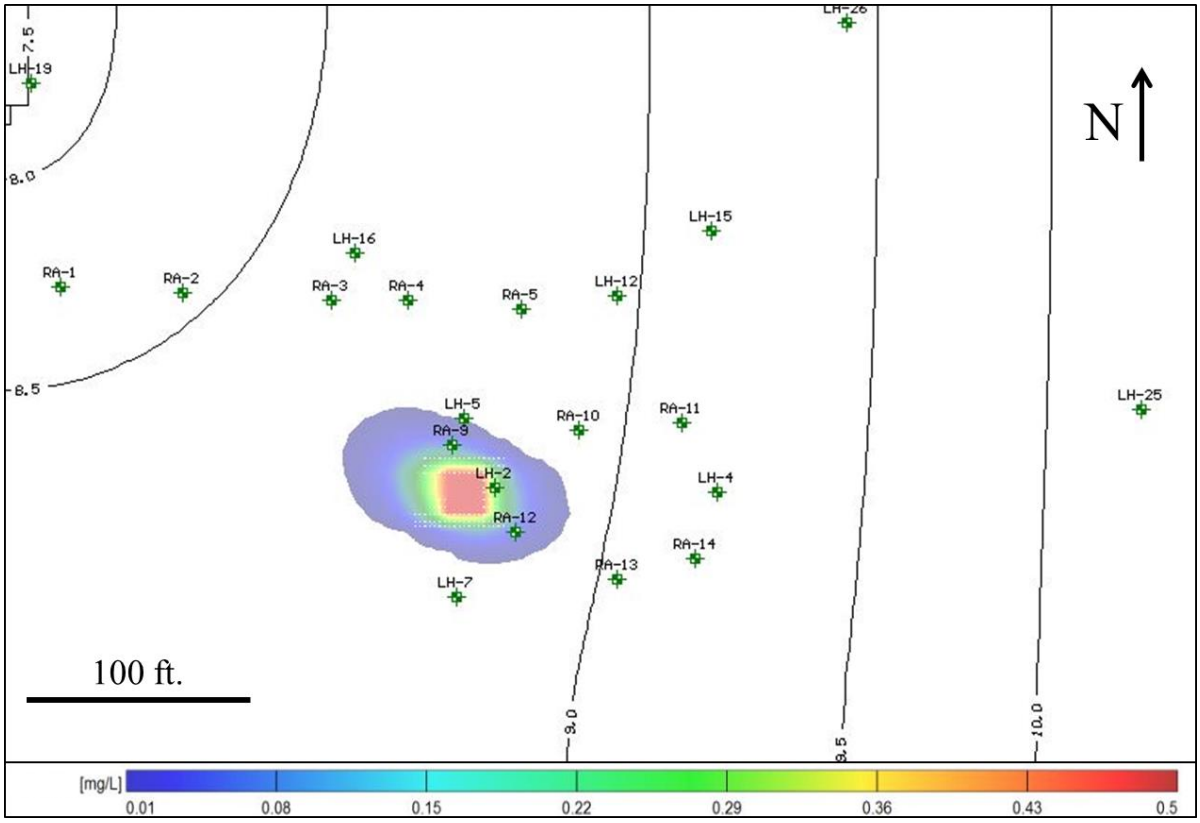

Figure 64. The distribution arsenic after 10 years with K_d = 10. The contours are the simulated hydraulic head values.

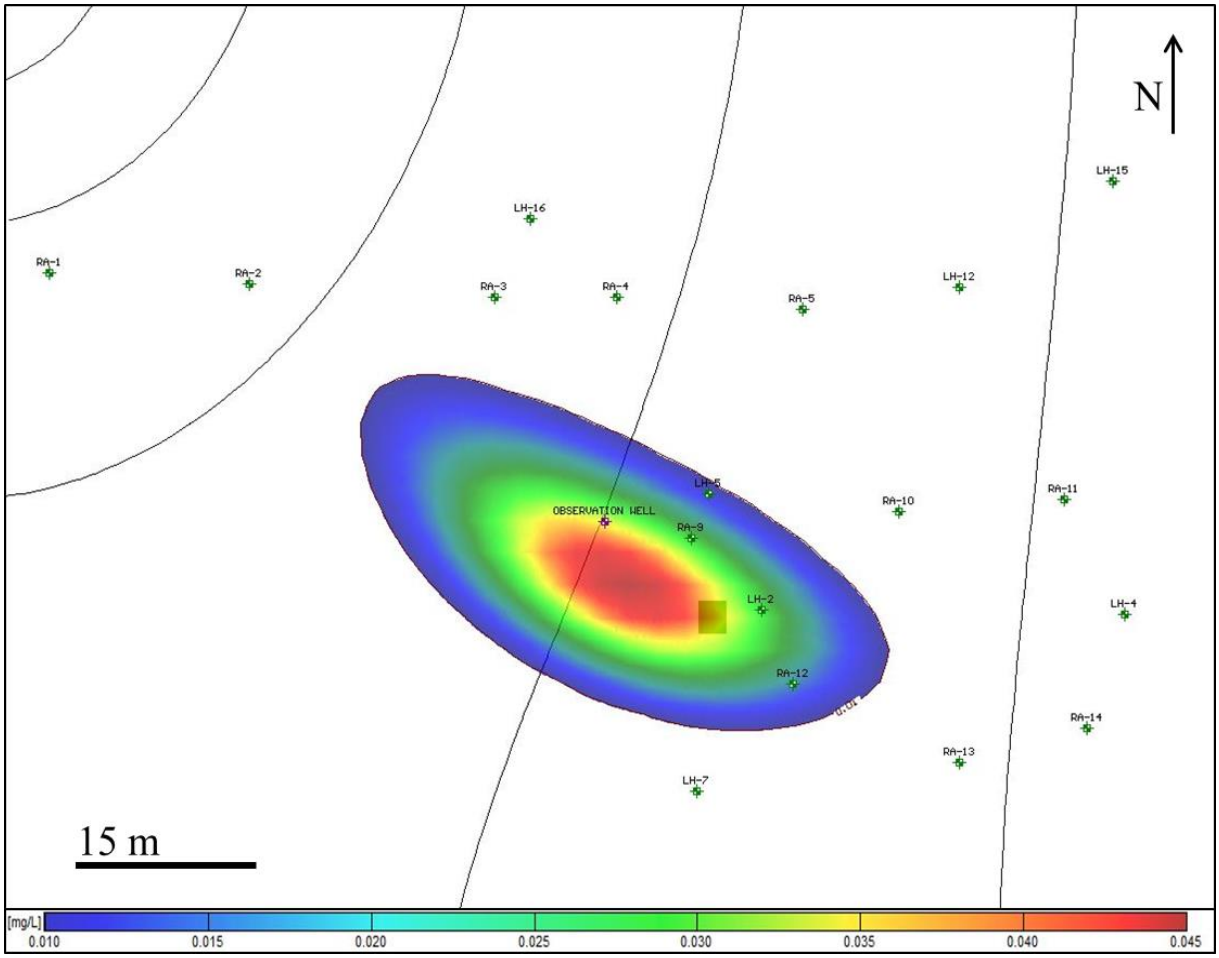

Figure 65. Calculated arsenic distribution for a discontinuous source with a $K_d = 0$ and 1 year after introduction. The highlighted cell is the source.

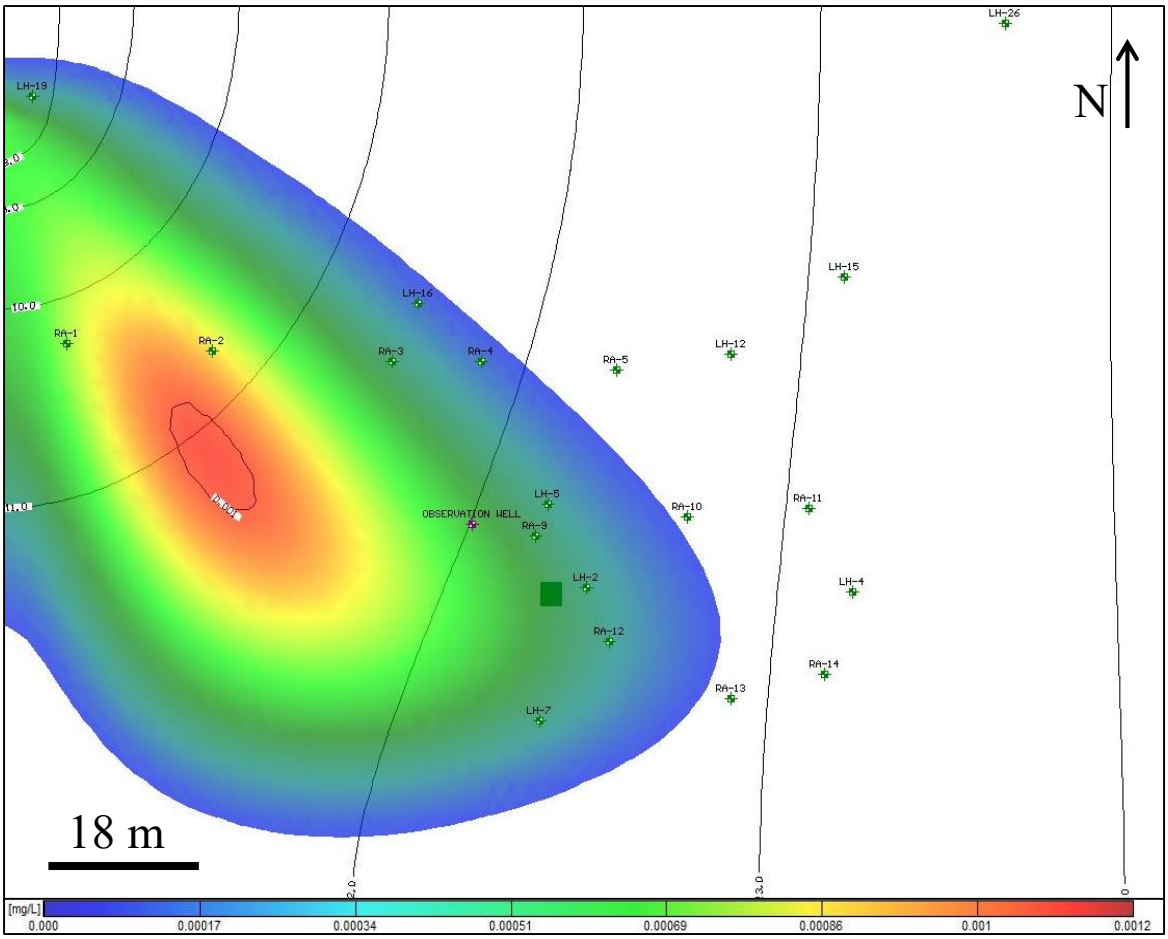

Figure 66. Calculated arsenic distribution for a discontinuous source with a $K_d = 0$ and 10 years after introduction. The highlighted cell is the source and the arsenic contour line shows the EPA limit of 0.01 mg/L.

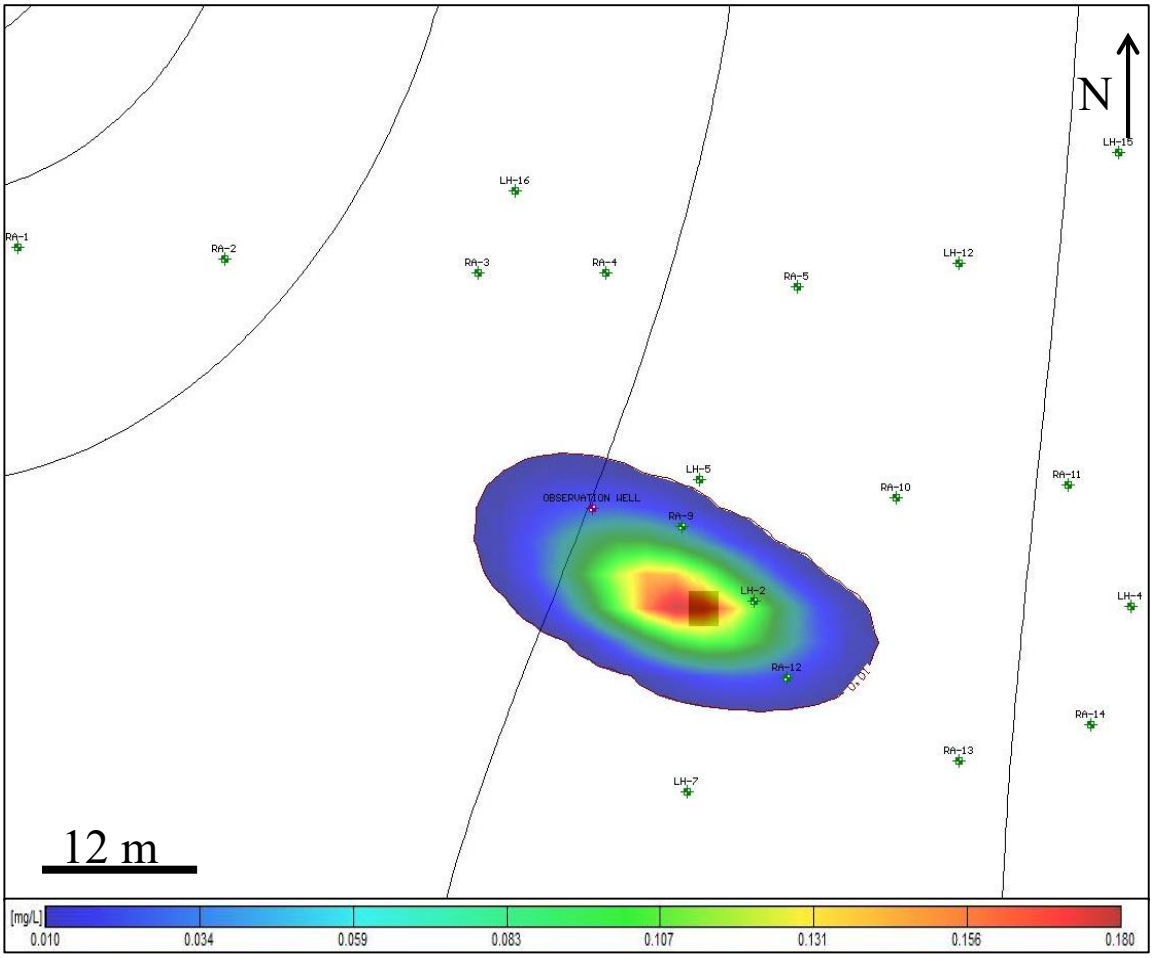

Figure 67. Calculated arsenic distribution for a discontinuous source with a $K_d = 0.5$ and 1 year after introduction. The highlighted cell is the source and the arsenic contour line shows the EPA limit of 0.01 mg/L.

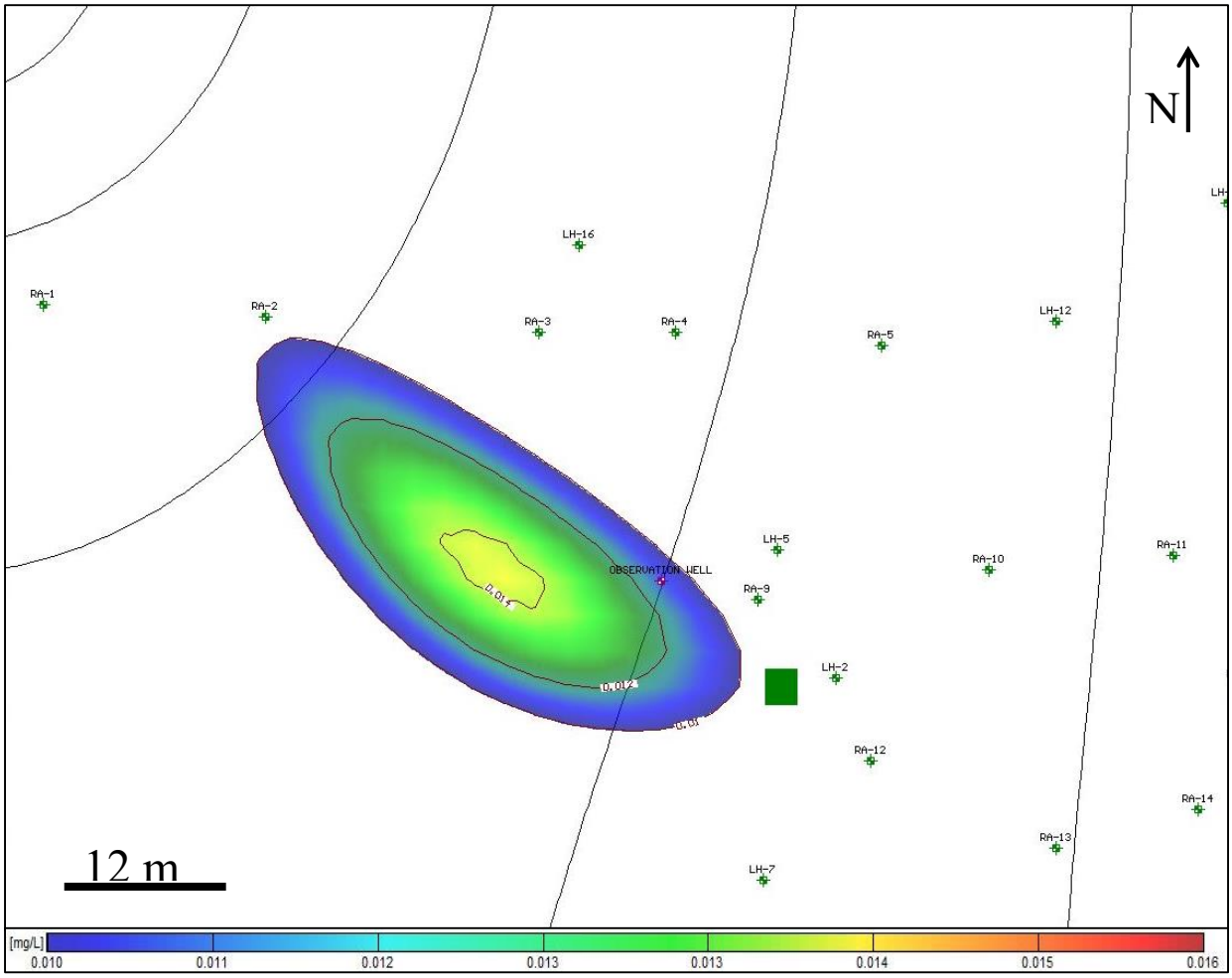

Figure 68. Calculated arsenic distribution for a discontinuous source with a $K_d = 0.5$ and 10 years after introduction. The highlighted cell is the source and the arsenic contour line shows the EPA limit of 0.01 mg/L.

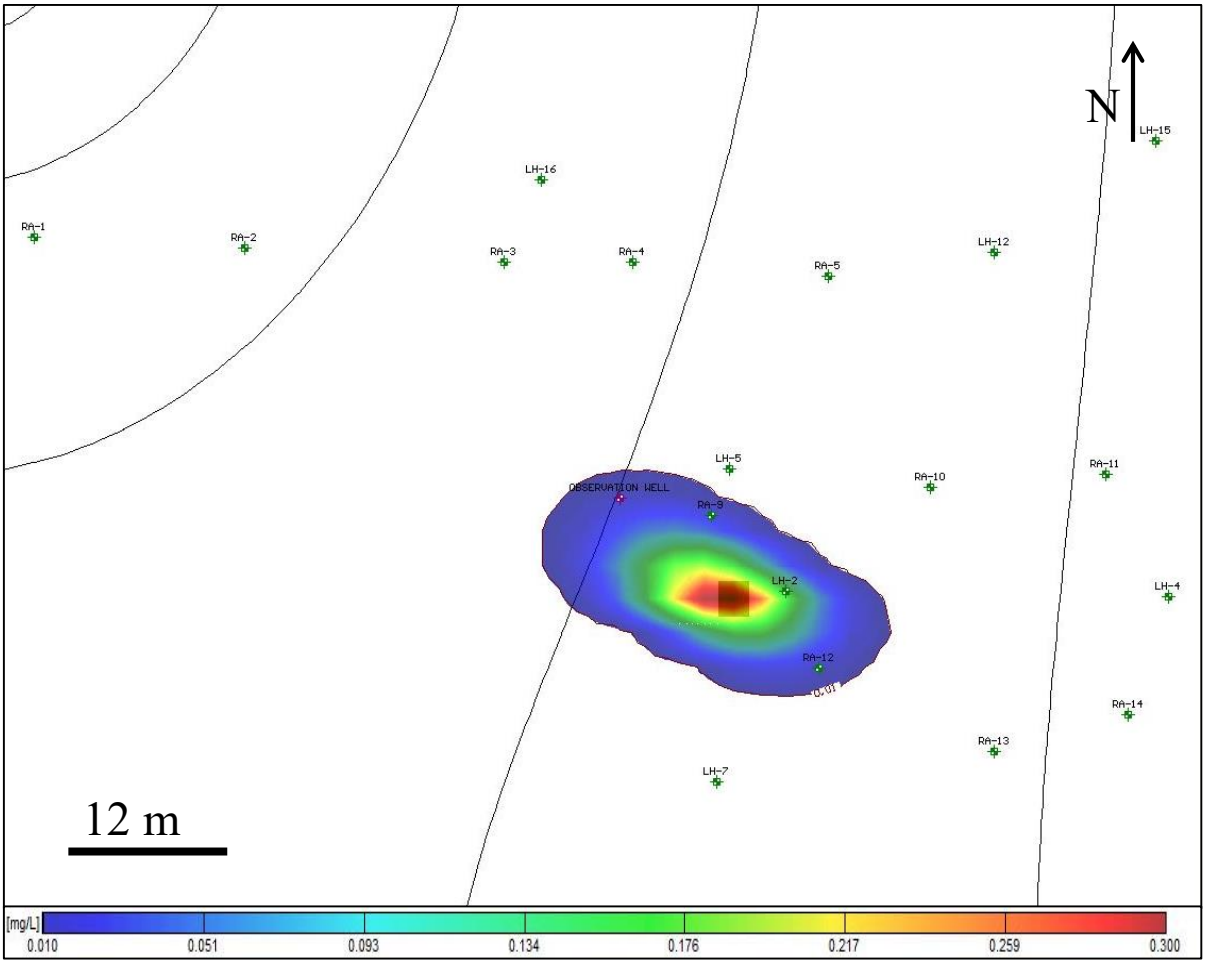

Figure 69. Calculated arsenic distribution for a discontinuous source with a $K_d = 1$ and 1 year after introduction. The highlighted cell is the source and the arsenic contour line shows the EPA limit of 0.01 mg/L.

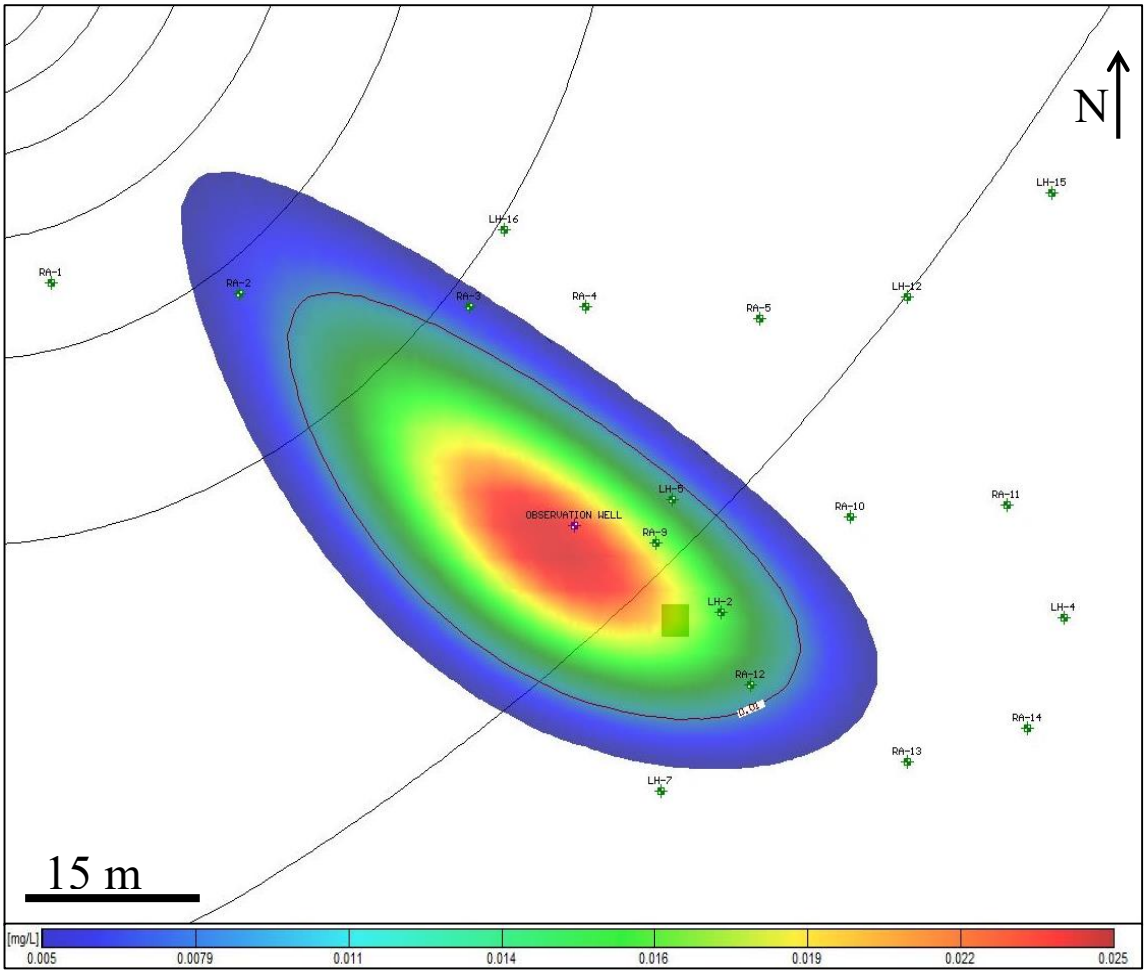

Figure 70. Calculated arsenic distribution for a discontinuous source with a $K_d = 1$ and 10 years after introduction. The highlighted cell is the source and the arsenic contour line shows the EPA limit of 0.01 mg/L.

The second discontinuous model was run for the same amount of time as the first with a K_d of 1 mL/g. This model represents an aquifer with a small amount of arsenic sorbed to sediments. After 1 year the leading edge of the plume traveled approximately 14 meters from the source (Figure 67). After 10 years the leading edge traveled approximately 50 meters from the source (Figure 68).

The third discontinuous contaminant transport model was run with the same conditions as the previous discontinuous models with the exception of distribution coefficient. The K_d used in this model was equal to 1 mL/g. This represents an aquifer that sorbs arsenic in a 2:1 ratio compared to the previous case with a K_d value of 0.5 ml/g. After a time of 1 year the plume traveled approximately 10 meters (Figure 69), which is significantly less than the previous lower K_d value of 0.5 mL/g. After 10 years the model showed the plume had traveled 37 meters from the source (Figure 70).

Discontinuous Breakthrough Curves

Plots of calculated arsenic concentrations recorded at the observation well versus time represent "breakthrough curves" that shows the front, center, and tail of a passing arsenic plume (Figure 71). Comparing breakthrough curves for the discontinuous shows the effects that K_d has on the travel time and peak concentration of arsenic plume when it reaches the observation well. The curve corresponding to $K_d = 0$ shows that the peak of the arsenic plume took 102 days to reach the observation well. The curve corresponding to $K_d = 0.5$ shows that arsenic took 311 days to reach the observation well, and the curve corresponding to $K_d = 1$ took 1048 days for the center mass to reach the same destination. The peak concentrations of plumes that reach the observation well are 0.060, 0.048, and 0.035 ppm for K_d values equal to 0, 0.5, and 1 mL/g, respectively.

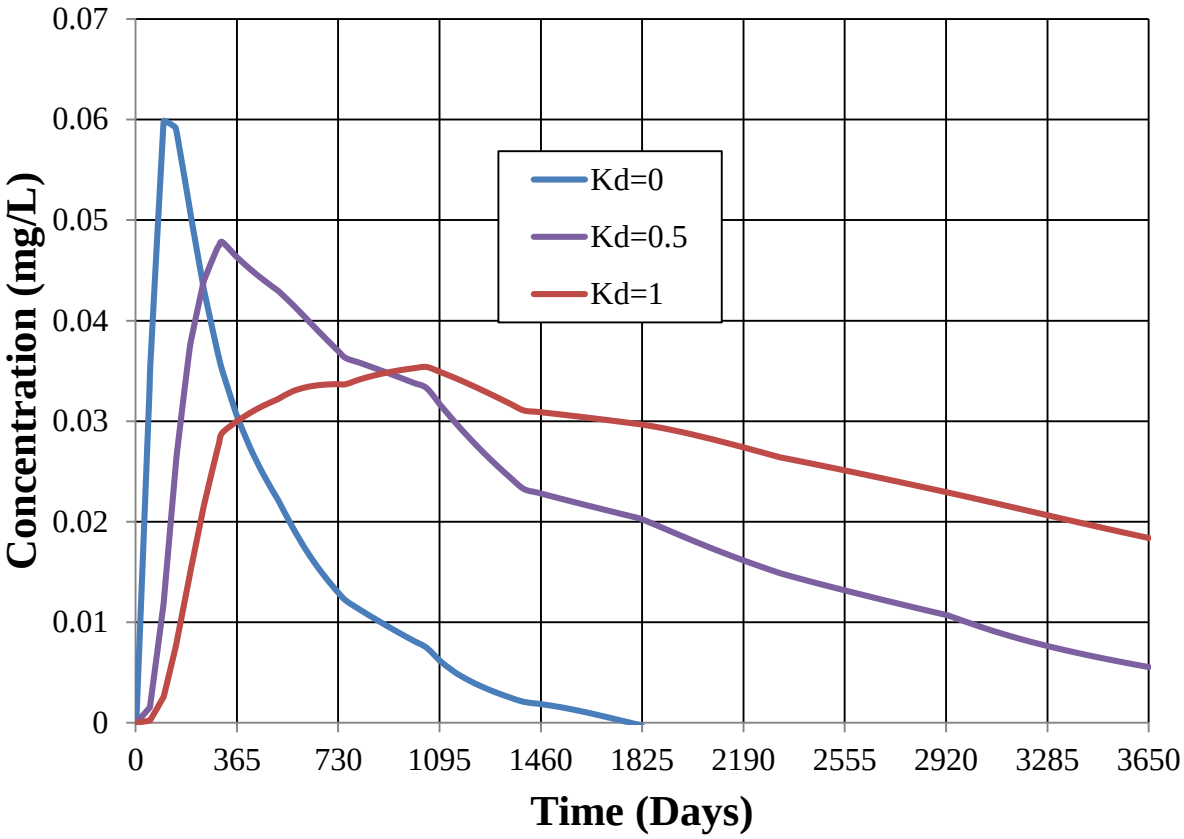

Figure 71. Breakthrough curves of calculated concentrations at the observation well in three discontinuous contaminant transport models.

The comparison of the breakthrough curves makes it easy to directly compare the effects of sorption on contaminant transport in relation to a given point (observation well). The higher the distribution coefficient (i.e., strong sorption) the longer it takes for the front of the arsenic plume to reach the well. High K_d values also lead to lower peak concentrations of the plumes.

Proposed Field Biostimulation and Expected Results

The results of the geochemical analyses and modeling suggest that the Lynn Haven industrial site contains hydrogeochemical conditions that may be amenable for immobilizing or sequestration of arsenic in groundwater via precipitation of biogenic pyrite. The pump-and-treat remediation activities have ceased at the Lynn Haven industrial site since the arsenic level has reduced within 13 to 28 percent of the historical maximum concentration of about 4500 µg/L (unfiltered). Bacterial sulfate reduction process may potentially provide more cost-effective solutions for remediating arsenic contaminants in groundwater than traditional pump-and-treat methods.

XRD and XRF analyses of sediment slurry in the wells show the formation of arsenic-rich iron sulfide solids, suggesting that sulfate reducing bacteria are removing some arsenic naturally at the site by precipitating colloidal pyrite, using very limited amount of dissolved sulfate and organic matter present in the hosting shallow aquifer. Saunders et al. (2005) performed a similar XRD and geochemical study at this site (Figure 72) and concluded that bacterial sulfate reduction and precipitation of pyrite were taking place.

The proposed in situ bioremediation approach would require engineering natural SRB with amendments of organic carbons, nutrients, and iron sulfate to make appropriate biominerals of Fe-sulfide with high-surface area for arsenic adsorption and co-precipitation (Saunders, 1998;

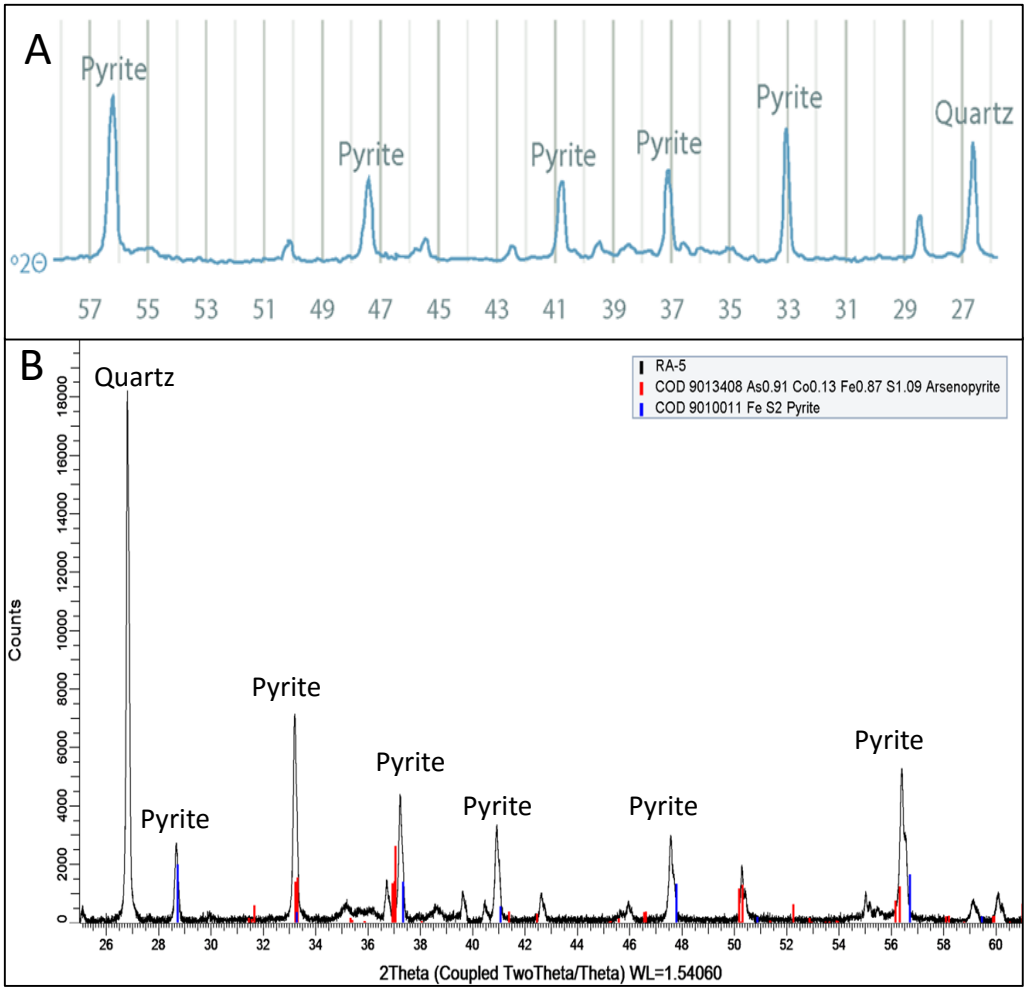

Figure 72. Plot A is an XRD spectrum of aquifer sediments taken from Saunders et al. (2005). Plot B is an XRD spectrum of aquifer sediments taken during the January 2015 sampling event. Both plots show sediment from well RA-5.

Saunders et al., 2008; Lutes et al., 2014). After amendments, we expect to see a rapid reduction in dissolved arsenic concentration once microbial sulfate reduction begins. It should be noted that injection of organic carbon may initially raise the dissolved Fe and arsenic concentration (approximately twice the initial level) during the early stage (first few weeks) because it creates Fe-reducing conditions and mobilizes arsenic from oxides in the aquifer (Saunders et al., 2008). Once biogenic sulfate reduction begins after about one month of injection, both Fe and As should decrease dramatically. Late in the experiment, arsenic may return to the background level either because the sulfate reduction ceases or when the treated groundwater is replaced by surrounding As-rich groundwater. New injection can proceed in this case to re-establish the sulfate reducing conditions and form more Fe-sulfide biominerals. Once Fe-sulfide biominerals stabilize in the aquifer they should continue to remove arsenic by sorption.

Conclusions

Geochemical field data and computer modeling techniques were used in this study to investigate interactions between arsenic-bearing groundwater and its hosting aquifer at the Lynn Haven industrial site in Bay County, Florida and Macon County, Alabama. The following conclusions can be made by combining the results of field survey, geochemical analysis, and numerical modeling.

Observed arsenic concentrations at the Lynn Haven retired substation ranged from 0.0002 ppm to 0.577 ppm in the sampled wells and the average As concentration was calculated (0.15 ppm) to be well above the EPA standard of 0.01 ppm. Due to the elevated concentrations of As and past remedial history the most viable option to cost effectively lower As concentrations is to implement an in-situ bioremediation technology.

The Lynn Haven field site is under moderately reducing conditions, as indicated by relatively low values of ORP and DO, as well as elevated dissolved sulfide and ferrous iron concentrations. The main hydrochemical facies of groundwater in the surficial aquifer is characterized as a Ca-HCO_3-Na-Cl type. Na shows largely conservative behavior but a few samples exhibit slightly enrichment or depletion relative to conservative mixing. Non-conservative behavior of Na may be explained by Na exchange or fixation on clays. Groundwater is strongly enriched in Ca and Mg and slightly enriched in K and SO_4 relative to the seawater dilution trend. The enrichment is attributed to a large degree by processes such as mixing of deeper groundwater from carbonate and clay-rich units as well as ion exchange. Carbonate rich groundwater would migrate upward into the surficial aquifer in place where the Jackson Bluff Formation is absent or functions as a semi-confining unit.

XRF analyses of selected sediments recovered from both the Macon County and Lynn Haven sites consistently resulted in major peaks for Fe, S, and As. XRD analyses confirmed the presence of iron sulfide (pyrite) and arsenic-bearing sulfide minerals. These results suggest that bacterial sulfate reduction has already led to the sequestration of arsenic in Fe-sulfides at both sites. The geochemical modeling conducted in this study also suggests that the surficial aquifer is currently at or near the conditions for sulfate reduction and the precipitation of As-bearing pyrite. The geochemical modeling results also show the sequence of minerals formed during bacterial sulfate reduction with a drop in Eh and amendments of $FeSO_4$. Ferrous iron in solution reacts with sulfide produced from sulfate reduction to form pyrite as the Eh drops below -0.08V. The precipitation of iron sulfide has the potential to significantly lower the concentration of arsenic in contaminated groundwater via adsorption and co-precipitation processes.

Results of hydrogeologic modeling with Basin2 and Visual MODFLOW at both regional and local scales suggest that groundwater and contaminants travel dominantly toward northwest of the site through time. Groundwater movement is driven by local and regional topographic relief or water table slope. The calculated flow velocities are on the order of a few to tens of meters per year. Contaminant transport models (with both continuous and discontinuous sources) show that the main factors influencing arsenic transport include advection, dispersion, and adsorption. Varying the distribution coefficient K_d values (1 to 10 ml/g) for different adsorption models showed that the higher the degree of sorption (high K_d values) the more arsenic transport is inhibited. Sensitivity analysis shows that adsorption tends to lower the peak concentration and cause time lag of arsenic transport.

The results of this study also have implications on how to bioremediate the Lynn Haven site. The geochemical data and modeling suggest that if site conditions are optimized for the

stimulation sulfate-reducing bacteria to precipitate iron sulfides, then this may be an effective bioremedial strategy. When iron sulfides begin to form from the SRB then arsenic will be adsorbed on to their surface. In order to optimize site conditions soluble sources of organic carbon, ferrous iron, and sulfate must be injected into the aquifer.

References

Allison, J.D., and Allison, T.L., 2005. Partition Coefficients for Metals in Surface Water, Soil, and Waste: U.S. EPA/600/R-05/074, 93 p.

Appelo, C.A.J., 1994, Cation and proton exchange, pH variations, and carbonate reactions in a freshening aquifer: Water Resources Research, Vol. 30, No. 10, 13p.

Bates, R.L., and Jackson, J.A., 1984, Dictionary of Geological Terms: New York, Anchor Books, 571 p.

Bethke, C. M., 2008, Geochemical and biogeochemical reaction modeling. Cambridge University Press, 543 pp.

Bethke, C.M., M.-K. Lee, H.A.M. Quinodoz, and W.N. Kreiling, 2003, Basin modeling with Basin2; A guide to using Basin2, B2plot, B2video, and B2view, Hydrogeology Program, University of Illinois, Urbana.

Charlet, L., and Polya, D.A., 2006. Arsenic in shallow, reducing groundwaters in southern Asia: an environmental health disaster: Elements 2, 91-96 p.

Cauwenberghe, L., and Roote, D.S., 1998. In Situ Bioremediation: Ground-Water Remediation Technologies Analysis Center O Series: TO-98-01, 24 p.

DeFlaun, M., Lanzon, J., Lodato, M., Henry, S., Onstott, T.E., Chan, E., and Otemuyiwa, B., 2009, Anaerobic Biostimulation for the In Situ Precipitation and Long-Term Sequestration of Metal Sulfides: SERDP Project ER1373, 175 p.

Domenico, P.A., and Schwartz, F.W., 1990, Physical and Chemical Hydrogeology: John Wiley and Sons Inc, 824 p.

Drever, J.I., 1997, The Geochemistry of Natural Waters: 3rd Edition, Prentice Hall, Upper Saddle River, New Jersey, 436 pp.

Dzombak, D.A., and Morel, F.M., 1990, Surface Complexation Modeling: Hydrous Ferrous Oxide: John Wiley and Sons, New York, New York, 393 p.

Fetter,C.W. 2001, Applied Hydrogeology, 4th ed., Prentice Hall, Upper Saddle River, NJ, 598 p.

Ford, R.G., Wilkin, R.T., and Puls, R.W., 2007, Monitored Natural Attenuation of Inorganic Contaminants in Groundwater Volume 2: U.S.EPA/600/R-07/140 108 p.

Frank, J.R., and Peters, R.W. 1992, Remediation of arsenic-oxide contamination: Phase I groundwater cleanup feasibility – treatability studies: Argonne National Laboratory, Argonne, Illinois, 19 p.

Freeze, A.R., and Cherry, J.A. (1979), Chemical Evolution of Natural Groundwater, In Groundwater: Prentice Hall, The University of Michigan, pp. 238-289.

Gelhar, L.W., Welty, C., and Rehfeldt, K.R., 1992, A critical review of data on field-scale dispersion in aquifers: Water Resources Research, 28, 1955-1974 p.

Harvey, C.F., Swartz, C.H., Badruzzman, B., Keon, N.E., Yu, W., Ali, A., Jay, J., Beckie, R., Niedan, V., Brabander, D., Oates, P., Ashfaque, K., Islam, S., Hemond, H.F., Ahmed, F., 2002, Arsenic mobility and groundwater extraction in Bangladesh: Science 298, 1602-1606 p.

Hem, J.D. (1986), Study and interpretation of the chemical characteristics of natural water, 3rd ed.: U.S. Geological Survey Water-Supply Paper 2254, 363 p.

Hounslow, A.W., 1980, Groundwater Geochemistry: Arsenic in Landfills: Ground Water 18, 331-333 p.

Huerta-Diaz, M.A., and J.W. Morse. 1992. Pyritization of trace metals in anoxic marine sediments: *Geochimica et Cosmochimica Acta*, *56*: 2681-2702.

Humayun, M., S.B. Simon, and L. Grossman, 2007. Tungsten and hafnium distribution in calcium-aluminum inclusions (CAIs) from Allende and Efremovka: *Geochim. Cosmochim. Acta*, 71, 4609-4627.

Humayun, M., F.A. Davis, and M.M. Hirschmann, 2010. Major element analysis of natural silicates by laser ablation ICP-MS: *J. Anal. At. Spectrom*., 25, 998-1005, DOI: 210.1039/C001391A

Keimowitz, A.R., Mailloux, B.J., Cole, P., Stute, M., Simpson, H.J., and Chillrud, S.N., 2007. Laboratory investigations of enhanced sulfate reduction as a groundwater arsenic remediation strategy: Environmental Science Technology, 41, 6718-6724

King, D.T., 1994. Upper Cretaceous depositional sequences in the Alabama gulf coastal plain: Their characteristics, origin, and constituent clastic aquifers: Journal of Sed. Res. B64, 2, 258-265 p.

Korte, N.E., and Fernando, Q., 1991, A Review of Arsenic (III) in Groundwater: Critical Reviews in Environmental Control 21, 1-39 p.

Lee, M.K., Saunders, J.A., 2003. Effects of pH on metals precipitation and sorption: field bioremediation and geochemical modeling approaches: Vadose Zone J. 2, 177-185 p.

Lehner, S.W., Savage, K.S., and Ayers, J.C., 2006, Vapor growth and characterization of pyrite (FeS_2) doped with Co, Ni, and As: Variations in semiconducting properties: Journal of Crystal Growth, 286, 306-317 pp.

Lowers, H.A., Breit, G.N., Foster A.L., Whitney, J., Yount, J., Uddin, M.N., and Muneem, A.A., 2007, Arsenic Incorporation into Authigenic Pyrite, Bengal Basin Sediment, Bangladesh: Geochimica, Cosmochimica, Acta 71, 2699-2717 p.

Lutes, C., Frizzell, A., Gillow, J., and Beckner, J. (2014), In situ Precipitation of Radionuclides in Groundwater at US DOE Savannah River Site – 14559: Waste Management Conference 2014, 14 p.

Markewich, H.W., and Christopher, R.A., 1982. Pleistocene and Holocene fluvial history of Uphapee Creek, Macon County, Alabama: A paleoenvironmental and paleoclimatic reconstruction of Holocene sedimentation and incision in an upper coastal plain stream valley: US Gov. Printing Office, Washington, DC.

McArthur, J.M., Ravenscroft, P., Safiulla, S., and Thirlwall, M.F., 2001, Arsenic in groundwater; testing pollution mechanisms for sedimentary aquifers in Bangladesh: Water Resources Research, 37, 109-118 p.

McDonald, M.G., and Harbaugh, A.W., 1988, Techniques of Water Resource Investigations of the United States Geological Survey, Chapter A1 – A modular three-dimensional finite difference ground-water flow model: United States Geological Survey Open-File Report 83-875, 484 p.

Mintz, J., and Miller, J., 1993, Lynn Haven Retired Substation Remedial Action Plan: Southern Company Services, 196 p.

Nesbitt, H.W., 1980, Characterization of mineral-solution interactions in Carboniferous sandstones and shales of the Illinois Sedimentary basin: American Journal of Science, v. 285, 607-630 p.

Nickson, R.T., McArthur, J.M., Ravenscroft, P., Burgess, W.G., and Ahmed, K.M., 2000, Mechanism of arsenic release to groundwater, Bangladesh and West Bengal: Applied Geochemistry, 15, 403-413 p.

O'Day, P.O., Vlassopoulos, D., Root, R., and Rivera, N., 2004, The Influence of Sulfur and Iron on Dissolved Arsenic Concentrations in the Shallow Subsurface under Changing Redox Conditions: Proceedings of the National Academy of Science, 101, 13703-13708, 6 p.

Penny, E., Lee, M.K., and Morton, C., 2003. Groundwater and microbial processes of the Alabama coastal plain aquifers: Water Resource Research, 39, 1320. doi: 10.1029/2003WR00196 17 p.

Saunders, J.A., Cook, R.B., Thomas, R.C., and Crowe, D.E., 1996.Coprecipitation of trace metals in pyrite: Implications for enhanced intrinsic bioremediation: In ed. S.H. Bottrell, Proc. Fourth International Symposium on the Geochemistry of the Earth's Surface (Ilkley, Yorkshire, England), 470-474 p.

Saunders, J.A., Pritchett, M.A., and Cook, R.B., 1997. Geochemistry of biogenic pyrite and ferromanganese stream coatings: a bacterial connection: Geomicrobiology. J. 14, 203-217 p.

Saunders, J.A., Lee, M.K., Uddin, A., Mohammad, S., Wilkin, R.T., Fayek, M., and Korte, N.E., 2005, Natural arsenic contamination of Holocene alluvial aquifers by linked linked tectonic, weathering, and microbial processes: Geochemistry Geophysics Geosystems J. V.6, 4. doi: 10.1029/2004GC00803.

Saunders, J.A., 2005, Sequestration of Arsenic in Iron Sulfide as a Potential Bioremediation Technique Using Sulfate Reducing Bacteria: Southern Company Generation Electric Power Research Institute, 22 p.

Saunders, J.A., Lee, M.K., Shamsudduha, M., Dhakal, P., Uddin, A., Chowdury, M.T., and Ahmed, K.M., 2008, Geochemistry and mineralogy of arsenic in (natural) anaerobic Groundwaters: Applied Geochem. 23, 3205-3214 p.

Schmidt, W. and Clark, M.W. 1980, Geology of Bay County, Florida: Florida Geological Survey Bulletin 57, 96 p.

Shamsudduha, M., Uddin, A., Saunders, J.A., and Lee, M.K., 2008. Quaternary stratigraphy, sediment characteristics and geochemistry of arsenic-contaminated alluvial aquifers in the Ganges-Brahmaputra floodplain in central Bangladesh: Journal of Contaminant Hydrology, 99, 112-136 p.

Smedley, P.L., and Kinniburgh, D.G., 2002, A review of the source, behavior and distribution of arsenic in natural waters: *Applied Geochemistry*, 17, 517-568 p.

Stueber, A.M., Walter, L.M., Huston, T.J., and Pushkar, P., 1993, Formation waters from Mississippian-Pennsylvanian reservoirs, Illinois basin, USA: Chemical and isotopic constraints on evolution and migration: Geochemica et Cosmochemica Acta, v. 57, 763-784 p.

USEPA, 1995, Contaminants and Remedial Options at Selected Metal-Contaminated Sites: Washington DC, Office of Research and Development, U.S. Environmental Protection Agency, EPA/540/R-95/512, 268 p.

USEPA, 1997, Technology Alternatives for the Remediation of Soils Contaminated with As, Cd, Cr, Hg, and Pb: Washington DC, Office of Emergency and Remedial Response, U.S. Environmental Protection Agency, EPA/540/S-97/500, 21 p.

USEPA, 2002, Proven Alternatives of Aboveground Treatment of Arsenic in Groundwater: Washington DC, Office of Solid Waste and Emergency Response, U.S. Environmental Protection Agency, EPA-542-S-02-002, 68 p.

Veach, O., and Stephenson, L.W., 1911, Preliminary Report of on the Geology of the Coastal Plain of Georgia: Georgia Geological Survey, Bulletin 26.

Welch, A.H., Westjohn, D.B., Helsel, D.R., and Wanty, R.B., 2000, Arsenic in ground water of the United States; occurrence and geochemistry: *Ground Water*, 38, 589-604 p.

Woolson, E.A. (1992), Introduction to arsenic chemistry and analysis, in Abstract Proceedings, Arsenic and Mercury Workshop on Removal, Recovery, Treatment, and Disposal: EPA/600/9-92/105.

Zheng, C., 1990, MT3D, A modular three-dimensional transport model for simulation of advection, dispersion, and chemical reactions of contaminants in groundwater systems: Report to the United States Environmental Protection Agency, Ada Oklahoma, 170 p.